Systematic identification of mammalian regulatory motifs' target genes and functions

Jason B Warner, Anthony A Philippakis, Savina A Jaeger, Fangxue Sherry He, Jolinta Lin & Martha L Bulyk

Supplementary figures and text:

Supplementary Figure 1: Schema of PhylCRM scoring scheme for a single motif.
Supplementary Figure 2: Phylogenetic tree of 8 mammals and schematization of PhylCRM scoring scheme.
Supplementary Figure 3: Schema of PhylCRM scoring scheme for multiple motifs.
Supplementary Figure 4: PhylCRM scan of positive control foreground and background regions using a range of phylogenies.
Supplementary Figure 5: Lever screen of all expression clusters using Boolean combinations of the MRF, MEF2, SRF and Tead motifs.
Supplementary Figure 6: Lever screen of all expression clusters and GO categories using Boolean combinations of the MRF, MEF2, SRF and Tead motifs.
Supplementary Figure 7: Schematic display of computationally predicted human CRMs and control sequences.
Supplementary Figure 8: Verification by Q-RT-PCR of transcriptional up-regulation during muscle differentiation of the genes immediately downstream of 6 predicted CRMs selected for experimental validation.
Supplementary Figure 9: Western blot analyses of the known myogenic TFs during the myogenic differentiation time-course.
Supplementary Figure 10: Western blot analyses after shRNA knockdown.
Supplementary Figure 11: Luciferase reporter assays of predicted CRMs after shRNA knockdown.
Supplementary Figure 12: Luciferase reporter assays for a synthetic CRM corresponding to the MRF AND MEF2 code.

Supplementary Table 1: Gene names and expression clusters.
Supplementary Table 2: GO attributes by cluster.
Supplementary Table 4: Predicted and tested CRM regions.

Supplementary Methods
Supplementary Results: Lever screen of 4 known myogenic regulatory motifs across 101 myogenic gene sets, and experimental validation of CRMs predicted by PhylCRM.

Note: Supplementary Table 3 is available on the Nature Methods website.

Supplementary Figure 1

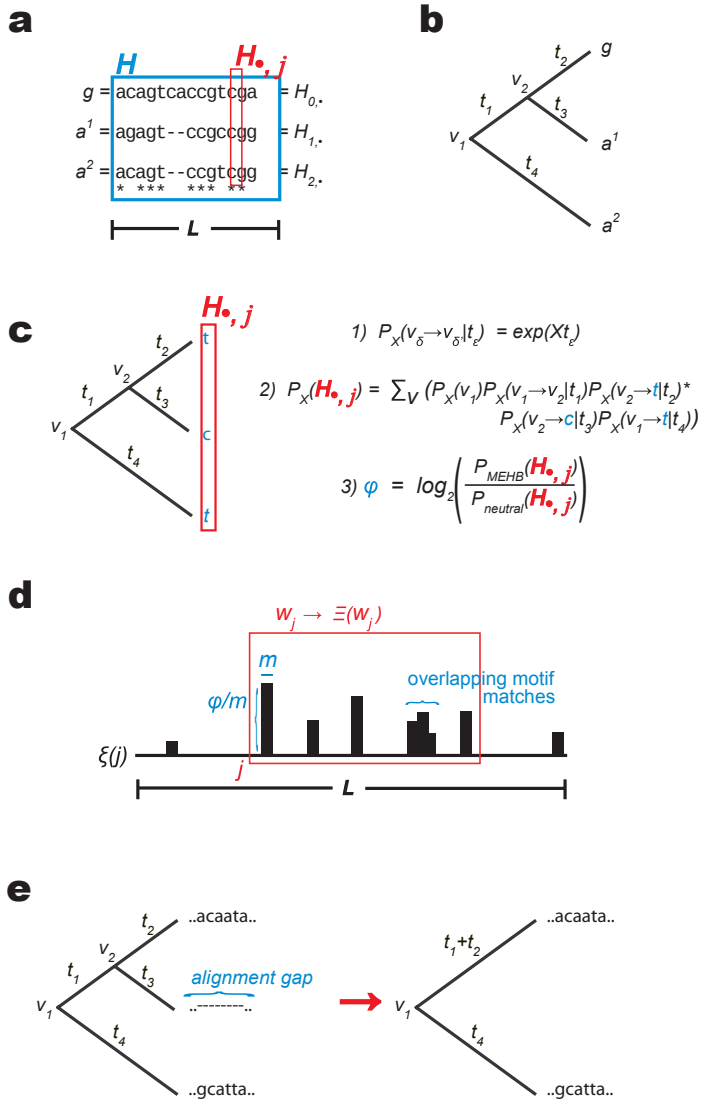

Supplementary Figure 1: PhylCRM scoring scheme for a single motif
(**a**) *g* represents the sequence being searched for CRMs and a^1 and a^2 are sequences from another organism aligned to it. *L* represents the length of the sequence, $H_{0,\bullet}=g$, $H_{i,\bullet}=a^{(i)}$, and $H_{\bullet,j}$ denotes the alignment column at position *j*. (**b**) Tree indicating the phylogeny of *g*, a^1, and a^2. (**c**) Scoring motif matches using the MEHB model. Here, the probability that a given nucleotide *a* turns into *b* during time *t* is given by a matrix exponential, for a suitably chosen rate-matrix *R*. This probability is then used to compute the probability of observing the set of nucleotides $H_{\bullet,j}$ under both the MEHB rate-matrix and the neutral matrix. The score of the motif φ is then taken to be the log-likelihood of the ratio of these probabilities. (**d**) Graphical image of scores for a motif *M* along *g*, where the height of the bars is φ/m. These scores are stored in an array ξ and the score of a window w_j (represented by $\Xi(w_j)$) is then given by summing ξ in w_j. **(e)** When there is no alignable sequence at a given position (or if there is no motif match there), the branch containing that sequence is removed and the pruned tree is used to compute φ.

Supplementary Figure 2

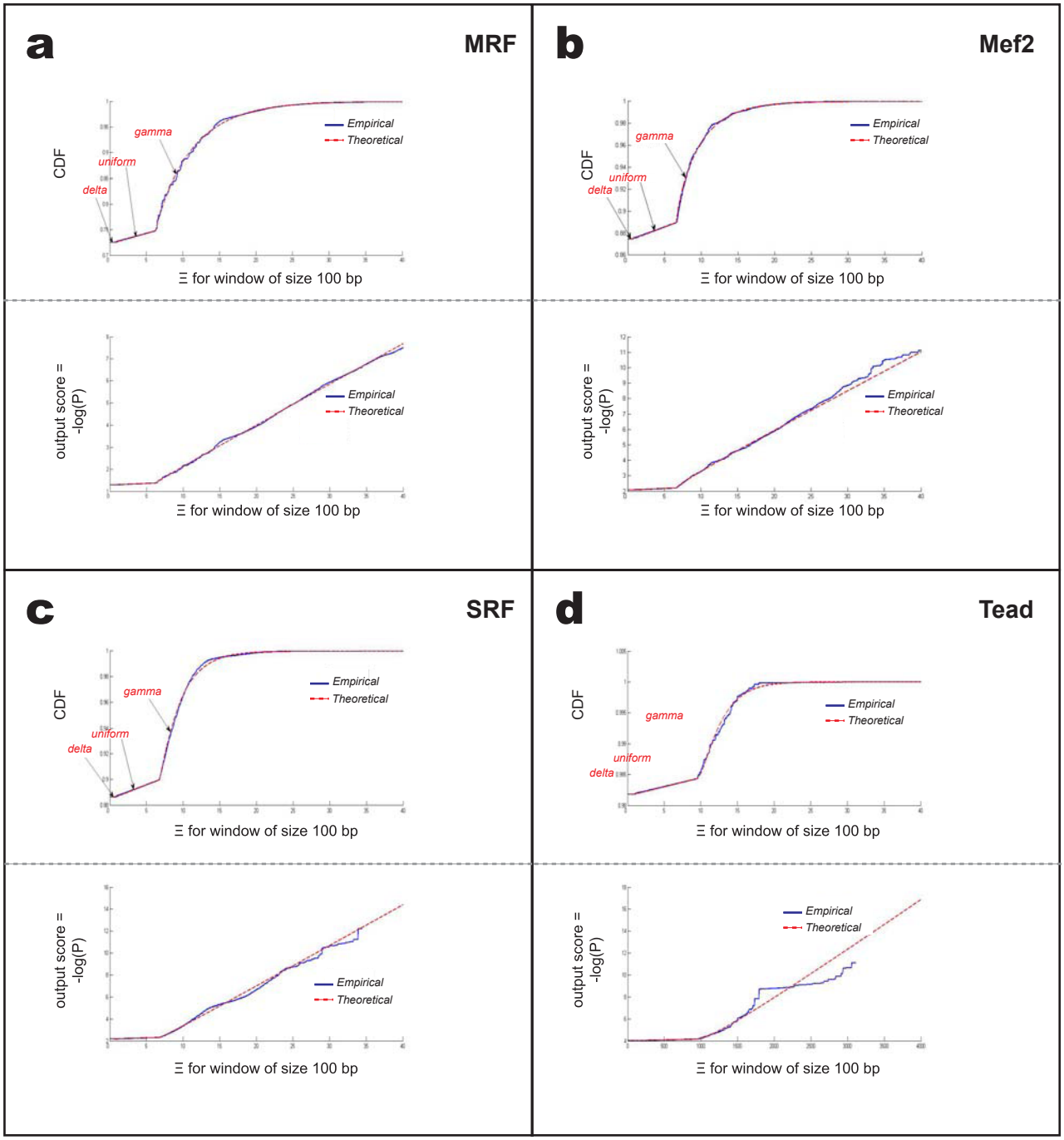

Supplementary Figure 2. Comparisons between the empirical and the fitted mixture of Delta, Uniform and Gamma distributions.
(**a**) **Upper panel** shows empirical cumulative distribution function (CDF) for MRF (in blue) and the corresponding CDF for the fitted mixture model (in red).
(**a**) **Lower panel** shows empirical output score for MRF (in blue) and the corresponding output score for the fitted mixture model (in red).
(**b**) **Upper panel** shows empirical CDF for MEF2 (in blue) and the corresponding CDF for the fitted mixture model (in red).
(**b**) **Lower panel** shows empirical output score for MEF2 (in blue) and the corresponding output score for the fitted mixture model (in red);
(**c**) **Upper panel** shows empirical CDF for SRF (in blue) and the corresponding CDF for the fitted mixture model (in red).
(**c**) **Lower panel** shows empirical output score for SRF (in blue) and the corresponding output score for the fitted mixture model (in red).
(**d**) **Upper panel** shows empirical CDF for TEAD (in blue) and the corresponding CDF for the fitted mixture model (in red).
(**d**) **Lower panel** shows empirical output score for TEAD (in blue) and the corresponding output score for the fitted mixture model (in red).

Supplementary Figure 3

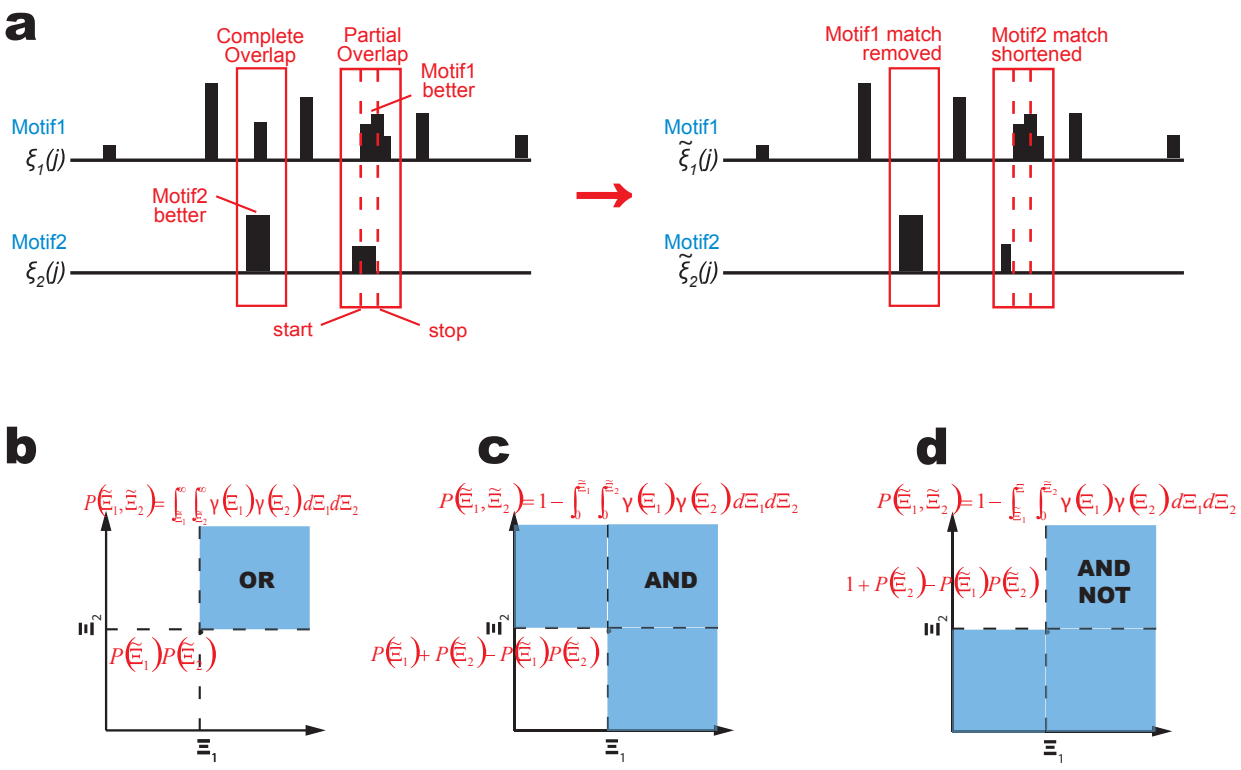

Supplementary Figure 3: Schema of scoring scheme for PhylCRM, for case of multiple motifs. (**a**) For two potentially overlapping motifs with positional scores ξ_1 and ξ_2, a de-overlapping step is performed (see text) where $\xi_i(j) = 0$ if $\xi_i(j) \neq \max\{\xi_1(j), \xi_2(j)\}$, $i \in \{1,2\}$. This step prevents motif-matches from being double-counted. (**b**) A restrictively-defined tail for the joint distribution of window scores $P(\Xi_1,\Xi_2)$. Here, a window can receive a good score (i.e., low $P(\Xi_1,\Xi_2)$) if it is enriched for either of the motifs, and thus this tail can be interpreted as an OR. (**c**) A generously-defined tail for the joint distribution of window scores $P(\Xi_1,\Xi_2)$. Here, a window must be enriched for both motifs in order to score well, and thus this tail can be interpreted as an AND. (**d**) A tail that is analogous to an "AND NOT" Boolean combination. Here, a window must be enriched for motif 1, but not enriched for motif 2 in order to score highly (i.e., low $P(\Xi_1,\Xi_2)$).

Supplementary Figure 4

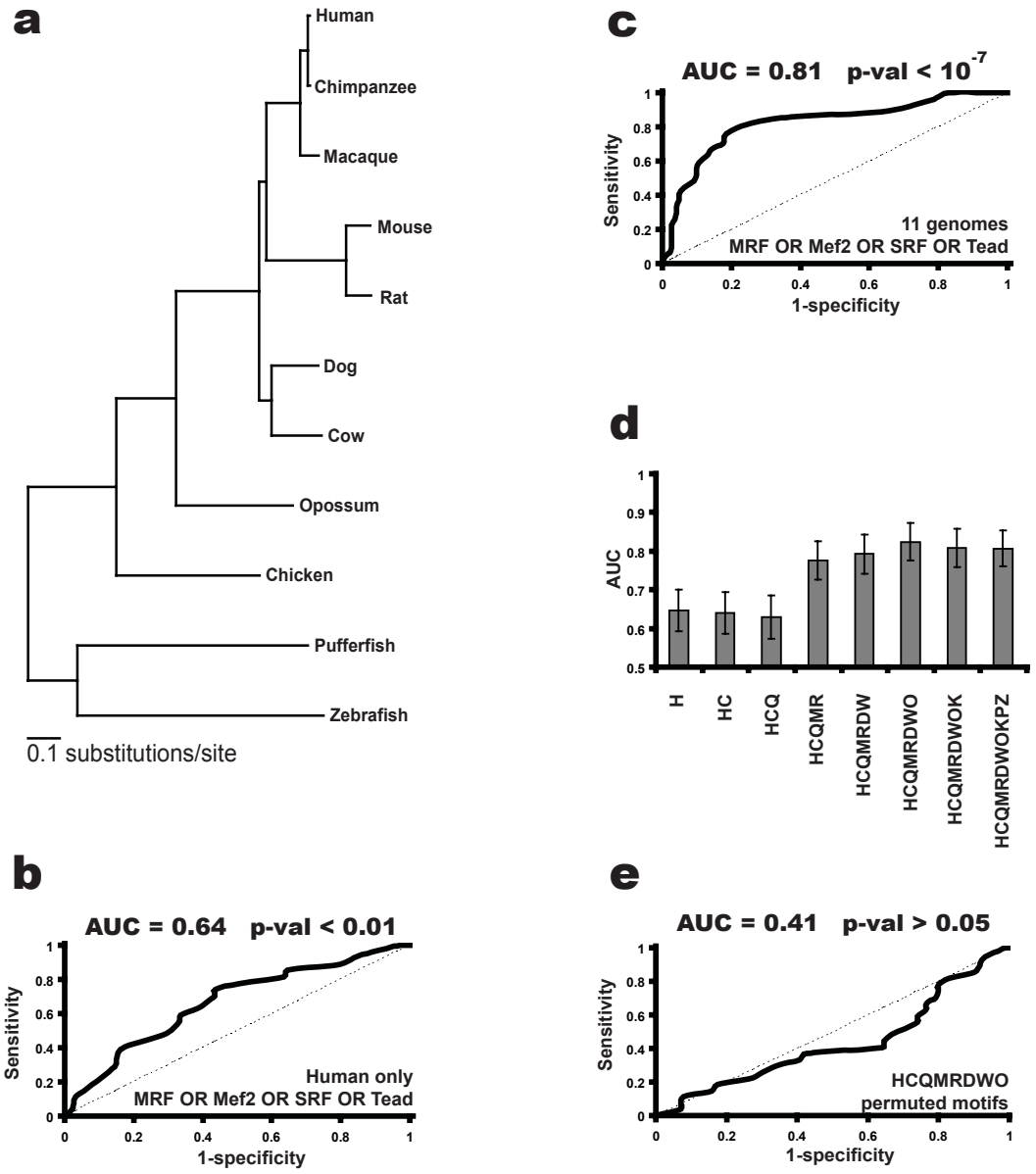

Supplementary Figure 4: Evaluation of PhylCRM and the effect of phylogeny
(**a**) Phylogenetic tree of 11 vertebrates utilized in this study. (**b**) Sensitivity and specificity of PhylCRM on a collection of 27 sequences of length 75 kb containing a CRM, as compared to a collection of length-matched sequences. Sequences were scanned with the OR combination of MRF, Mef2, SRF and Tead, and using only human sequence. (**c**) Similar to (**b**) but using all 11 vertebrate genomes. (**d**) AUC values when using progressively larger phylogenies. H=Human, C=Chimpanzee, Q=Macaque, M=Mouse, R=Rat, D=Dog, W=Cow, O=Opposum, K=Chicken, P=Pufferfish, Z=Zebrafish. (**e**) Sensitivity and specificity when using the phylogeny HCQMRDWO and a permuted form of these motifs.

Supplementary Figure 5

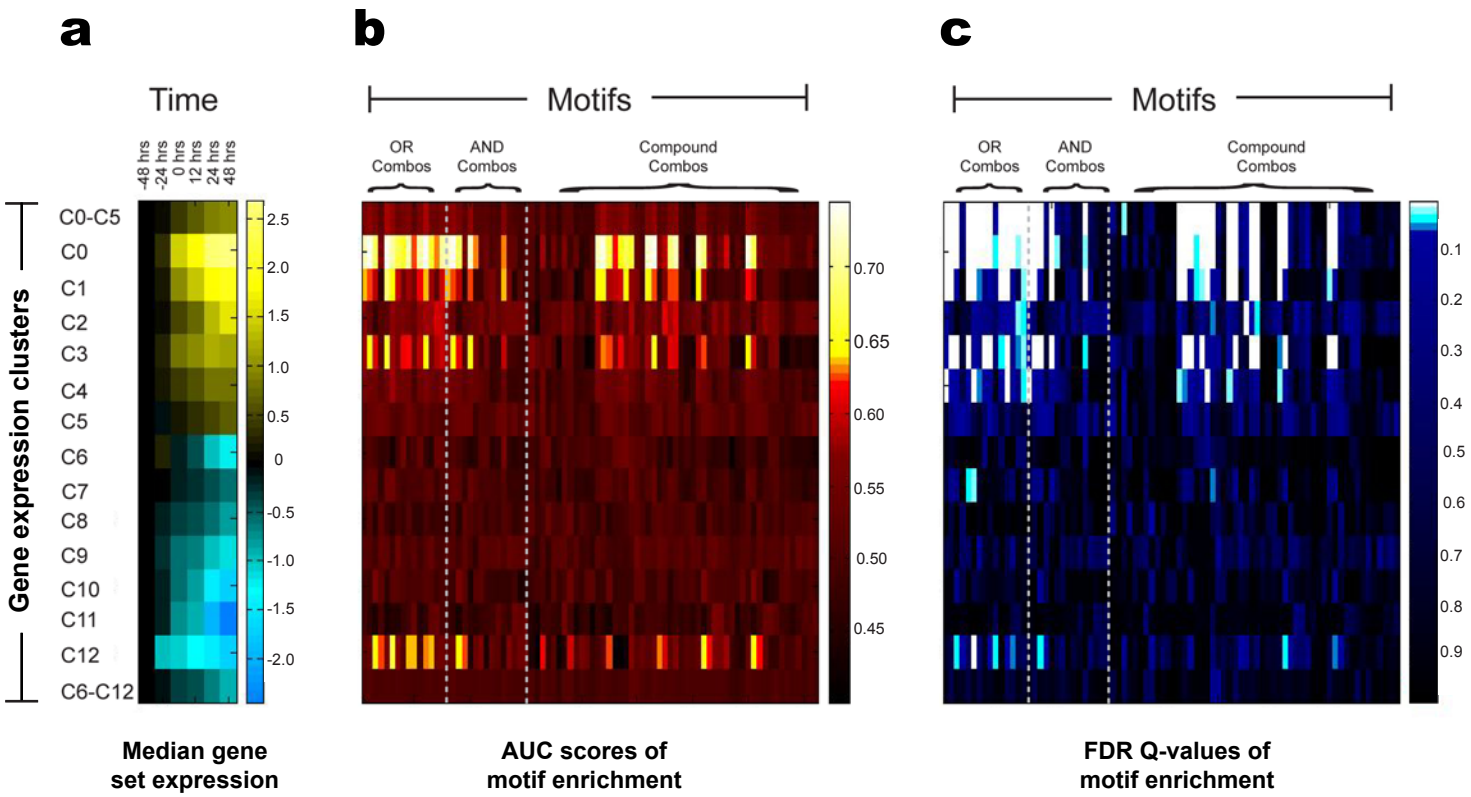

Supplementary Figure 5: Lever screen of time course of human skeletal muscle differentiation. (**a**) Median arcsinh value (relative to –48 hrs) of each considered expression cluster or combination of clusters. (**b**) AUC values for each TF binding site motif combination and gene set (GM-pair). (**c**) FDR q-value for each GM pair computed by Lever using a permutation test.

Supplementary Figure 6

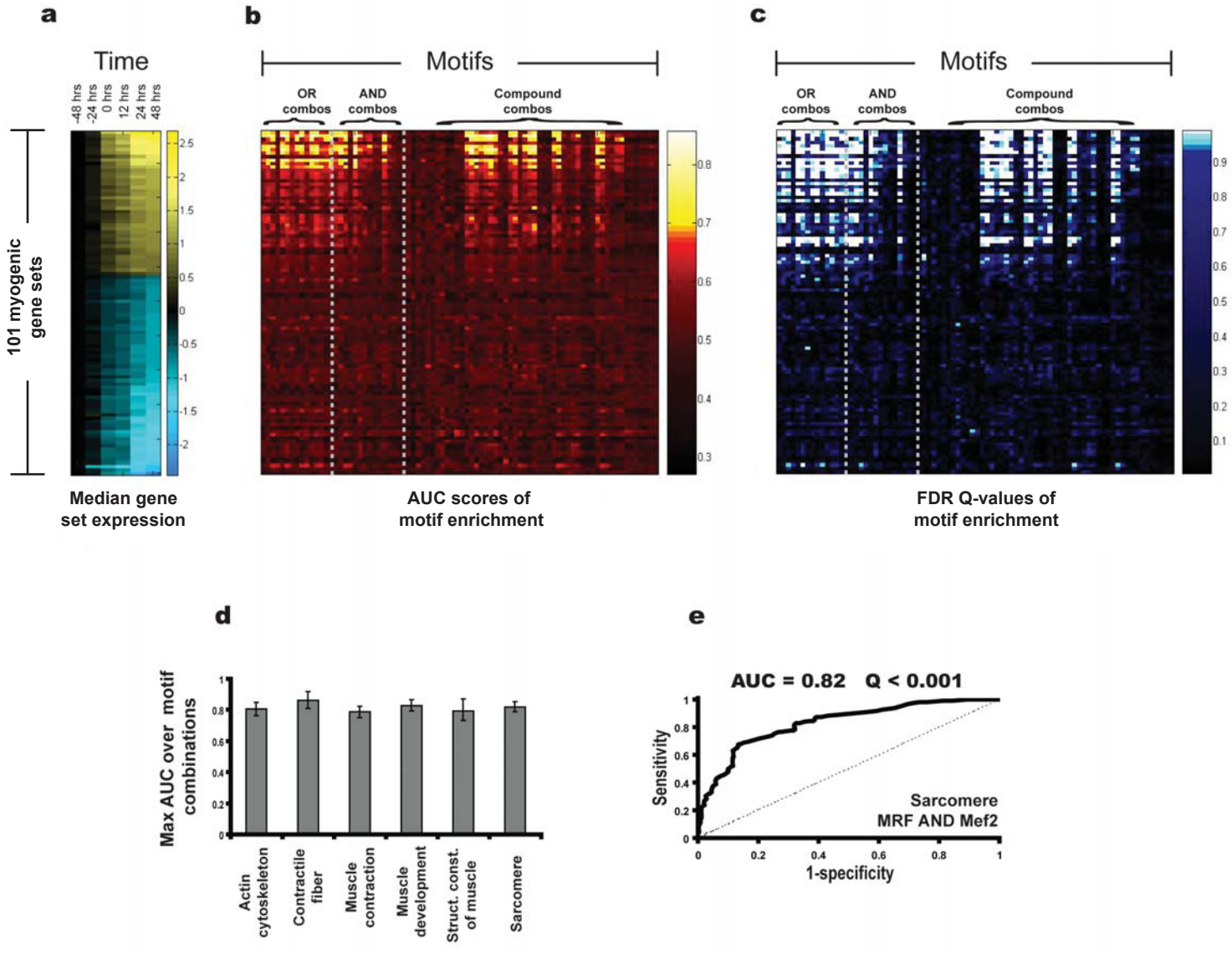

Supplementary Figure 6: Lever screen of 101 myogenic gene sets using Boolean combinations of MRF/Mef2/SRF/Tead myogenic motifs.
(**a**) Median signal intensity throughout the time-course of gene expression profiling for each of the 101 gene sets derived from GO categories and expression clusters.
(**b**) AUC values for each GM-pair using 75-kb regions surrounding transcription start.
(**c**) FDR Q-value for each GM- pair.
(**d**) Bar graphs indicating the maximum AUCs across all considered Boolean combinations of the motifs for these gene sets
(**e**) Sensitivity vs.specificity curves for the MRF AND MEF2 combination on the sarcomere gene set.

Supplementary Figure 7

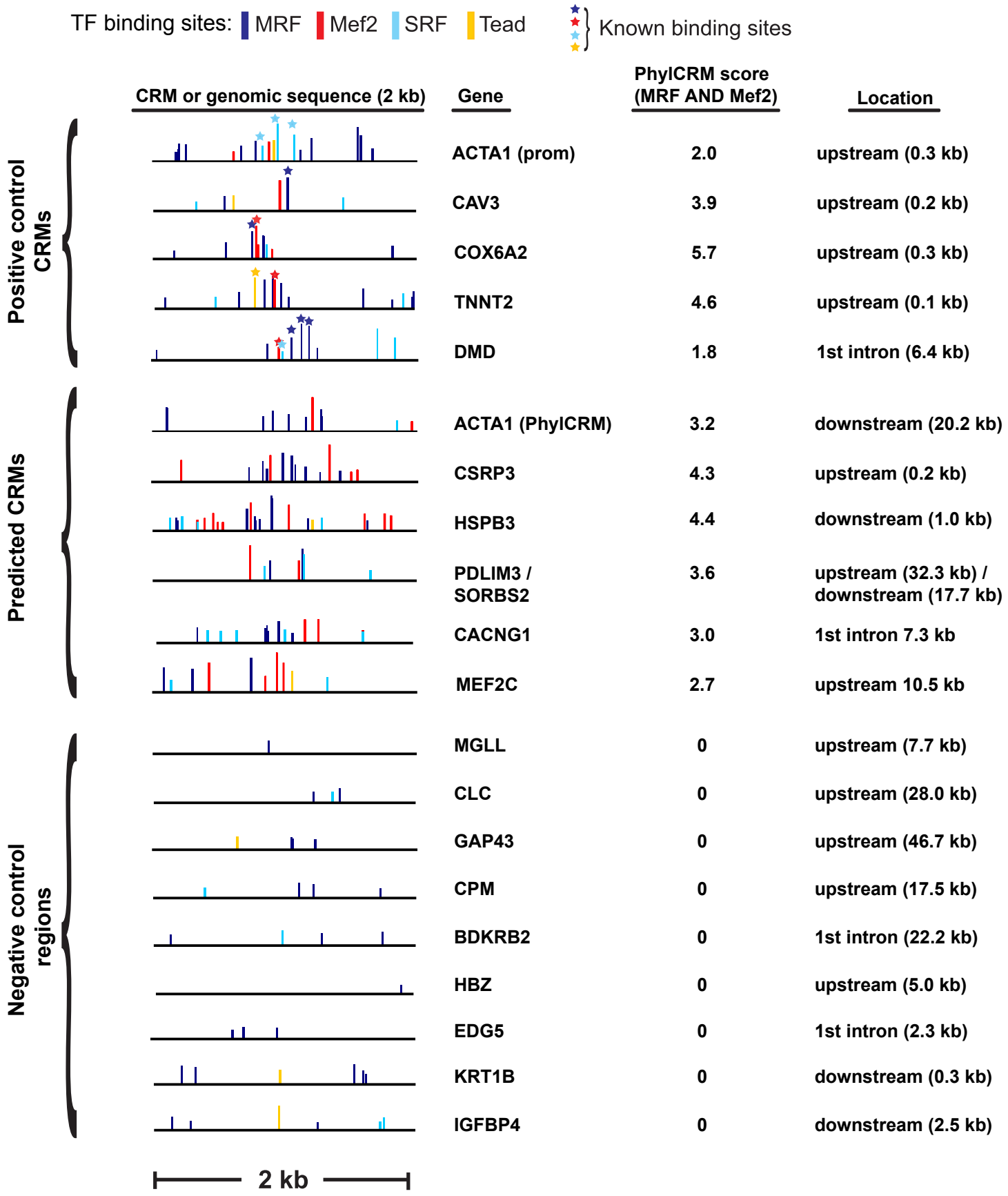

Supplementary Figure 7. Schematic display of comptutationally predicted human CRMs and control sequences. Previously described CRMs were used as positive controls in ChIP assays; see Supplementary Methods for full descriptions of the known and candidate CRMs. Negative control regions used in ChIP assays were chosen to not contain matches to the MRF AND Mef2 motif combinations, and to also not be enriched for the other binding sites under consideration (MRF = blue, Mef2 = red, SRF = cyan, Tead = gold), where stars indicate known binding sites. The PhylCRM score of the degree of enrichment for MRF AND Mef2 is shown (see Supplementary Methods for a description of the PhylCRM scoring scheme). Locations of sequence windows in relation to transcriptional start (if upstream or intronic) or stop (if downstream) are shown. We note that the region labeled "PDLIM3/SORBS2" was located between the PDLIM and SORBS2 genes. Also, we note that "ACTA 1 (prom)" refers to a previously known CRM located at transcriptional start, while "ACTA 1 (PhylCRM)" refers to a novel PhylCRM prediction.

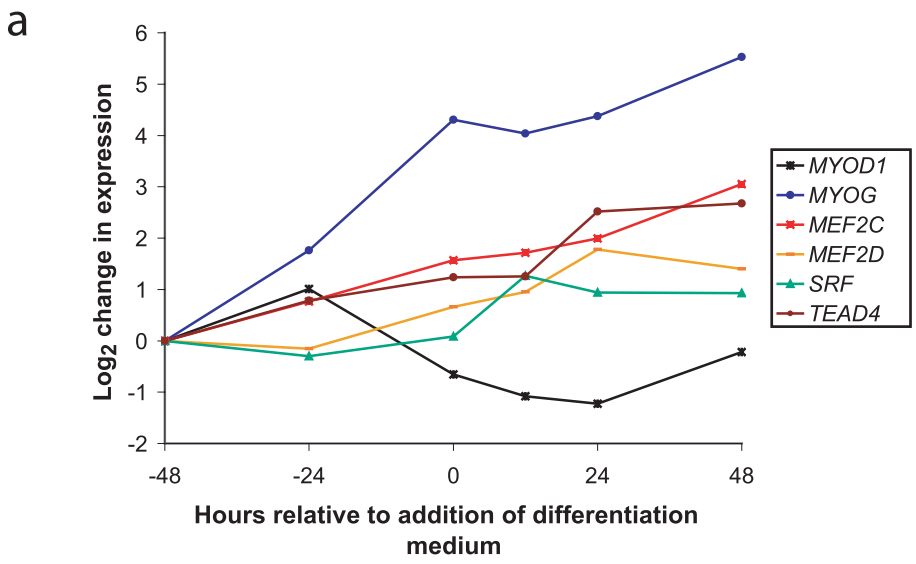

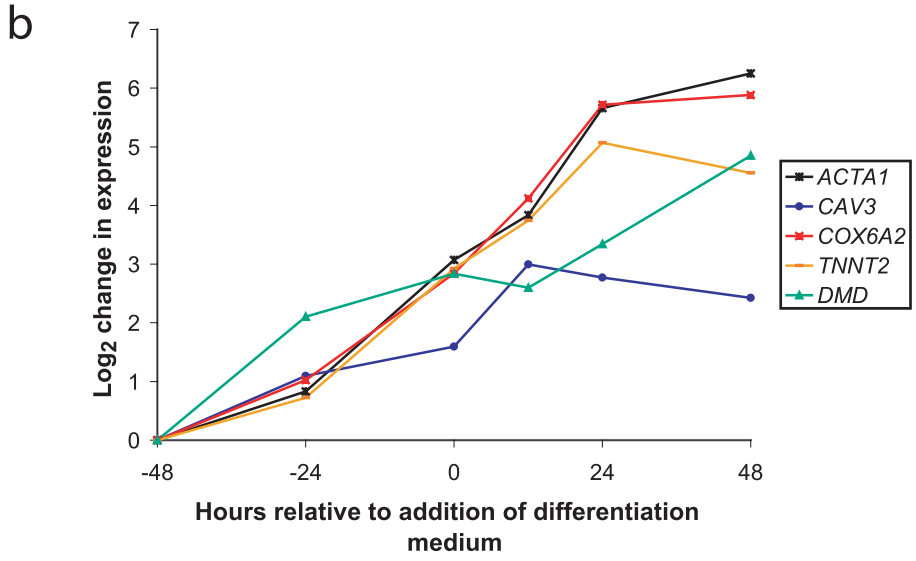

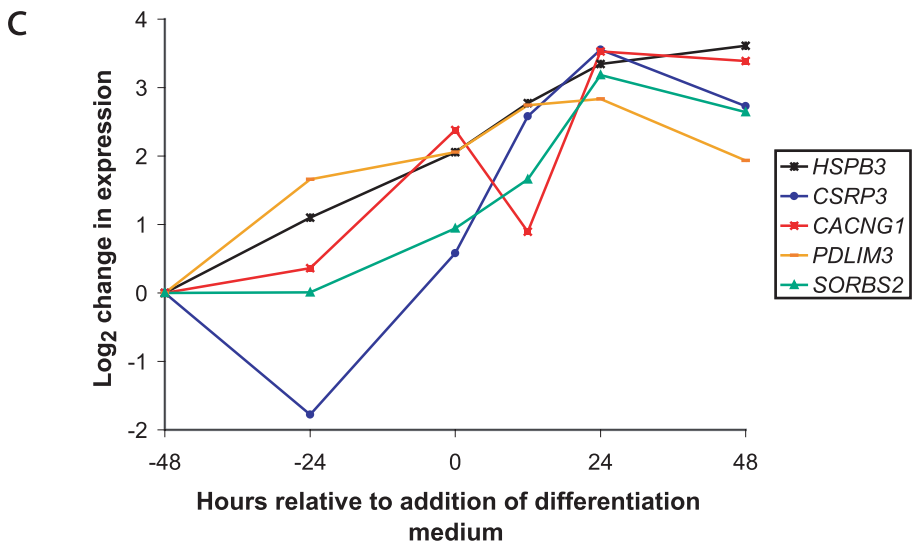

Supplementary Figure 8 - Verification of transcription upregulation during muscle differentiation. Total RNA from primary human cells was extracted and processed as described in **Supplementary Methods.** The following sets of transcripts were normalized to *RPS18*: (**a**) muscle transcription factors, (**b**) genes regulated by positive control CRMs, (**c**) genes associated with predicted CRMs.

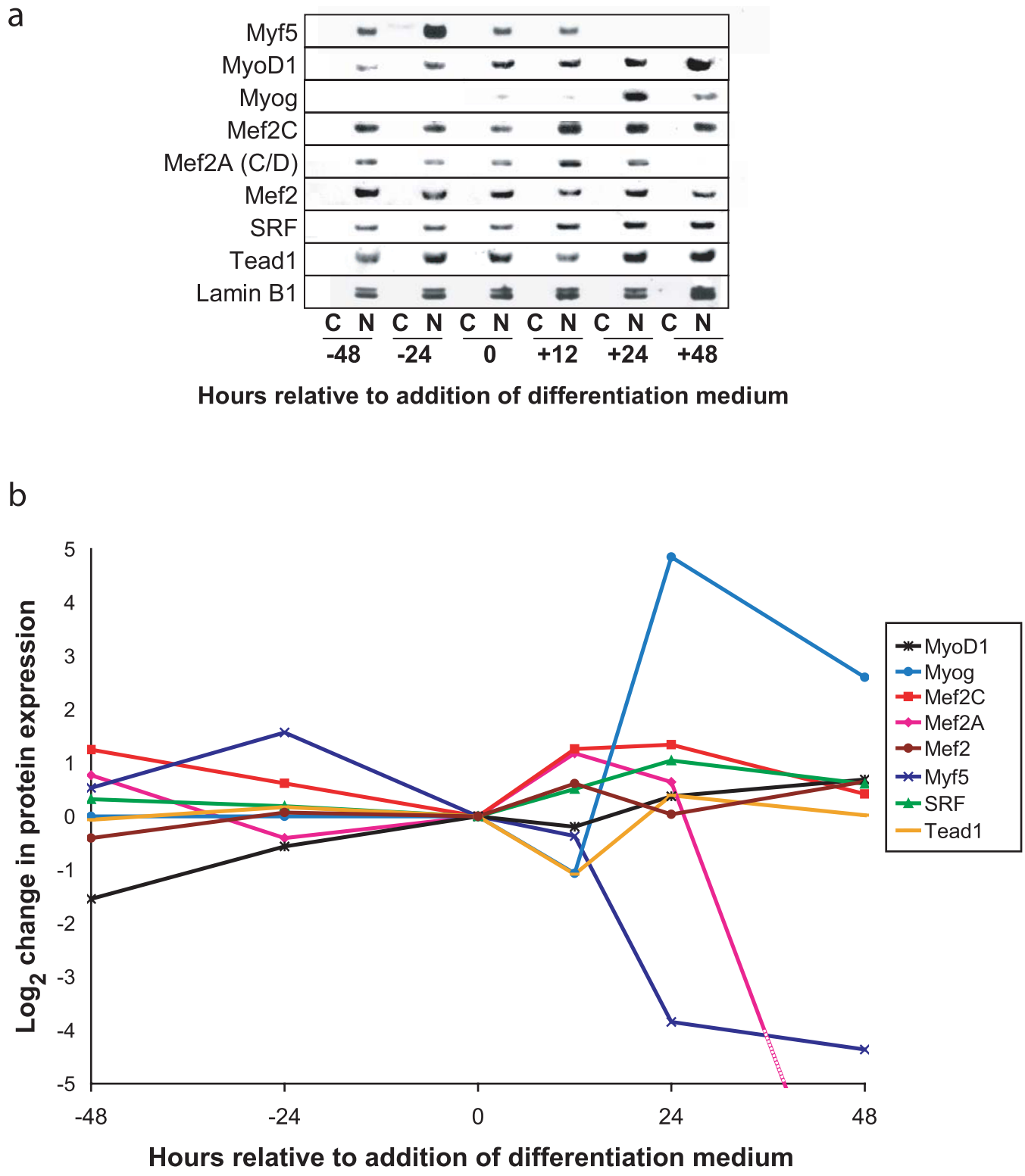

Supplementary Figure 9: Western blots to detect levels of muscle transcription factors.
(**a**) Western blots were performed as described in **Supplementary Methods** to detect known muscle transcription factors. A lamin B1 antibody was used as normalization control. (**b**) Quantitation of bands in panel **a** was performed using lamin B1 for normalization relative to 0 hours.

Supplementary Figure 10

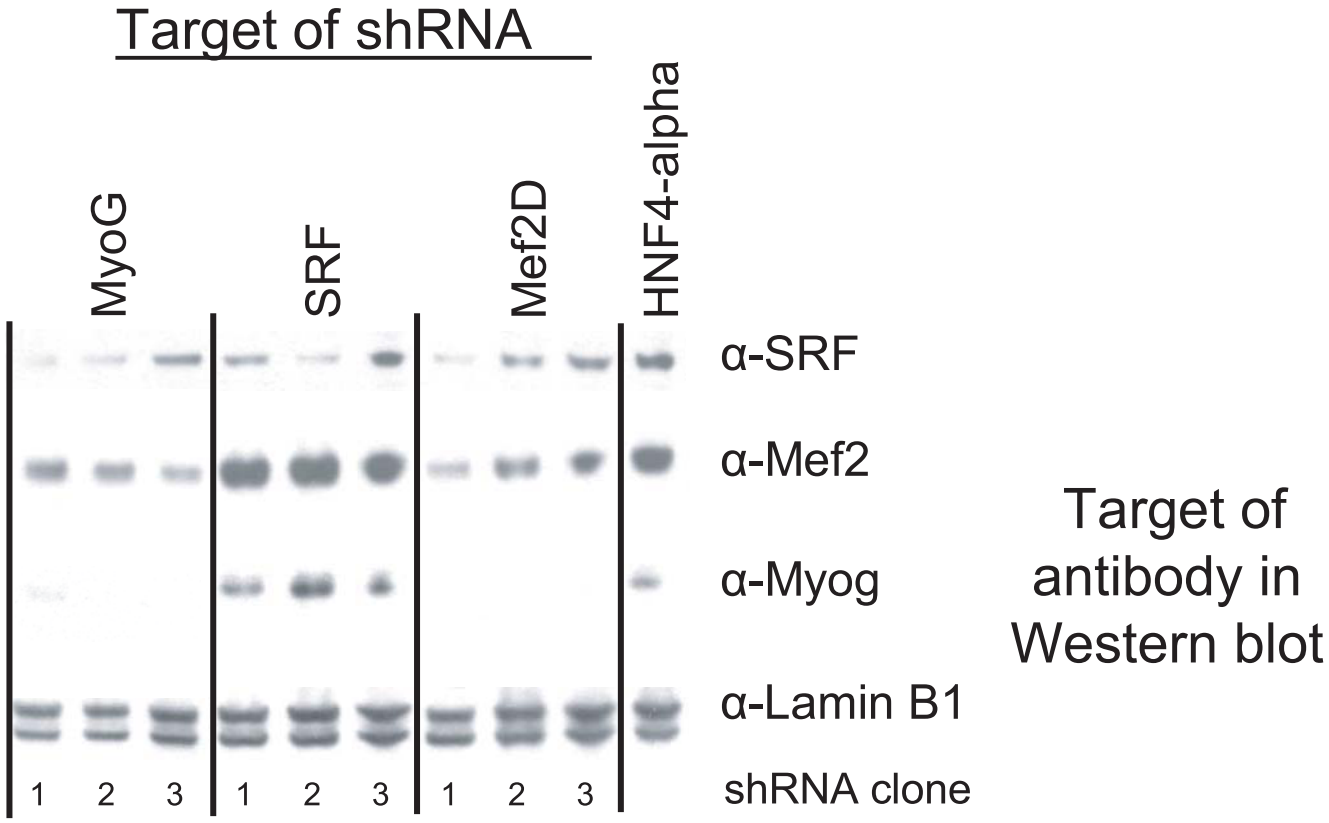

Supplementary Figure 10: Western blot analyses after RNAi knockdown. An antibody against Lamin B1 was used to control for gel loading.

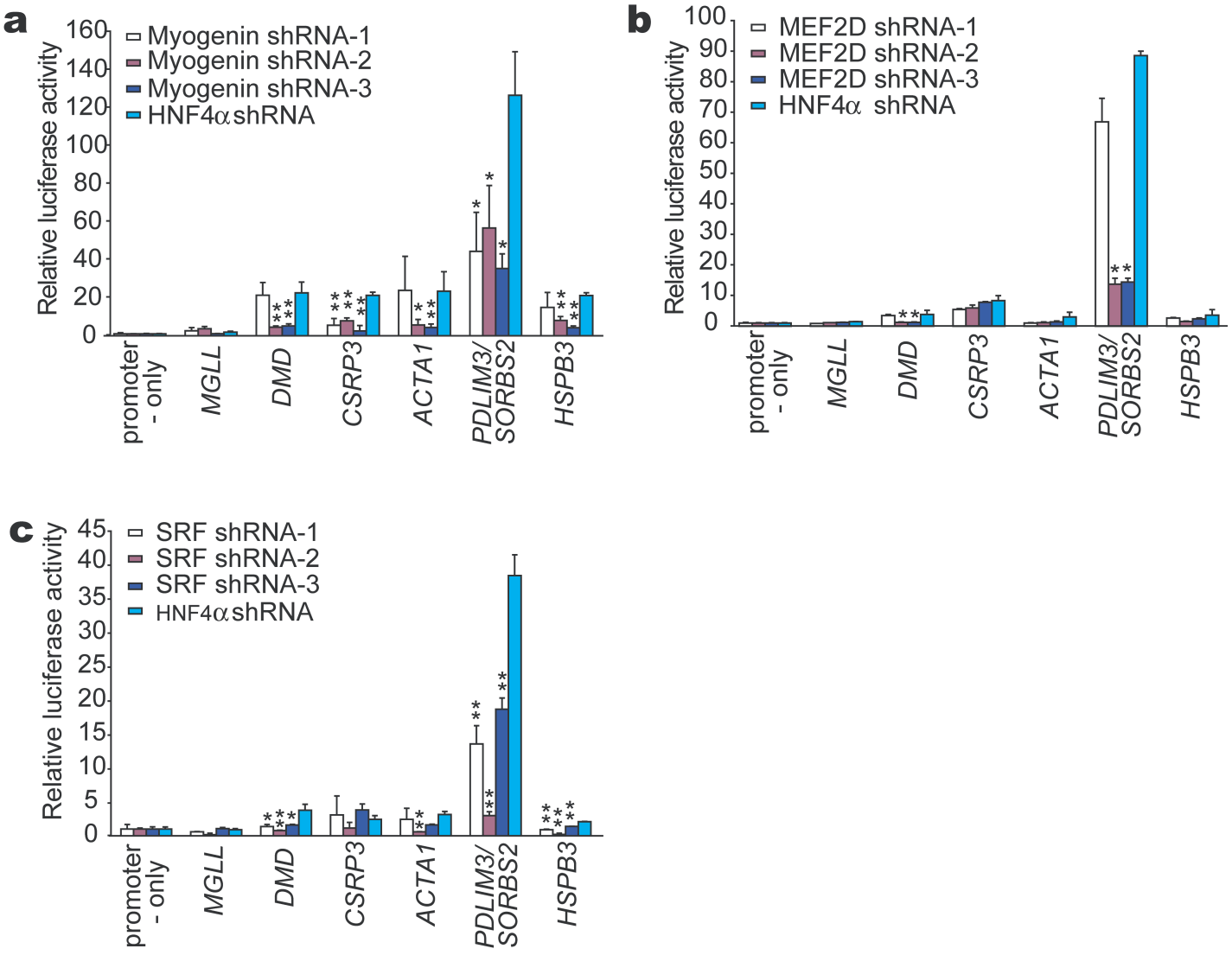

Supplementary Figure 11: Luciferase reporter assays of predicted CRMs after shRNA knockdown. (a-c) C2C12 myoblasts were infected with lentivirus encoding shRNAs directed against known myogenic TFs. In all experiments, lentivirus encoding shRNA against HNF4α, a liver-specific TF, was used as a negative control. Experimental knockdowns were directed against **(a)** Myogenin, **(b)** MEF2D, and **(c)** SRF. In **(a-c)**, * indicates $P < 0.05$, while vertically stacked double asterisks indicate $P < 0.005$, comparing luciferase activity in the experimental knockdown versus the HNF4α knockdown.

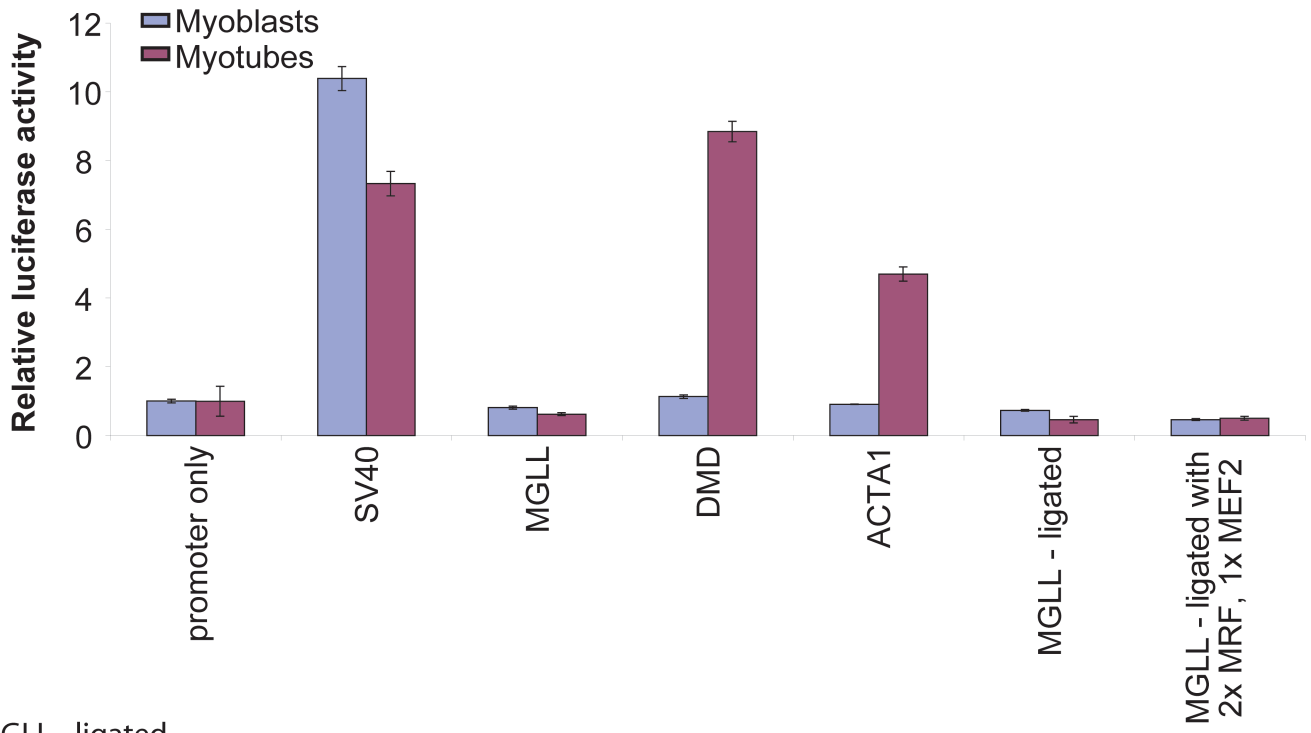

>MGLL - ligated
catgatgcattcacctcccaccaggccccaccttcaacattggggattacagttcaaaatgaggtttggtggggacacagatccaaaccatatca
ACTTGTAGGGGCAGAAAGACGTCACCTTTACTTGAATTGCAACCCTTACCTTTTCATCGCAGGCTGTAGGAG

>MGLL - ligated with MRF/Mef2/MRF sites
catgatgcattcacctcccaccaggccccaccttcaacattggggCAGCTGgttcaaaatgaggtttggtggggacacagatccaaaccatatca
ACTTGTAGGGGCAGAACTAAAAATAGTTTACTTGAATTGCAACCCTTACCTTTTCATCGCAGGCTGCAGCTG

Supplementary Figure 12: Luciferase reporter assays for a synthetic CRM containing binding sites for MRF AND Mef2. Putative and control CRMs were cloned either upstream (BglII) or downstream (BamHI) of the luciferase reporter gene of the pGL3-Promoter vector (Promega) in order to reflect the genomic location of the CRM. As positive controls, we used an SV40 enhancer, one of the five previously known muscle CRMs used in our ChIPs (DMD), and a novel CRM that we verified previously CRM (ACTA1, Fig 6). As a negative control we used a human noncoding genomic region (MGLL) not enriched for matches to the four known myogenic motifs. As described in Supplementary Methods, we created variants of a shorter 167-bp MGLL negative control region by ligating segments of the original MGLL region (MGLL - ligated) or by ligating segments of the MGLL region that have two consensus MRF sites (shown in blue) and one consensus Mef2 site (shown in red). C2C12 cells were cultured in 6-well plates (9.4 cm^2 per well) 24 hours prior to transfection at 3 x 10^4 cells per well for myoblasts or 1.5 x 10^5 cells per well for myotubes. The cells were then cotransfected in triplicate with 1 µg of experimental vector (pGL3-P with or without inserted region) and 50 ng of the normalization vector (pRL-TK) using FuGENE 6 transfection reagent (Roche) according to the manufacturer's protocols. Cell extracts were obtained from an aliquot of the proliferating myoblasts 24 hours after transfection. The remaining cell cultures were then switched to differentiation medium, and cell extracts were obtained after 96 hours in differentiation medium. Luciferase reporter assays were performed using the Dual-Luciferase® Reporter Assay System (Promega) according to the manufacturer's protocols. Firefly luminescence intensities were normalized by the luminescence intensities of the internal Renilla control.

Supplementary Table 1: Gene names and expression clusters

Cluster	Genbank/Refseq ID	Symbol	Expression fold changles (arcsinh units relative to -48 hrs) NEG48	NEG24	ZERO	POS12	POS24	POS48
0	AB014513	LDB3	0	0.13	1.68	2.22	3.17	3.34
0	AB032993	GRIPAP1	0	0.46	1.42	1.46	2.19	2.51
0	AF086254	MYOM3	0	0.49	1.66	1.89	3.07	2.63
0	AF255910	JAM2	0	-0.07	0.74	1.39	2.84	3.35
0	AK022290	SMYD1	0	0.32	1.72	2.23	2.63	1.72
0	AK022746	FLJ12684	0	1.3	1.83	1.61	2.18	2.73
0	AK023391	FBXO32	0	0.5	1.54	2.44	2.73	2.87
0	AK025273	EGLN3	0	0.05	1.68	1.61	2.6	2.74
0	AL133109	ARPP-21	0	0.25	1.04	1.63	2.25	2.54
0	BU629989	Cep152	0	0.29	1.5	1.81	2.24	2.36
0	J05200	RYR1	0	0.27	1.3	1.67	2.6	2.56
0	L09102	L09102	0	0.41	2.26	2.07	2.64	2.64
0	M20642	MYL1	0	0.55	1.69	2.53	3.22	3.8
0	NM_000041	APOE	0	0	1.17	0.96	2.59	3.21
0	NM_000129	F13A1	0	0.52	1.44	1.3	2.26	2.49
0	NM_000727	CACNG1	0	0.18	1.45	1.71	2.72	2.78
0	NM_000954	PTGDS	0	0.28	1.81	2.38	2.75	2.9
0	NM_001103	ACTN2	0	0.48	1.38	1.83	2.74	2.64
0	NM_001232	CASQ2	0	0.77	1.59	2.16	3.28	3.87
0	NM_001541	HSPB2	0	0.15	1.14	1.54	2.41	2.57
0	NM_001733	C1R	0	0.37	1.33	1.5	2.17	2.61
0	NM_001976	ENO3	0	0.6	1.66	1.91	2.67	2.6
0	NM_002152	HRC	0	0.13	1.33	1.73	2.6	2.76
0	NM_002476	MYL4	0	0.62	1.96	2.3	3.41	3.84
0	NM_003063	SLN	0	0.16	0.77	1.18	2.29	3.52
0	NM_003280	TNNC1	0	0.35	1.59	2.32	3.2	3.12
0	NM_003281	TNNI1	0	0.7	2.08	2.2	2.98	3.31
0	NM_003282	TNNI2	0	0.38	1.85	1.94	2.9	2.86
0	NM_003283	TNNT1	0	0.54	1.32	1.51	2.2	2.51
0	NM_003881	WISP2	0	0.4	1.25	2.4	2.3	2.04
0	NM_004010	DMD	0	0.82	1.2	1.57	2.22	2.71
0	NM_004076	CRYBB3	0	0.12	0.6	1.5	2.06	3.26
0	NM_004102	FABP3	0	0.28	0.89	1.75	2.78	2.86
0	NM_005205	COX6A2	0	0.28	1.4	1.9	2.87	2.97
0	NM_005359	SMAD4	0	0.3	1.17	1.68	2.35	2.72
0	NM_006308	HSPB3	0	0.28	1.54	1.76	2.29	2.47
0	NM_006705	GADD45G	0	0.85	2.38	2.45	2.22	2.05
0	NM_006757	TNNT3	0	0.41	1.61	2	3.15	3.53
0	NM_013292	MYLPF	0	-0.99	1	1.85	2.93	2.32
0	NM_016243	NQO3A2	0	0.69	1.82	2.02	2.33	2.21
0	NM_016300	ARPP-21	0	0.35	1.86	1.94	2.7	2.85
0	NM_016599	MYOZ2	0	-0.56	0.93	1.29	2.52	2.91
0	X98114	TTN	0	0.14	0.98	1.95	2.52	2.33
1	AB023217	MYH15	0	-0.33	1.03	1.66	2.04	1.59
1	AB033088	SYNE1	0	-0.04	1.2	1.42	1.71	1.91
1	AB037751	ALPK3	0	0.62	1.29	1.62	1.63	1.68
1	AB037815	KIAA1394	0	-0.01	1.29	1.37	1.78	1.91
1	AF086028	ERBB3	0	0.27	1.58	1.91	2.28	1.64

1	AF111783	MYH4	0	0.12	1.42	1.68	2.09	2.24
1	AF131839	OLFM2	0	0	0.94	1.44	1.73	1.29
1	AF311287	CARD9	0	0.13	0.91	1.17	2.04	2.48
1	AJ010482	SYNPO2	0	0.27	1.33	1.72	2.11	2.16
1	AJ227899	GRASP	0	-0.25	0.84	1.2	1.93	2.23
1	AK022567	FLJ12505	0	0	1.22	1.05	1.73	1.48
1	AK022983	SYNPO2L	0	0.6	1.45	1.66	1.77	1.41
1	AK023172	C2orf23	0	-0.23	0.86	1.47	2.42	2.5
1	AK023481	POSTN	0	-0.16	0.25	1.1	2.05	2.41
1	AK023521	FER1L4	0	0.14	0.82	0.88	1.64	2.09
1	AK024578	CCDC3	0	0.06	1.15	1.3	1.68	1.89
1	AK025783	SH3MD1	0	0.72	1.27	1.19	1.59	1.96
1	AK027224	IQCG	0	0.32	1.3	1.35	1.77	2
1	AL359586	DKFZp762	0	-0.23	0.39	1.6	1.72	1.91
1	AL389956	FBXO32	0	0.37	0.99	2.32	2.31	1.95
1	AL833529	C10orf72	0	-0.02	1.13	1.21	1.65	1.59
1	L09080	IGHV@	0	0.04	1.19	1.53	2.28	1.75
1	M64108	COL14A1	0	0.21	0.44	1.33	2	1.97
1	NM_000256	MYBPC3	0	0	0.94	1.16	1.51	1.62
1	NM_000431	MVK	0	0.28	0.53	1.46	1.68	1.63
1	NM_000432	MYL2	0	0.37	0.91	1.33	1.7	1.84
1	NM_000900	MGP	0	-0.14	0.58	1.52	2.26	2.25
1	NM_001085	SERPINA3	0	0.31	1.53	1.38	2.07	1.89
1	NM_001234	CAV3	0	0.26	1.09	1.66	1.56	1.47
1	NM_001647	APOD	0	0.37	1.09	0.91	1.37	1.82
1	NM_001734	C1S	0	-0.2	0.76	1.13	1.86	2.13
1	NM_001845	COL4A1	0	0.38	0.69	1.02	1.72	2.25
1	NM_001854	COL11A1	0	0.3	0.97	1.39	1.52	2.11
1	NM_001885	CRYAB	0	0.33	0.81	1	1.98	2.26
1	NM_002397	MEF2C	0	0.44	1.24	1.56	2.08	2.1
1	NM_002480	PPP1R12A	0	-0.08	0.82	0.99	1.75	2.22
1	NM_002510	GPNMB	0	0.33	0.55	1.47	1.73	2.14
1	NM_002889	RARRES2	0	0.14	1.02	1.54	1.59	1.71
1	NM_003279	TNNC2	0	0.09	0.74	1.19	2.31	2.64
1	NM_003764	STX11	0	0.11	1.06	1.12	1.9	2.1
1	NM_003826	NAPG	0	0.13	1.01	1.17	1.78	1.98
1	NM_004265	FADS2	0	-0.09	0.57	1.59	2.29	2.7
1	NM_004274	AKAP6	0	0.22	0.93	0.91	1.78	1.9
1	NM_004533	MYBPC2	0	0.38	0.92	1.04	1.73	1.84
1	NM_004574	38599	0	0.22	0.79	0.65	1.9	2.41
1	NM_004734	DCAMKL1	0	0.19	1.08	1.51	1.82	1.39
1	NM_006063	KBTBD10	0	0.17	1.27	1.62	1.71	1.51
1	NM_006574	CSPG5	0	0.19	0.96	1.83	2.19	2.19
1	NM_007193	ANXA10	0	0.93	1.17	0.99	1.96	1.67
1	NM_012219	MRAS	0	0.19	1.11	1.5	1.65	1.56
1	NM_012237	SIRT2	0	0.12	1.49	1.38	1.8	1.64
1	NM_014332	SMPX	0	0.55	0.88	1.04	2.2	1.84
1	NM_015719	COL5A3	0	0.05	1.17	1.47	2.1	1.85
1	NM_017431	PRKAG3	0	0.3	1.37	1.4	1.71	1.36
1	NM_017644	DRE1	0	0.31	0.61	1.29	1.67	1.63
1	NM_017766	FLJ20321	0	0.04	1.27	1.46	1.91	1.54
1	NM_018661	DEFB103A	0	1.1	1.44	1.82	1.82	2.2

1	NM_019841	TRPV5	0	-0.24	0.69	1.56	1.5	2.15
1	U17327	NOS1	0	0.2	1.08	1.16	2.02	2.45
1	X98115	TTN	0	0.48	1.34	1.79	2.25	1.96
1	Y11710	COL14A1	0	0.21	0.71	1.31	2.02	2.12
1	Y18213	GNAO1	0	0.14	0.83	0.92	1.56	2.14
2	AB007950	TMCC2	0	0.09	0.53	0.89	1.17	1.36
2	AB014557	KIAA0657	0	0.15	0.51	0.91	1.85	2.04
2	AB023154	DTX4	0	-0.12	0.19	0.27	1.1	1.45
2	AB023197	KIAA0980	0	0.24	0.41	0.24	0.94	1.51
2	AB040930	LRRN1	0	0.1	0.35	0.58	1.57	1.63
2	AB046776	OBSCN	0	-0.28	0.53	0.63	1.17	1.21
2	AB048791	HES4	0	-0.28	0.51	0.75	1.49	1.46
2	AF000381	FOLR1	0	-0.19	0.41	0.59	1.17	1.37
2	AF010236	SGCD	0	-0.05	0.72	0.54	1.35	1.47
2	AF114264	NEXN	0	0.02	0.43	0.8	1.26	1.4
2	AF205632	ZFP106	0	0.3	0.54	0.74	1.8	2.23
2	AF217989	GDPD5	0	-0.07	0.43	0.87	1.18	1.27
2	AF218006	EFHD1	0	-0.1	0.22	0.6	1.35	1.88
2	AJ278018	CLSTN2	0	0.08	0.47	0.68	1.39	2.37
2	AK000757	SORT1	0	-0.11	0.63	1.1	1.47	1.75
2	AK022059	SNAG1	0	-0.11	0.26	1.24	1.59	1.48
2	AK022383	ARGBP2	0	0.25	0.31	0.84	1.35	1.21
2	AK022878	ABHD4	0	0.37	0.26	1.32	1.33	1.57
2	AK023760	RAPGEF1	0	0.02	0.7	0.78	1.11	1.52
2	AK025950	FHOD3	0	0.14	0.54	0.69	1.58	1.38
2	AK026945	TRIB3	0	-0.06	0.13	0.34	1.21	1.74
2	L27560	IGFBP5	0	0.15	0.6	0.84	1.02	1.69
2	M92642	COL16A1	0	0.18	0.3	0.66	1.28	1.94
2	NM_000063	C2	0	0.39	0.51	0.87	1.31	1.63
2	NM_000064	C3	0	-0.05	0.67	1.07	1.49	1.6
2	NM_000376	VDR	0	0.03	0.16	0.48	1.18	1.55
2	NM_000385	AQP1	0	0.15	0.26	0.38	1.42	2.7
2	NM_000553	WRN	0	-0.1	0.11	0.22	1.22	1.86
2	NM_000723	CACNB1	0	0.2	0.51	0.92	1.63	1.69
2	NM_000854	GSTT2	0	-0.08	0.61	0.52	1.13	1.43
2	NM_000950	PRRG1	0	-0.46	0.72	0.62	1.41	1.46
2	NM_001148	ANK2	0	0.31	0.78	0.56	1.33	1.63
2	NM_001360	DHCR7	0	0.19	0.47	1.17	1.69	1.65
2	NM_001460	FMO2	0	0.14	0.18	0.46	0.96	1.61
2	NM_001553	IGFBP7	0	0.26	0.59	0.51	1.16	1.88
2	NM_001567	INPPL1	0	-0.2	0.61	0.65	1.17	1.24
2	NM_001825	CKMT2	0	0.07	0.29	0.28	1.17	1.56
2	NM_001909	CTSD	0	0.5	0.8	0.81	1.13	1.68
2	NM_001939	DRP2	0	0.24	0.67	0.66	1.34	1.84
2	NM_002004	FDPS	0	-0.2	-0.13	0.56	1.32	1.7
2	NM_002461	MVD	0	-0.13	0.29	0.79	1.53	1.83
2	NM_002475	MLC1SA	0	0.25	1.1	0.07	1.99	1.9
2	NM_002579	PALM	0	0.49	0.48	0.98	1.04	2.1
2	NM_003239	TGFB3	0	0	0.58	0.67	1.31	1.51
2	NM_003355	UCP2	0	0.11	0.75	0.65	1.83	2.11
2	NM_003508	FZD9	0	0.14	0.69	0.54	1.4	1.31
2	NM_003603	ARGBP2	0	0.32	0.49	0.75	1.22	1.57

2	NM_003657	BCAS1	0	-0.03	0.33	0.25	1.26	2.07
2	NM_003759	SLC4A4	0	-0.28	0.35	0.71	1.3	1.66
2	NM_003790	TNFRSF25	0	-0.06	0.71	0.87	1.53	1.98
2	NM_004210	NEURL	0	-0.09	0.24	0.71	1.32	1.19
2	NM_004221	IL32	0	0.04	0.5	0.2	0.47	2.08
2	NM_004390	CTSH	0	0.1	0.38	0.87	1.4	1.63
2	NM_004460	FAP	0	0.01	0.35	0.61	1.05	1.5
2	NM_004615	TSPAN7	0	0.28	0.55	0.72	0.85	2.06
2	NM_004673	ANGPTL1	0	-0.01	0.53	0.79	1.35	1.47
2	NM_005446	P2RXL1	0	-0.87	0.38	0.84	1.51	1.34
2	NM_006475	POSTN	0	-0.06	0.08	0.99	1.69	2.36
2	NM_006789	APOBEC2	0	0.01	0.63	0.79	1.67	1.63
2	NM_007069	HRASLS3	0	0.25	0.67	1.06	1.45	1.76
2	NM_007098	CLTCL1	0	0.33	0.71	0.82	1.02	1.9
2	NM_012211	ITGA11	0	-0.22	0.26	0.69	1.05	1.7
2	NM_012326	MAPRE3	0	-0.02	0.59	0.64	1.73	1.92
2	NM_013239	PPP2R3B	0	0.25	0.6	0.27	1.65	1.92
2	NM_013402	FADS1	0	0.19	0.5	0.96	1.06	1.53
2	NM_014840	ARK5	0	-0.29	0.89	0.93	1.42	1.45
2	NM_016730	FOLR1	0	0.09	0.71	0.79	1.52	1.77
2	NM_017980	LIMS2	0	-0.14	0.31	0.86	1.33	1.7
2	NM_019598	KLK12	0	0.05	0.5	0.17	0.68	1.97
2	NM_020433	JPH2	0	0.11	0.44	0.88	1.58	1.35
2	NM_022173	TIA1	0	0.13	0.61	0.83	1.56	1.92
3	AB002360	MCF2L	0	0.15	0.7	1.13	0.8	0.94
3	AB002384	C6orf32	0	0.23	1.33	1.6	1.71	0.85
3	AB007972	PPP1R12B	0	0.31	0.7	0.79	0.95	1
3	AB011174	PACS2	0	0.1	0.86	1.04	1.32	1.12
3	AB014526	MFAP3L	0	0	0.72	0.93	1.11	0.81
3	AB014533	COBL	0	0.55	1.29	1.06	1.07	1.22
3	AB018264	TSPYL4	0	0.07	0.96	1.04	1.29	1.31
3	AB020704	PPFIA4	0	0.31	0.94	1.17	1.22	1.08
3	AB037718	APEG1	0	0.12	0.76	0.98	1.06	0.65
3	AB040945	MYH7B	0	0.29	0.68	1.04	1.62	1.12
3	AB046769	KIAA1549	0	0.37	0.48	1.1	1.23	1.2
3	AF001893	TncRNA	0	-0.26	0.66	1.13	0.95	0.89
3	AF086527	AF086527	0	-0.03	0.86	1.03	1.16	1.05
3	AF143880	SORBS1	0	0.43	0.83	1.32	1.53	0.81
3	AF176705	FBXO10	0	0.45	0.99	0.84	0.89	0.84
3	AF217967	TSPAN9	0	0.02	0.73	1.01	1.35	1.3
3	AF230801	GHR	0	0.65	1.2	0.9	0.98	1.09
3	AF272036	RRAGD	0	0.27	0.39	0.85	1.27	0.92
3	AK001057	MGC1638	0	0.45	0.63	0.89	1.15	1.17
3	AK021598	COL5A1	0	0.52	0.62	0.95	1.23	0.98
3	AK022228	AK022228	0	0.13	0.68	0.95	0.9	0.83
3	AK022632	UAP1L1	0	0.17	0.13	1.68	1.34	1.19
3	AK022845	C9orf58	0	0.06	1.18	0.8	1.88	1.26
3	AK024449	C10orf54	0	-0.27	0.71	1.52	1.35	1.52
3	AK024472	BMF	0	0.21	0.79	1.33	1.06	0.84
3	AK025674	CORO7	0	0.3	1.05	0.79	0.96	0.77
3	AL109698	DKFZp547	0	0.16	0.92	1.13	0.97	0.85
3	AL133074	TP53INP1	0	0.2	0.63	1.14	1.16	1.27

3	BC023609	LDB3	0	0.11	0.76	1.19	1	1.34
3	D13631	ARHGEF6	0	0.28	0.97	0.92	1.28	0.93
3	NM_000022	ADA	0	0.18	0.54	1.22	1.1	0.57
3	NM_000476	AK1	0	0.16	0.76	0.97	1.44	1.33
3	NM_000592	C4B	0	-0.04	0.74	0.81	1.52	1.24
3	NM_000747	CHRNB1	0	0.1	1.01	0.89	1.23	1.16
3	NM_001311	CRIP1	0	0.09	0.93	1.48	1.79	1.08
3	NM_001462	FPRL1	0	0.58	1.03	0.84	0.92	1.18
3	NM_001730	KLF5	0	0.15	0.68	1.11	1.26	1.21
3	NM_001928	DF	0	0.06	0.85	1.22	1.31	1.19
3	NM_002206	ITGA7	0	0.12	0.79	1.12	1.09	0.69
3	NM_002615	SERPINF1	0	0.02	1.04	1.02	1.07	1.16
3	NM_002673	PLXNB1	0	-0.12	0.49	1.28	1.2	0.86
3	NM_003039	SLC2A5	0	0.67	1.33	0.95	0.88	1.02
3	NM_003748	ALDH4A1	0	0.87	0.89	0.73	1.22	1.56
3	NM_004089	TSC22D3	0	0.95	1.3	0.78	1.07	1.24
3	NM_004305	BIN1	0	0.18	0.98	0.94	1.41	1.46
3	NM_004393	DAG1	0	0.26	1.21	0.73	0.88	0.96
3	NM_004933	CDH15	0	-0.03	0.85	0.75	0.95	0.87
3	NM_005068	SIM1	0	0.29	0.98	0.85	0.85	0.7
3	NM_005195	CEBPD	0	0.24	0.96	0.71	0.79	0.79
3	NM_005312	RAPGEF1	0	0.08	0.62	1.02	1.31	1.18
3	NM_005923	MAP3K5	0	0.29	0.74	1.02	1.49	1.42
3	NM_006287	TFPI	0	0.17	0.84	1.11	1.13	1.25
3	NM_006472	TXNIP	0	0.98	1.48	1.06	1.29	1.14
3	NM_006675	TSPAN9	0	0.15	0.66	0.78	1.19	1.24
3	NM_007008	RTN4	0	0.11	0.91	0.97	1.31	1.07
3	NM_014067	LRP16	0	0.17	0.75	0.59	0.96	1.27
3	NM_014370	STK23	0	0.42	1.09	1.26	1.56	1.33
3	NM_014476	PDLIM3	0	0.22	0.85	0.9	0.97	0.72
3	NM_014585	SLC40A1	0	0.23	0.51	1.02	1.23	1.25
3	NM_015385	SORBS1	0	0.29	1.16	1.53	1.57	1.09
3	NM_015513	CRELD1	0	0.25	0.56	0.61	1.29	1.15
3	NM_016582	SLC15A3	0	0.73	0.96	0.86	1.04	1.1
3	NM_016613	DKFZp434	0	0.46	0.88	1.26	1.34	1.2
3	NM_017414	USP18	0	-0.02	0.9	0.94	1.05	0.76
3	NM_017707	DDEFL1	0	0.26	0.75	0.78	1.02	1.19
3	NM_017988	SCYL2	0	0.67	0.71	0.85	0.92	1.2
3	NM_018645	HES6	0	0.01	0.85	0.78	1.45	1.33
3	NM_018949	UTS2R	0	0.08	1.14	0.98	1.33	1.13
3	NM_020524	PBXIP1	0	0.28	1.04	1.41	1.43	1.29
3	U66044	IDS	0	0.31	0.51	1.03	0.99	1.02
3	Y11312	PIK3C2B	0	0.29	0.43	1.02	1.34	1.31
4	AB002339	N4BP3	0	-0.2	0.57	0.6	1.16	1.18
4	AB002374	KIAA0376	0	0.18	0.41	0.48	0.9	1.35
4	AB007978	KIAA0509	0	0.2	0.39	0.97	0.82	0.89
4	AB011154	KIAA0582	0	0.75	0.63	0.69	0.71	0.9
4	AB011540	LRP4	0	0.16	0.25	0.34	0.93	0.93
4	AB013452	ATP8A1	0	0.31	0.42	0.55	0.96	0.86
4	AB014567	TIP120B	0	-0.07	0.41	0.54	1.08	0.97
4	AB014607	THEA	0	0.15	0.44	0.77	0.94	1.13
4	AB023151	KIAA0934	0	0.04	0.26	0.46	0.96	0.8

4	AB023222	KIAA1005	0	0.05	0.77	0.49	0.7	0.79
4	AB029025	KIAA1102	0	-0.14	0.09	0.4	0.99	0.9
4	AB032965	CASKIN2	0	-0.08	0.46	0.58	0.81	0.69
4	AB033016	ZNF651	0	0.2	0.46	0.44	0.57	0.84
4	AB037771	USP53	0	0	0.25	0.98	0.82	0.54
4	AB046782	PCDH18	0	0.38	0.48	0.93	0.66	0.73
4	AB046822	KIAA1602	0	0.05	0.32	0.4	0.68	1.04
4	AF019225	APOL1	0	0.18	0.33	0.37	0.72	0.84
4	AF038192	TOM1L2	0	0.08	0.11	0.77	0.93	1.11
4	AF043469	NXPH4	0	0.1	0.55	0.56	1.14	0.92
4	AF052117	CLCN4	0	0.19	0.22	0.6	0.71	1.46
4	AF052152	AF052152	0	0.2	0.64	0.83	1.11	0.63
4	AF055020	SEMA6C	0	0.1	0.41	0.72	0.73	0.66
4	AF055033	IGFBP5	0	0.02	0.25	0.53	0.54	0.95
4	AF070587	KIAA1509	0	-0.07	0.51	0.87	0.82	0.52
4	AF075028	AF075028	0	-0.09	0.39	0.76	0.65	0.42
4	AF086393	NANOS1	0	-0.02	0.26	0.52	0.68	0.82
4	AF088008	DKFZP564	0	0.24	0.35	0.53	0.78	0.58
4	AF124432	HOM-TES	0	0.32	0.5	0.49	0.61	0.71
4	AF159092	NDRG2	0	0.18	0.51	0.55	0.73	0.88
4	AF161339	ARHGAP9	0	0.1	0.59	0.49	0.66	0.7
4	AF161345	ZFHX1B	0	0.2	0.55	0.7	0.92	0.82
4	AF163762	ADAMTS1	0	0.29	0.12	0.39	1.05	0.98
4	AF174600	LMO7	0	0.12	0.28	0.51	0.82	0.78
4	AF204173	POPDC2	0	0.01	0.3	0.36	0.76	1.05
4	AF209930	CHRD	0	0.11	0.55	0.49	1.23	0.82
4	AF251025	ZFYVE1	0	0.15	0.05	0.74	0.56	0.72
4	AF315683	MMP28	0	0.1	0.63	0.72	1	1.04
4	AK000992	PDE4DIP	0	0.17	0.1	0.8	0.79	0.63
4	AK001398	FHOD3	0	0	0.28	0.69	1.09	0.79
4	AK002078	ZNF449	0	0.33	0.33	1.01	0.72	0.77
4	AK002164	MGC3509	0	0.21	0.34	0.51	0.64	0.72
4	AK021594	FLJ22594	0	0.24	0.52	0.55	0.82	1.04
4	AK021793	LOC28602	0	-0.14	0.29	0.49	1.23	0.75
4	AK021807	LRP11	0	0.23	0.46	0.57	0.56	0.54
4	AK021985	FBXL7	0	0.48	0.61	0.74	0.81	0.76
4	AK022013	NPAS2	0	0.45	0.13	0.67	0.75	1.08
4	AK022035	COL11A1	0	0.12	0.09	0.69	1.17	1.22
4	AK023362	AK023362	0	0.45	0.44	0.99	0.95	0.79
4	AK024004	C6orf60	0	0.37	0.3	0.43	0.66	1.44
4	AK024016	APG10L	0	0.11	0.23	0.19	0.68	1.36
4	AK024311	FLJ14249	0	0.18	0.18	0.9	0.88	0.63
4	AK024438	FLJ38705	0	0.28	0.55	0.73	0.76	0.71
4	AK024947	CTBP2	0	0.26	0.09	0.58	0.74	1.11
4	AK025076	GTF2IRD2	0	0.36	0.52	0.42	0.59	0.65
4	AK025665	ADPN	0	0.13	0.03	0.4	0.48	1.26
4	AK025948	MGC1081	0	-0.01	0.54	0.34	0.6	1.11
4	AK026146	MGC4692	0	0.39	0.34	0.39	0.64	1.28
4	AK026654	CYBRD1	0	-0.29	0.48	1.07	1.02	0.85
4	AK026666	MGC3207	0	0.38	0.35	0.6	0.9	0.77
4	AK027157	CEAL1	0	0.22	0.27	0.68	1.01	0.95
4	AK027246	AK027246	0	0.21	0.41	1.01	1.03	0.63

4	AL035295	LOC92346	0	0.08	0.52	0.33	1.04	0.96
4	AL050012	GOLGA1	0	0.2	0.55	0.44	0.52	0.97
4	AL050107	WWTR1	0	0.22	0.3	0.27	0.77	1.13
4	AL050374	ABTB2	0	-0.04	0.26	0.51	1.17	1.18
4	AL110203	LOC15886	0	0	0.26	0.75	0.89	0.52
4	AL117666	LRIG1	0	0.06	0.41	0.9	0.75	0.67
4	AL137450	RPL37	0	0.01	0.38	0.65	0.55	0.69
4	AL137616	AL137616	0	0.21	0.57	0.76	0.65	1.24
4	AL137698	PGM5	0	-0.05	0.08	0.47	0.77	1.32
4	AL162078	KNSL8	0	0.26	0.29	0.48	0.58	0.71
4	AL390078	SHD	0	0.13	0.75	0.6	0.76	0.73
4	AL390144	ZNRF1	0	0.13	0.4	0.41	0.58	0.8
4	AL832149	LOC28401	0	0.03	0.51	0.31	0.69	0.66
4	BC017044	CYP27A1	0	0.09	0.53	0.86	0.87	0.49
4	D16951	D16951	0	0.23	0.43	0.27	0.65	1.14
4	M26747	THRB	0	0.39	0.35	0.58	0.45	0.76
4	NM_000023	SGCA	0	-0.09	0.6	0.77	0.79	0.68
4	NM_000029	AGT	0	0.13	0.41	0.38	0.8	0.73
4	NM_000069	CACNA1S	0	-0.14	0.22	0.39	0.95	1.06
4	NM_000152	GAA	0	0.02	0.55	0.45	0.7	0.81
4	NM_000161	GCH1	0	0.2	0.25	0.64	0.65	0.8
4	NM_000238	KCNH2	0	-0.15	0.57	0.43	0.84	0.77
4	NM_000271	NPC1	0	0.29	0.41	0.91	0.85	1.06
4	NM_000308	PPGB	0	0.05	0.36	0.72	0.64	0.75
4	NM_000316	PTHR1	0	0.08	0.55	0.58	0.78	0.77
4	NM_000383	AIRE	0	-0.24	0.1	0.49	1.18	0.97
4	NM_000393	COL5A2	0	0.16	0.55	0.58	0.52	0.92
4	NM_000612	IGF2	0	0.09	0.74	0.85	0.72	0.93
4	NM_000681	ADRA2A	0	0.25	0.69	0.33	0.63	0.92
4	NM_000876	IGF2R	0	0.03	0.3	0.5	0.66	0.78
4	NM_001448	GPC4	0	0.22	0.34	0.53	0.52	0.72
4	NM_001549	IFIT3	0	0.06	0.22	0.94	1.04	0.73
4	NM_001681	ATP2A2	0	0	0.23	0.86	1.1	0.88
4	NM_001711	BGN	0	0.28	0.44	0.45	0.81	1.27
4	NM_001974	EMR1	0	0.17	0.34	0.49	0.41	0.95
4	NM_002085	GPX4	0	-0.08	0.36	0.66	0.61	0.63
4	NM_002130	HMGCS1	0	-0.43	-0.34	1.18	1.56	0.81
4	NM_002168	IDH2	0	0.24	0.46	0.4	0.51	1.03
4	NM_002317	LOX	0	0.35	0.18	0.26	0.63	0.87
4	NM_002332	LRP1	0	0.28	0.35	0.44	0.49	0.98
4	NM_002335	LRP5	0	0.3	0.78	0.85	0.79	0.63
4	NM_002340	LSS	0	0.26	0.27	0.82	1.24	1.13
4	NM_002345	LUM	0	0.33	0.64	0.98	0.64	0.92
4	NM_002428	MMP15	0	-0.11	-0.03	0.76	0.99	0.84
4	NM_002481	PPP1R12B	0	0.03	0.42	0.52	0.97	0.77
4	NM_002611	PDK2	0	0.11	0.55	0.7	0.8	0.75
4	NM_002648	PIM1	0	-0.27	0.15	0.75	0.92	1.25
4	NM_002763	PROX1	0	-0.15	0.63	1.08	0.84	0.83
4	NM_002861	PCYT2	0	0.24	0.2	0.42	0.7	1.08
4	NM_003118	SPARC	0	0.05	0.18	0.54	0.79	1.13
4	NM_003204	NFE2L1	0	0.37	0.38	0.36	0.63	1
4	NM_003273	TM7SF2	0	0.1	0.5	0.49	0.93	1.05

4	NM_003289	TPM2	0	0.13	0.4	0.53	0.95	1.29
4	NM_003528	HIST2H2B	0	-0.02	0.3	0.88	0.63	0.82
4	NM_003565	ULK1	0	0.2	0.32	0.46	0.83	0.81
4	NM_003613	CILP	0	-0.01	-0.07	0.06	0.73	1.51
4	NM_003706	PLA2G4C	0	0.07	0.43	0.79	0.86	0.78
4	NM_003803	MYOM1	0	0.3	0.18	0.24	0.95	1.22
4	NM_003829	MPDZ	0	0.41	0.37	0.24	0.68	0.8
4	NM_003885	CDK5R1	0	0.07	0.49	0.69	1.04	0.43
4	NM_003900	SQSTM1	0	-0.13	0.2	1.3	0.85	0.95
4	NM_004121	GGTLA1	0	0.23	0.64	0.37	0.47	0.92
4	NM_004521	KIF5B	0	-0.28	0.33	0.41	0.76	0.88
4	NM_004678	BPY2	0	-0.19	0.39	0.3	0.78	0.82
4	NM_004740	TIAF1	0	0.09	0.29	0.54	0.8	0.69
4	NM_004937	CTNS	0	0.28	0.19	1.17	0.71	0.82
4	NM_004975	KCNB1	0	0.19	0.48	0.39	0.57	0.82
4	NM_005031	FXYD1	0	-0.26	0.39	0.6	0.88	1.32
4	NM_005070	SLC4A3	0	-0.12	0.23	0.56	1.18	0.73
4	NM_005087	FXR1	0	0.26	0.35	0.47	0.64	0.62
4	NM_005165	ALDOC	0	0.13	0.79	0.66	0.96	0.72
4	NM_005307	GRK4	0	0.31	0.31	0.36	0.65	0.63
4	NM_005318	H1F0	0	0.06	-0.24	1.13	0.42	0.89
4	NM_005419	STAT2	0	0.03	0.35	0.88	0.78	0.7
4	NM_005547	IVL	0	0.13	0.48	0.41	0.46	1.17
4	NM_005891	ACAT2	0	0.17	-0.2	0.52	1.07	1.27
4	NM_005892	FMNL1	0	-0.19	0.6	0.65	0.78	0.65
4	NM_005938	MLLT7	0	0.36	0.56	0.68	0.82	1.04
4	NM_005992	TBX1	0	0.2	0.7	0.92	0.88	0.67
4	NM_006011	ST8SIA2	0	0.43	0.55	0.58	1.1	0.81
4	NM_006034	TP53I11	0	0.02	0.16	0.49	1.1	0.96
4	NM_006097	MYL9	0	0.05	0.18	0.46	0.95	1.16
4	NM_006352	ZNF238	0	0.03	0.85	0.68	0.75	0.62
4	NM_006386	DDX17	0	0.33	0.45	0.88	0.88	0.98
4	NM_006482	DYRK2	0	-0.51	0.33	0.74	1.05	0.77
4	NM_006934	SLC6A9	0	0.21	0.17	1	0.76	1.06
4	NM_007112	THBS3	0	0.22	0.28	0.59	0.94	1.24
4	NM_007124	UTRN	0	0.12	0.33	0.29	0.9	1.4
4	NM_007315	STAT1	0	-0.01	0.16	0.71	0.67	0.68
4	NM_012249	RHOQ	0	0.23	0.28	0.45	0.76	1.15
4	NM_013231	FLRT2	0	-0.07	0.35	0.5	0.82	1.03
4	NM_013401	RAB3IL1	0	0.47	0.42	0.47	0.77	0.63
4	NM_014391	ANKRD1	0	0.08	0.47	0.52	1.37	0.83
4	NM_014432	IL20RA	0	-0.2	0.66	0.93	0.75	0.72
4	NM_014467	SRPX2	0	0.04	0.25	0.62	0.61	0.68
4	NM_014746	RNF144	0	0.05	0.41	0.72	0.62	0.67
4	NM_014781	RB1CC1	0	-0.18	0.35	0.61	0.84	0.91
4	NM_014909	KIAA1036	0	0.11	0.27	0.59	1.08	0.95
4	NM_014945	ABLIM3	0	-0.02	0.5	0.69	1.11	1.09
4	NM_015642	ZBTB20	0	0.16	0.6	0.98	0.74	0.54
4	NM_016081	KIAA0992	0	0.11	0.43	0.51	0.57	0.91
4	NM_016423	ZNF219	0	0.03	0.38	0.53	0.87	0.94
4	NM_016532	SKIP	0	0.1	0.13	0.45	0.71	0.94
4	NM_017506	OR7A5	0	0.32	0.56	0.42	1.08	0.77

4	NM_017622	FLJ20014	0	0.37	0.4	0.79	0.86	0.75
4	NM_018013	FLJ10159	0	0.17	0.41	0.31	0.59	0.9
4	NM_018194	HHAT	0	-0.04	0.08	0.41	0.77	1.04
4	NM_018487	HCA112	0	0.3	0.91	0.6	0.7	0.94
4	NM_018723	A2BP1	0	-0.11	0.7	0.56	0.88	0.62
4	NM_020185	DUSP22	0	0.42	0.29	0.37	0.85	1.23
4	NM_020422	LOC57146	0	0.08	0.31	0.47	0.65	0.94
4	U03106	CDKN1A	0	-0.04	0.27	0.7	0.96	1.21
4	U16850	CALM2	0	-0.25	0.41	0.88	0.77	0.8
4	U30889	PC	0	0.01	0.41	0.28	1.19	1.13
4	U34249	TRIM15	0	0.07	0.26	0.46	0.92	1.24
4	U66052	IDS	0	0.22	0.31	0.94	1.07	0.84
4	X90978	RUNX1	0	0.15	0.42	1.04	1	0.78
4	Y11709	COL14A1	0	0.22	0.33	0.74	1.1	0.83
5	AB002297	DOCK3	0	-0.2	0.03	0.09	0.31	0.42
5	AB004857	SLC11A2	0	-0.08	0.03	0.31	0.36	0.46
5	AB007925	SRGAP2	0	0.04	0.04	0.35	0.61	0.66
5	AB011133	MAST3	0	-0.1	0.04	0.16	0.28	0.34
5	AB011182	SPG20	0	0.05	0.09	0.33	0.44	0.44
5	AB011539	EGFL3	0	0.03	0.1	0.03	0.44	0.51
5	AB028947	KIAA1024	0	0	0.14	0.48	0.43	0.37
5	AB028949	KIAA1026	0	0.09	0.14	0.12	0.3	0.45
5	AB033025	KIAA1199	0	-0.06	0.08	0.53	0.54	0.74
5	AB037765	KIAA1344	0	-0.4	0.08	0.26	0.44	0.64
5	AF019618	PAR5	0	-0.23	0.32	0.32	0.54	0.43
5	AF026943	AF026943	0	-0.19	-0.11	0.48	0.59	0.47
5	AF075030	AF075030	0	-0.15	0.12	0.48	0.67	0.94
5	AF085961	YPEL2	0	0.12	0.28	0.45	0.65	0.65
5	AF086425	MTHFD1L	0	-0.33	-0.15	0.13	0.48	0.45
5	AF086439	DHX35	0	0.02	0.06	0.33	0.38	0.57
5	AF152529	PCDHGB8	0	-0.03	0.2	0.64	0.59	0.55
5	AF250226	ADCY6	0	0.1	0.23	0.4	0.31	0.63
5	AF261758	DHCR24	0	-0.24	-0.42	0.27	0.59	0.78
5	AF305239	HIPK3	0	-0.35	0.22	0.05	0.68	0.69
5	AF305550	MOAP1	0	0.1	0.25	0.37	0.57	0.75
5	AJ404615	FN3K	0	0.05	0	0.27	0.33	0.42
5	AK000401	TANC	0	-0.12	0.03	0.41	0.64	0.73
5	AK000685	CCNL2	0	-0.14	-0.06	0.49	0.46	0.45
5	AK021699	ZNF556	0	-0.37	0.21	0.62	0.67	0.38
5	AK021981	AK021981	0	-0.27	0.08	0.23	0.22	0.4
5	AK022404	RERE	0	-0.03	0.15	0.26	0.25	0.49
5	AK022583	AK022583	0	-0.24	0.03	0.1	0.29	0.54
5	AK022961	PANK3	0	-0.14	-0.1	0.18	0.27	0.45
5	AK023448	Cep63	0	-0.07	0.29	0.16	0.41	0.8
5	AK023505	RSNL2	0	-0.16	0.3	0.64	0.5	0.48
5	AK023609	PSCD3	0	-0.23	0.23	0.59	0.59	0.55
5	AK023696	LOC40150	0	0.19	0.38	0.25	0.44	0.53
5	AK023707	CCDC2	0	-0.02	0.16	0.27	0.41	0.49
5	AK024177	AK024177	0	-0.08	-0.05	0.28	0.34	0.54
5	AK024431	AKNA	0	-0.08	0.29	0.28	0.55	1.07
5	AK024470	RPS27	0	-0.12	0.19	0.58	0.57	0.43
5	AK024549	ARHGAP1	0	0.13	0.16	0.3	0.74	0.71

5	AK024599	AK024599	0	-0.12	-0.04	0.21	0.49	0.45
5	AK024739	C10orf118	0	-0.17	0.24	0.51	0.71	0.62
5	AK025004	AK025004	0	0.08	0.23	0.53	0.59	0.66
5	AK025112	AK025112	0	0.08	0.21	0.17	0.51	0.53
5	AK025269	FLJ21616	0	-0.1	0.08	0.33	0.53	0.62
5	AK025419	SPIB	0	-0.27	0.02	0.06	0.3	0.34
5	AK025886	SLC24A6	0	-0.06	0.14	0.56	0.4	0.71
5	AK026026	BID	0	-0.04	0.34	0.38	0.48	0.57
5	AK026295	AK026295	0	0	0.08	0.39	0.6	0.67
5	AK026642	AK026642	0	-0.61	-0.03	0.38	0.45	0.48
5	AK026720	LOC28353	0	-0.49	0.21	0.3	0.65	1.16
5	AK026723	AK026723	0	0.04	0.04	0.84	0.45	0.77
5	AL049964	AL049964	0	-0.2	0.26	0.53	0.76	0.49
5	AL117482	ULK3	0	-0.18	0.06	0.34	0.82	0.77
5	AL133577	MBTD1	0	-0.04	0.32	0.48	0.55	0.53
5	AL359627	COL12A1	0	-0.35	0.12	0.54	0.47	0.46
5	BC031485	ACACA	0	-0.21	0.11	0.19	0.42	0.42
5	BF184738	TAGLN	0	-0.06	0.09	0.16	0.29	0.6
5	BF345435	e(y)2	0	0.01	0.31	-0.03	0.26	0.73
5	D16877	D16877	0	0.04	0.36	0.34	0.63	0.57
5	D17220	D17220	0	0.18	0.37	0.34	0.38	0.8
5	D38145	PTGIS	0	0.21	0.29	0.39	0.36	0.61
5	D82061	HSD17B8	0	0.11	0.42	0.17	0.41	0.6
5	D86985	KIAA0232	0	-0.18	0.09	0.37	0.51	0.31
5	D87742	KIAA0268	0	-0.02	0.32	0.12	0.6	0.62
5	L26494	POU3F1	0	0.06	0.03	0.35	0.29	0.93
5	M30262	NPPA	0	-0.64	-0.7	-0.21	0.91	0.94
5	NM_000028	AGL	0	0.15	0.05	0.29	0.73	0.74
5	NM_000072	CD36	0	0.15	0.35	0.28	0.58	0.76
5	NM_000195	HPS1	0	-0.06	0.23	0.42	0.44	0.58
5	NM_000313	PROS1	0	-0.06	-0.03	0.14	0.69	0.59
5	NM_000719	CACNA1C	0	-0.22	0.22	0.13	0.26	0.56
5	NM_000943	PPIC	0	0.07	0.15	0.16	0.36	0.56
5	NM_001105	ACVR1	0	-0.31	-0.23	0.49	0.51	0.83
5	NM_001257	CDH13	0	0.08	0.38	0.56	0.49	0.61
5	NM_001313	CRMP1	0	-0.51	-0.25	0.17	0.38	0.76
5	NM_001375	DNASE2	0	0.1	0.29	0.42	0.44	0.65
5	NM_001393	ECM2	0	0.09	-0.18	0.34	0.79	0.59
5	NM_001398	ECH1	0	0.07	0.24	0.34	0.43	0.45
5	NM_001456	FLNA	0	-0.36	-0.4	0.19	0.22	0.71
5	NM_001481	GAS8	0	-0.27	0.28	0.26	0.63	0.65
5	NM_002230	JUP	0	-0.07	-0.02	0.09	0.62	1.29
5	NM_002413	MGST2	0	0.27	0.24	0.29	0.61	0.72
5	NM_002446	MAP3K10	0	-0.18	0.02	0.3	0.32	0.72
5	NM_002462	MX1	0	0.1	0.29	0.39	0.33	0.9
5	NM_002821	PTK7	0	0.03	0.34	0.09	0.28	0.77
5	NM_002959	SORT1	0	0.14	0.16	0.12	0.55	0.78
5	NM_003040	SLC4A2	0	0.15	0.38	0.46	0.53	0.61
5	NM_003107	SOX4	0	-0.01	0.21	0.23	0.52	0.68
5	NM_003129	SQLE	0	-0.11	-0.03	0.26	0.84	0.73
5	NM_003287	TPD52L1	0	-0.19	-0.01	0.21	0.5	1.02
5	NM_003401	XRCC4	0	-0.18	0.03	0.34	0.49	0.66

5	NM_003532	HIST1H3E	0	-0.31	0.03	0.61	0.83	0.74
5	NM_003722	TP73L	0	-0.15	0.17	-0.01	0.43	0.67
5	NM_003768	PEA15	0	0.1	0.01	0.47	0.75	0.7
5	NM_003882	WISP1	0	0.01	-0.01	0.02	0.57	0.89
5	NM_003982	SLC7A7	0	0.03	0.32	0.39	0.64	0.65
5	NM_004227	PSCD3	0	-0.27	0.32	0.41	0.66	0.51
5	NM_004351	CBLB	0	-0.01	0.11	0.67	0.5	0.42
5	NM_004422	DVL2	0	-0.15	-0.02	0.37	0.44	0.64
5	NM_004443	EPHB3	0	0.05	0.22	0.38	0.7	0.55
5	NM_004508	IDI1	0	-0.12	0.26	0.21	0.7	0.78
5	NM_004529	MLLT3	0	0.04	0.18	0.03	0.48	0.54
5	NM_004720	EDG4	0	-0.04	0.01	0.36	0.32	0.41
5	NM_005010	NRCAM	0	-0.16	0.14	0.3	0.39	0.66
5	NM_005098	MSC	0	-0.44	-0.13	0.18	0.71	1.05
5	NM_005213	CSTA	0	-0.1	0.2	0.32	0.26	0.48
5	NM_005296	GPR23	0	-0.14	0.21	0.33	0.26	0.46
5	NM_005725	TSPAN2	0	-0.43	0.15	0.43	0.41	0.7
5	NM_005738	ARL4A	0	-0.01	-0.04	0.44	0.82	0.67
5	NM_005785	RNF41	0	-0.12	-0.09	0.12	0.58	0.93
5	NM_005832	KCNMB2	0	-0.08	0.34	0.47	0.65	0.72
5	NM_005908	MANBA	0	0.04	0.25	0.46	0.65	0.57
5	NM_006033	LIPG	0	-0.08	0.1	0.17	0.7	0.58
5	NM_006162	NFATC1	0	-0.16	0.16	0.34	0.67	0.85
5	NM_006212	PFKFB2	0	0.02	0.12	0.36	0.35	0.51
5	NM_006432	NPC2	0	-0.14	-0.08	0.59	0.53	0.57
5	NM_006561	CUGBP2	0	0.07	0.37	0.44	0.54	0.66
5	NM_006623	PHGDH	0	0.06	0.14	-0.02	0.31	0.46
5	NM_006640	38604	0	0.17	0.35	0.27	0.34	0.55
5	NM_006743	RBM3	0	0.24	-0.05	0.49	0.34	0.57
5	NM_006790	TTID	0	0.16	0.06	0.44	0.53	0.82
5	NM_007097	CLTB	0	0.18	0.1	0.2	0.41	0.86
5	NM_007281	SCRG1	0	-0.3	-0.16	-0.03	0.44	0.72
5	NM_012090	MACF1	0	-0.18	0.1	0.27	0.57	0.62
5	NM_012257	HBP1	0	0	-0.2	0.57	0.63	0.75
5	NM_012266	DNAJB5	0	-0.27	0.07	0.05	0.46	0.73
5	NM_013352	SART2	0	-0.24	0.02	0.19	0.29	0.44
5	NM_013400	REPIN1	0	0.13	0.23	0.51	0.39	0.46
5	NM_013974	DDAH2	0	0.09	0.06	0.13	0.32	0.7
5	NM_014028	OSTM1	0	-0.17	-0.05	0.32	0.5	0.7
5	NM_014133	NM_01413	0	-0.09	0	0.49	0.55	0.77
5	NM_014241	PTPLA	0	-0.15	-0.1	0.46	0.89	0.84
5	NM_014405	CACNG4	0	-0.17	0.08	0.28	0.71	0.73
5	NM_014549	DKFZP434	0	0.02	0.17	0.45	0.6	0.74
5	NM_014811	KIAA0649	0	-0.19	0.06	0.35	0.41	0.5
5	NM_014862	ARNT2	0	-0.28	0.03	0.39	0.78	0.75
5	NM_014900	COBLL1	0	-0.17	-0.37	-0.03	0.22	0.7
5	NM_014921	LPHN1	0	-0.1	0.19	0.08	0.27	0.37
5	NM_014965	OIP106	0	-0.11	0.01	0.29	0.55	0.54
5	NM_015071	ARHGAP2	0	-0.26	0.26	0.32	0.32	0.49
5	NM_015379	BRI3	0	0.05	0.2	0.56	0.53	0.74
5	NM_015696	GPX7	0	-0.14	-0.01	0.16	0.56	0.47
5	NM_015900	PLA1A	0	0.07	-0.07	0.15	0.42	0.66

5	NM_015922	NSDHL	0	0.11	-0.32	0.35	0.6	0.77
5	NM_015983	UBE2D4	0	-0.18	0.02	0.09	0.38	0.54
5	NM_016108	AIG1	0	0.2	0.25	0.25	0.58	0.49
5	NM_016206	VGL-3	0	-0.41	0.16	0.39	0.44	0.52
5	NM_016332	SEPX1	0	0.05	0.24	0.45	0.59	0.47
5	NM_016733	LIMK2	0	0.13	0.24	0.1	0.73	0.77
5	NM_017673	C1orf26	0	0.37	0.33	0.41	0.48	0.54
5	NM_018009	TAPBPL	0	0.13	0.22	0.43	0.36	0.62
5	NM_018017	C10orf118	0	-0.27	0.24	0.57	0.51	0.55
5	NM_018370	FLJ11259	0	-0.15	-0.16	0.43	0.2	0.87
5	NM_018542	NM_01854	0	-0.02	0.37	0.39	0.72	0.56
5	NM_018558	GABRQ	0	0.27	0.26	0.3	0.43	0.85
5	NM_019096	GTPBP2	0	-0.05	-0.06	0.05	0.32	0.42
5	NM_020164	ASPH	0	-0.12	0.2	0.13	0.4	0.56
5	NM_020233	MDS006	0	-0.18	0.15	0.26	0.56	0.43
5	NM_020379	MAN1C1	0	-0.13	-0.11	0.43	0.58	0.73
5	U01147	ABR	0	-0.01	0.21	0.33	0.48	0.37
5	U17989	STRN3	0	0.12	0.29	0.41	0.56	0.44
5	U42977	THPO	0	-0.02	0.12	0.04	0.31	0.74
5	U52076	U52076	0	0.27	0.3	0.26	0.38	0.95
5	U66048	U66048	0	0.1	0.24	0.62	0.46	0.58
5	U79271	AKT3	0	-0.02	0.22	0.15	0.45	0.71
5	X75693	X75693	0	0.06	0.29	0.46	0.46	0.49
6	AB007932	PLXNA2	0	0.81	-0.2	-0.96	-1.55	-1.45
6	AB012643	ALPL	0	0.34	0.1	-0.42	-0.8	-0.95
6	AB040907	ZNF537	0	0.19	-0.29	-0.77	-0.85	-0.93
6	AB044661	XAB1	0	0.21	-0.52	-0.54	-0.89	-1.22
6	AF086287	PRKCA	0	0	-0.32	-0.22	-1.08	-1.25
6	AF131784	RAB27B	0	-0.03	-0.21	0.85	-0.65	-1.64
6	AF164797	MRPL17	0	0.64	0.1	-0.52	-1.08	-0.52
6	AF254067	IL21R	0	0.21	-0.06	-0.66	-1.12	-1.04
6	AK000450	MRPL52	0	0.41	-0.4	-0.37	-0.77	-0.81
6	AK000660	CDK6	0	0.08	-0.03	-0.4	-0.66	-1.35
6	AK021788	TRPM3	0	0.5	-0.12	-0.09	-0.74	-1.31
6	AK022287	SFXN1	0	0.07	-0.19	-0.46	-0.94	-0.91
6	AK023015	WDR54	0	0.17	-0.52	-0.44	-1.02	-1.24
6	AK024513	CAV2	0	0.01	-0.29	-0.47	-0.94	-1.16
6	AK025855	CDH4	0	-0.09	-0.23	-0.48	-1.2	-1.37
6	AK026663	DOCK5	0	0.58	-0.07	-0.3	-0.52	-1.05
6	AL117477	PHF19	0	0.4	-0.3	-0.5	-1.01	-1.5
6	AL137764	LOC64744	0	-0.07	-0.23	-0.6	-0.93	-1.62
6	AL157504	AL157504	0	0.29	-0.21	-0.34	-0.73	-1.05
6	AL160131	C22orf18	0	0.37	0.04	-0.03	-0.94	-1.81
6	BC008376	CXCL5	0	1.34	0.34	-0.15	-1.08	-1.73
6	D87450	KIAA0261	0	-0.01	-0.27	-0.4	-1.16	-1.13
6	M34671	CD59	0	0.22	-0.36	-0.87	-0.88	-1
6	NM_000693	ALDH1A3	0	-0.26	-0.13	-0.28	-0.9	-1.66
6	NM_000956	PTGER2	0	0.25	-0.04	-0.27	-0.71	-1.31
6	NM_001047	SRD5A1	0	0.14	-0.25	-0.32	-0.73	-1.17
6	NM_001071	TYMS	0	0.26	0.04	-0.45	-1.27	-1.37
6	NM_001078	VCAM1	0	0.04	-0.08	-0.6	-0.9	-1.13
6	NM_001191	BCL2L1	0	0.54	0.36	-0.2	-0.94	-0.88

6	NM_001218	CA12	0	0.42	0.32	-0.2	-0.7	-1.11
6	NM_001444	FABP5	0	0.65	-0.21	-0.21	-1.55	-1.49
6	NM_001627	ALCAM	0	0.08	-0.51	-0.41	-1.03	-1.25
6	NM_001809	CENPA	0	0.55	-0.18	-0.91	-1.08	-1.42
6	NM_001840	CNR1	0	0.25	0.13	-0.36	-0.58	-1.2
6	NM_002105	H2AFX	0	0.64	-0.09	-0.49	-1.36	-1.34
6	NM_002128	HMGB1	0	0.32	-0.29	-0.53	-0.93	-0.74
6	NM_002388	MCM3	0	0.95	-0.2	-0.4	-1.33	-1.56
6	NM_002452	NUDT1	0	0.52	-0.06	-0.54	-1.16	-0.94
6	NM_002692	POLE2	0	0.22	-0.36	-0.42	-1.13	-0.96
6	NM_002823	PTMA	0	0.08	-0.32	-0.56	-0.86	-1.58
6	NM_002882	RANBP1	0	0.2	-0.41	-0.61	-1.04	-0.97
6	NM_003004	SECTM1	0	0.29	0.43	0.27	-0.75	-1.66
6	NM_003012	SFRP1	0	0.15	-0.37	-0.58	-1.14	-1.2
6	NM_003016	SFRS2	0	0.09	-0.27	-0.69	-0.82	-1.62
6	NM_003524	HIST1H2B	0	1.1	0.81	-0.75	-2.09	-2.02
6	NM_003545	HIST1H4E	0	0.19	-0.23	-0.42	-1.09	-1.21
6	NM_003546	HIST1H4L	0	0.92	0.49	0.11	-1.18	-2.28
6	NM_003744	NUMB	0	0.23	-0.07	-0.59	-0.53	-1.06
6	NM_004126	GNG11	0	0.03	-0.12	-0.46	-1.27	-1.48
6	NM_004170	SLC1A1	0	0.04	-0.29	-0.46	-0.84	-1.15
6	NM_004207	SLC16A3	0	0.2	-0.27	-0.83	-1.11	-0.97
6	NM_004292	RIN1	0	0.05	-0.1	-0.41	-1.12	-1.23
6	NM_004298	NUP155	0	0.52	-0.15	-0.86	-0.94	-0.58
6	NM_004318	ASPH	0	-0.3	-0.21	0.06	-0.98	-1.23
6	NM_004516	ILF3	0	0.13	0.05	-0.2	-0.75	-0.91
6	NM_004834	MAP4K4	0	0.38	-0.49	-0.3	-0.76	-0.89
6	NM_005004	NDUFB8	0	0.32	-0.12	-0.28	-0.38	-1.12
6	NM_005110	GFPT2	0	-0.14	-0.05	-0.11	-0.58	-1.5
6	NM_005321	HIST1H1E	0	-0.05	-0.36	-0.25	-1.09	-1.07
6	NM_005441	CHAF1B	0	0.04	-0.31	-0.56	-1.03	-0.96
6	NM_005544	IRS1	0	-0.05	-0.04	-0.21	-0.54	-1.4
6	NM_005576	LOXL1	0	0.4	0	-1.01	-1.2	-0.77
6	NM_005733	KIF20A	0	0.46	-0.13	-0.4	-1.25	-1.47
6	NM_005863	NET1	0	0.07	-0.07	-0.73	-1.18	-1.55
6	NM_005994	TBX2	0	0.67	0.07	-0.62	-1.01	-1.26
6	NM_006442	DRAP1	0	0.24	-0.29	-0.54	-1.09	-1.33
6	NM_006666	RUVBL2	0	0.51	0.04	-0.42	-1.23	-0.81
6	NM_007086	WDHD1	0	0.13	-0.42	-0.38	-1	-1
6	NM_007172	NUP50	0	0.28	-0.41	-0.52	-0.98	-1.12
6	NM_012177	FBXO5	0	0.78	-0.28	-0.64	-1.12	-1.63
6	NM_012449	STEAP1	0	0.41	-0.72	-0.71	-1.14	-1.23
6	NM_012484	HMMR	0	0.57	-0.44	-0.24	-1	-1.19
6	NM_014344	FJX1	0	0.33	0.42	-0.52	-1.12	-1.12
6	NM_014380	NGFRAP1	0	-0.01	-0.2	-0.52	-0.72	-1.38
6	NM_015865	SLC14A1	0	0.33	-0.14	-0.24	-1.17	-1.27
6	NM_016260	ZNFN1A2	0	0.48	-0.28	-0.37	-0.57	-0.98
6	NM_016395	HSPC121	0	0.05	-0.45	-0.35	-0.75	-1.21
6	NM_018087	FLJ10407	0	0.57	-0.01	-0.04	-0.53	-0.97
6	NM_018092	NETO2	0	0.7	0.62	-0.03	-0.82	-1.34
6	NM_018283	NUDT15	0	0	-0.29	-0.45	-0.97	-1.51
6	NM_018323	PI4K2B	0	0.25	-0.07	-0.32	-0.87	-0.8

6	NM_018340	FLJ11151	0	0.16	-0.13	-0.85	-1.2	-0.64
6	NM_018492	PBK	0	0.34	-0.61	-0.16	-0.97	-1.57
6	NM_019013	FLJ10156	0	0.13	-0.23	-0.5	-1.26	-1.54
6	NM_020038	ABCC3	0	-0.19	-0.12	-0.18	-0.99	-1.63
6	NM_020242	KIF15	0	0.13	-0.35	-0.47	-0.76	-1.18
6	NM_020467	LOC57228	0	0.3	-0.28	-0.44	-0.74	-0.95
6	U96131	TRIP13	0	0.83	-0.11	-0.49	-0.9	-0.96
7	AB002444	AB002444	0	-0.06	-0.11	-0.18	-0.42	-0.83
7	AB013384	HIP1R	0	-0.18	-0.3	-0.32	-0.6	-0.39
7	AB019573	HOP	0	-0.09	-0.18	-0.25	-0.36	-0.46
7	AB020640	CAMTA1	0	0.03	0.01	-0.24	-0.51	-0.58
7	AB023166	CIT	0	0.42	-0.13	-0.45	-0.75	-0.73
7	AB026436	DUSP10	0	0.37	0.06	0.23	-0.34	-1.2
7	AB032964	TCEB3BP	0	-0.15	-0.27	-0.16	-0.35	-0.64
7	AB032996	FAM40B	0	-0.05	-0.33	-0.14	-0.3	-0.43
7	AB033091	SLC39A10	0	0.06	-0.14	-0.03	-0.35	-0.61
7	AB037794	AMSH-LP	0	0.89	0.09	-0.07	-0.41	-0.57
7	AB040879	KIAA1446	0	0.28	-0.24	-0.43	-0.21	-0.59
7	AB040903	TD-60	0	-0.16	-0.2	-0.34	-0.55	-0.39
7	AF007192	AF007192	0	0.18	0.11	-0.15	-0.37	-0.77
7	AF022913	PIGK	0	0.39	0.04	-0.25	-0.5	-0.46
7	AF038202	STX6	0	-0.08	-0.1	-0.36	-0.42	-0.42
7	AF070600	TUBB	0	0.31	-0.25	-0.49	-0.67	-0.35
7	AF072810	BAZ1B	0	0.18	-0.17	-0.27	-0.36	-0.76
7	AF085966	SKIV2L2	0	0.18	-0.06	-0.21	-0.32	-0.99
7	AF086234	C6orf125	0	0.14	-0.35	-0.35	-0.37	-0.77
7	AF086517	AF086517	0	-0.13	-0.05	-0.53	-0.44	-0.54
7	AF086543	CD44	0	-0.16	-0.21	-0.29	-0.47	-0.51
7	AF086924	PPP2R2C	0	0.12	0.02	-0.32	-0.32	-0.31
7	AF087993	NR2F2	0	-0.09	-0.21	-0.26	-0.25	-0.47
7	AF110265	EPS15L1	0	-0.06	-0.04	-0.23	-0.27	-0.38
7	AF131762	CHST11	0	-0.22	-0.12	-0.31	-0.42	-0.58
7	AF133332	AF133332	0	0.14	-0.23	-0.39	-0.4	-0.35
7	AF159141	BRMS1	0	-0.12	-0.36	-0.06	-0.47	-0.75
7	AF161371	C6orf153	0	-0.23	-0.28	-0.3	-0.41	-0.48
7	AF172327	AF172327	0	-0.08	-0.13	-0.13	-0.46	-0.49
7	AF172929	HCST	0	0.05	0.04	-0.3	-0.56	-0.4
7	AF182419	MDS018	0	0.02	-0.27	-0.26	-0.39	-0.5
7	AF202092	APG3L	0	0.33	-0.48	-0.34	-0.38	-0.76
7	AF205435	MRPL46	0	0.21	-0.22	-0.52	-0.7	-0.43
7	AF239156	PDF	0	0.05	-0.26	-0.01	-0.18	-1.09
7	AF249267	SLC2A4R(	0	-0.02	0.11	-0.26	-0.24	-0.32
7	AF286164	PLEKHA2	0	0.11	0.01	-0.38	-0.26	-0.33
7	AF309553	REC14	0	0.05	-0.07	-0.41	-0.41	-0.31
7	AJ131244	SEC24A	0	-0.02	-0.08	-0.3	-0.37	-0.55
7	AJ224875	ALG8	0	0.04	-0.32	-0.31	-0.4	-0.56
7	AJ249900	SMOC1	0	0.25	0.05	-0.06	-0.37	-1
7	AJ277442	XYLT2	0	-0.07	-0.16	-0.1	-0.48	-0.62
7	AK000407	DERPC	0	-0.11	-0.34	-0.02	-0.41	-0.51
7	AK000529	PIGX	0	-0.14	-0.24	-0.4	-0.34	-0.52
7	AK002036	AK002036	0	-0.11	-0.16	-0.03	-0.43	-0.59
7	AK021454	LOC16359	0	-0.24	-0.27	-0.36	-0.3	-0.6

7	AK021539	C18orf4	0	0.03	0.07	0.09	-0.56	-0.81
7	AK021560	LRRC17	0	-0.03	0.14	-0.24	-0.48	-0.93
7	AK022207	MLPH	0	0.06	-0.16	-0.25	-0.57	-0.68
7	AK022667	FLJ11712	0	-0.03	-0.31	-0.37	-0.37	-0.53
7	AK022874	COG4	0	-0.16	-0.16	-0.22	-0.4	-0.68
7	AK023089	SLC30A7	0	0	-0.21	-0.07	-0.34	-0.81
7	AK023109	ARL6IP6	0	0.11	-0.35	-0.27	-0.53	-0.74
7	AK023149	DRF1	0	0.63	0.01	-0.11	-0.52	-0.73
7	AK023214	SKD3	0	-0.01	-0.24	-0.31	-0.44	-0.49
7	AK023511	C13orf7	0	0.03	-0.09	-0.05	-0.34	-0.41
7	AK023827	AK023827	0	0.16	-0.01	-0.1	-0.2	-0.38
7	AK024048	FBXO22	0	-0.11	-0.36	-0.21	-0.5	-0.6
7	AK024524	CIDEC	0	0.17	0.29	0.09	-0.29	-1.25
7	AK024810	FNBP3	0	0.1	-0.11	-0.31	-0.45	-0.42
7	AK024998	AK024998	0	0.08	-0.24	-0.38	-0.38	-0.81
7	AK025168	OSBPL6	0	0.09	-0.01	-0.42	-0.17	-0.59
7	AK025455	C14orf169	0	-0.08	-0.16	-0.07	-0.26	-0.58
7	AK025686	MGC2165	0	0.11	-0.08	-0.17	-0.68	-0.63
7	AK026383	AK026383	0	0.19	0.27	-0.17	-0.54	-0.44
7	AK026495	SLC2A13	0	-0.15	0.03	-0.17	-0.53	-0.66
7	AL050173	C21orf25	0	-0.02	-0.16	-0.1	-0.53	-0.47
7	AL117635	RTTN	0	0.22	-0.14	-0.34	-0.46	-0.79
7	AL137548	VKORC1L	0	0.51	-0.09	-0.17	-0.66	-0.44
7	AL137679	3'HEXO	0	0.45	-0.06	-0.15	-0.36	-0.33
7	AL390147	FAM20C	0	0.04	0.16	-0.35	-0.46	-0.52
7	AV740891	AV740891	0	0.09	-0.04	-0.25	-0.67	-0.8
7	AY004175	PLCB1	0	0.08	0.01	-0.39	-0.42	-0.39
7	AY007117	SHKBP1	0	-0.21	-0.18	-0.22	-0.37	-0.67
7	BC000401	SF3B2	0	0.08	-0.26	-0.18	-0.44	-0.44
7	BC001123	TMED9	0	-0.19	-0.32	-0.21	-0.24	-0.6
7	BC007318	MAPRE2	0	-0.1	-0.31	-0.16	-0.45	-0.59
7	BC009187	CKLFSF6	0	0.16	-0.03	-0.25	-0.33	-0.35
7	BC012304	DDX46	0	0.02	-0.24	-0.28	-0.45	-0.35
7	D17267	CSNK2A2	0	-0.12	-0.16	-0.13	-0.29	-0.75
7	D26018	POLD3	0	0.29	-0.22	-0.37	-0.57	-0.85
7	D28589	KIAA0114	0	-0.06	-0.23	-0.1	-0.58	-0.74
7	D42055	NEDD4	0	0.12	0.02	-0.26	-0.33	-0.37
7	D87076	PHF15	0	0.15	-0.2	-0.29	-0.49	-0.49
7	J03250	TOP1	0	-0.06	-0.22	-0.32	-0.43	-0.57
7	L05096	RPL39L	0	0.07	-0.18	-0.28	-0.56	-0.31
7	L15616	RNU15A	0	0	-0.19	-0.15	-0.26	-0.67
7	M33197	GAPD	0	-0.11	0.03	-0.06	-0.72	-0.63
7	M59979	PTGS1	0	-0.09	-0.13	-0.31	-0.43	-0.43
7	M69181	MYH10	0	0.06	-0.18	-0.33	-0.44	-0.55
7	NM_000048	ASL	0	0.19	-0.09	-0.37	-0.67	-0.69
7	NM_000107	DDB2	0	0.04	-0.09	-0.22	-0.41	-0.44
7	NM_000119	EPB42	0	-0.11	-0.22	-0.49	-0.52	-0.5
7	NM_000188	HK1	0	0.02	-0.27	-0.32	-0.57	-0.57
7	NM_000240	MAOA	0	0.38	0.38	0.07	-0.16	-0.67
7	NM_000276	OCRL	0	0.04	-0.21	-0.24	-0.36	-0.31
7	NM_000289	PFKM	0	-0.09	-0.13	-0.06	-0.24	-0.63
7	NM_000291	PGK1	0	-0.26	0.1	-0.07	-0.53	-0.83

7	NM_000408	GPD2	0	0.53	-0.25	-0.07	-0.6	-0.72
7	NM_000418	IL4R	0	-0.08	-0.18	-0.39	-0.37	-0.4
7	NM_000544	TAP2	0	0.11	-0.19	-0.25	-0.33	-0.57
7	NM_000737	CGB	0	0.32	-0.52	-0.6	-0.66	-0.41
7	NM_000916	OXTR	0	0.1	-0.29	0.44	-0.69	-0.99
7	NM_000937	POLR2A	0	-0.11	-0.18	-0.06	-0.4	-0.74
7	NM_001029	RPS26	0	0.25	-0.11	-0.27	-0.47	-0.33
7	NM_001127	AP1B1	0	0	-0.18	-0.37	-0.49	-0.6
7	NM_001154	ANXA5	0	-0.05	-0.34	-0.36	-0.64	-0.49
7	NM_001228	CASP8	0	0.06	-0.1	-0.08	-0.27	-0.49
7	NM_001275	CHGA	0	-0.12	-0.08	-0.11	-0.34	-0.76
7	NM_001326	CSTF3	0	0	-0.09	-0.16	-0.32	-0.48
7	NM_001336	CTSZ	0	0.15	-0.05	-0.16	-0.22	-1.14
7	NM_001350	DAXX	0	-0.04	-0.2	-0.18	-0.62	-0.57
7	NM_001397	ECE1	0	0.14	-0.01	-0.08	-0.37	-0.64
7	NM_001419	ELAVL1	0	-0.27	-0.26	-0.32	-0.51	-0.49
7	NM_001467	SLC37A4	0	-0.05	-0.26	-0.39	-0.65	-0.32
7	NM_001499	GLE1L	0	0.18	-0.09	-0.13	-0.42	-0.32
7	NM_001500	GMDS	0	-0.31	-0.19	-0.26	-0.34	-0.51
7	NM_001521	GTF3C2	0	-0.06	-0.28	-0.06	-0.39	-0.66
7	NM_001649	APXL	0	-0.08	-0.24	-0.58	-0.28	-0.66
7	NM_001659	ARF3	0	0.08	-0.14	-0.34	-0.4	-0.6
7	NM_001752	CAT	0	0.33	-0.13	-0.18	-0.17	-0.57
7	NM_001794	CDH4	0	0.13	-0.04	-0.32	-0.69	-0.5
7	NM_001955	EDN1	0	0.01	-0.27	-0.23	-0.32	-0.63
7	NM_001962	EFNA5	0	0	0.14	-0.15	-0.32	-0.75
7	NM_001994	F13B	0	0.12	-0.2	-0.21	-0.48	-0.54
7	NM_002070	GNAI2	0	-0.05	-0.15	-0.35	-0.47	-0.61
7	NM_002133	HMOX1	0	-0.11	-0.17	0.04	-0.37	-0.98
7	NM_002136	HNRPA1	0	-0.03	-0.11	-0.48	-0.58	-0.58
7	NM_002137	HNRPA2B	0	-0.06	-0.24	-0.32	-0.47	-0.73
7	NM_002224	ITPR3	0	0	-0.43	-0.19	-0.41	-0.43
7	NM_002396	ME2	0	-0.04	-0.21	-0.23	-0.54	-0.75
7	NM_002451	MTAP	0	0.14	-0.3	-0.43	-0.64	-0.35
7	NM_002469	MYF6	0	0.4	0.08	0	-0.48	-0.4
7	NM_002486	NCBP1	0	-0.08	-0.16	-0.3	-0.22	-0.81
7	NM_002533	NVL	0	-0.18	-0.33	-0.09	-0.4	-0.64
7	NM_002576	PAK1	0	0.13	-0.3	-0.49	-0.67	-0.56
7	NM_002654	PKM2	0	0.1	0.02	0.08	-0.47	-0.71
7	NM_002685	EXOSC10	0	0.02	-0.43	-0.17	-0.52	-0.64
7	NM_002708	PPP1CA	0	0.25	-0.03	-0.3	-0.31	-0.3
7	NM_002710	PPP1CC	0	-0.01	-0.16	-0.33	-0.44	-0.48
7	NM_002752	MAPK9	0	0.07	-0.15	-0.28	-0.3	-0.32
7	NM_002813	PSMD9	0	-0.2	-0.31	-0.29	-0.34	-0.52
7	NM_002851	PTPRZ1	0	0.09	-0.08	-0.33	-0.28	-0.45
7	NM_002855	PVRL1	0	-0.1	-0.17	-0.34	-0.53	-0.54
7	NM_002860	ALDH18A1	0	0.48	0.24	-0.02	-0.69	-0.55
7	NM_002890	RASA1	0	-0.26	-0.25	-0.28	-0.5	-0.49
7	NM_002947	RPA3	0	0.76	0.04	-0.14	-0.51	-0.73
7	NM_002986	CCL11	0	0.11	-0.35	-0.25	-0.33	-0.62
7	NM_003002	SDHD	0	0.25	-0.14	-0.17	-0.21	-0.76
7	NM_003018	SFTPC	0	-0.04	0.01	-0.32	-0.52	-0.41

7	NM_003087	SNCG	0	0	-0.19	-0.48	-0.72	-0.51
7	NM_003139	SRPR	0	-0.08	-0.18	-0.13	-0.37	-0.3
7	NM_003201	TFAM	0	0.03	-0.28	-0.21	-0.64	-0.47
7	NM_003345	UBE2I	0	-0.02	-0.25	-0.35	-0.5	-0.37
7	NM_003348	UBE2N	0	-0.03	-0.16	-0.45	-0.48	-0.69
7	NM_003364	UPP1	0	0.58	-0.25	-0.56	-0.67	-0.61
7	NM_003390	WEE1	0	0.19	-0.24	-0.26	-0.57	-0.62
7	NM_003420	ZNF35	0	-0.17	-0.23	-0.36	-0.43	-0.57
7	NM_003487	TAF15	0	-0.28	-0.17	-0.19	-0.25	-0.68
7	NM_003653	COPS3	0	-0.08	-0.12	-0.37	-0.41	-0.4
7	NM_003757	EIF3S2	0	0.25	-0.01	-0.29	-0.3	-1.06
7	NM_003761	VAMP8	0	0.02	-0.31	-0.02	-0.36	-0.85
7	NM_003774	GALNT4	0	0.12	-0.35	-0.28	-0.62	-0.61
7	NM_003816	ADAM9	0	0.15	0.08	0.13	-0.35	-0.62
7	NM_003883	HDAC3	0	0.33	-0.11	-0.28	-0.42	-0.45
7	NM_003902	FUBP1	0	0.07	-0.14	-0.52	-0.41	-0.32
7	NM_003909	CPNE3	0	0.23	-0.12	-0.36	-0.45	-0.93
7	NM_003910	G10	0	-0.08	-0.19	-0.45	-0.33	-0.53
7	NM_003914	CCNA1	0	-0.22	0.03	0.05	-0.35	-0.82
7	NM_003944	SELENBP	0	-0.01	0.25	0.16	-0.26	-0.65
7	NM_004044	ATIC	0	0.04	-0.21	-0.4	-0.54	-0.61
7	NM_004052	BNIP3	0	0.17	0.31	-0.36	-0.64	-0.46
7	NM_004074	COX8A	0	0.08	-0.16	-0.39	-0.58	-0.59
7	NM_004077	CS	0	0.09	-0.37	-0.44	-0.39	-0.53
7	NM_004106	FCER1G	0	0.09	-0.31	-0.29	-0.71	-0.48
7	NM_004140	LLGL1	0	-0.09	-0.19	-0.21	-0.46	-0.36
7	NM_004146	NDUFB7	0	0.06	-0.12	-0.1	-0.26	-1.03
7	NM_004206	SEC22L3	0	0.1	-0.22	-0.33	-0.49	-0.44
7	NM_004260	RECQL4	0	0.3	-0.2	-0.15	-0.49	-0.68
7	NM_004278	PIGL	0	-0.16	-0.31	-0.25	-0.47	-0.62
7	NM_004285	H6PD	0	0.16	0.15	-0.33	-0.67	-0.34
7	NM_004328	BCS1L	0	0.19	-0.27	-0.54	-0.58	-0.43
7	NM_004341	CAD	0	-0.05	-0.35	-0.28	-0.48	-0.45
7	NM_004401	DFFA	0	-0.23	-0.28	-0.36	-0.55	-0.44
7	NM_004454	ETV5	0	0.06	-0.21	-0.54	-0.38	-0.67
7	NM_004553	NDUFS6	0	0.07	-0.13	-0.25	-0.32	-0.44
7	NM_004704	RNU3IP2	0	0.15	-0.15	-0.33	-0.49	-0.65
7	NM_004724	ZW10	0	0.19	-0.34	-0.3	-0.39	-0.59
7	NM_004739	MTA2	0	-0.15	-0.16	-0.34	-0.41	-0.37
7	NM_004750	CRLF1	0	0.29	0.08	-0.07	-0.56	-0.62
7	NM_004765	BCL7C	0	0.28	-0.09	-0.38	-0.54	-0.47
7	NM_004774	PPARBP	0	-0.07	-0.14	-0.16	-0.52	-0.35
7	NM_004819	SYMPK	0	-0.08	-0.21	-0.16	-0.29	-0.43
7	NM_004891	MRPL33	0	0.05	0	-0.27	-0.4	-0.45
7	NM_004892	SEC22L1	0	0.19	-0.09	0.01	-0.46	-0.63
7	NM_004964	HDAC1	0	0.15	-0.11	-0.37	-0.38	-0.7
7	NM_005109	OXSR1	0	0	-0.15	-0.39	-0.48	-0.53
7	NM_005119	THRAP3	0	0.03	-0.1	-0.09	-0.32	-0.53
7	NM_005271	GLUD1	0	-0.08	-0.03	-0.24	-0.29	-0.42
7	NM_005333	HCCS	0	-0.05	-0.26	-0.35	-0.4	-0.4
7	NM_005335	HCLS1	0	-0.05	-0.24	-0.35	-0.66	-0.51
7	NM_005401	PTPN14	0	-0.01	-0.08	-0.48	-0.53	-0.75

7	NM_005481	THRAP5	0	-0.08	-0.22	-0.17	-0.27	-0.43
7	NM_005536	IMPA1	0	0.19	-0.25	-0.32	-0.41	-0.8
7	NM_005647	TBL1X	0	0.07	-0.04	-0.17	-0.39	-0.41
7	NM_005662	VDAC3	0	-0.18	-0.3	-0.24	-0.25	-0.65
7	NM_005805	PSMD14	0	-0.16	-0.29	-0.57	-0.44	-0.37
7	NM_005884	PAK4	0	0.08	-0.18	-0.51	-0.72	-0.57
7	NM_005898	M11S1	0	-0.13	-0.14	-0.21	-0.31	-0.3
7	NM_005905	SMAD9	0	0.35	-0.15	-0.44	-0.41	-0.55
7	NM_006076	HRBL	0	0.48	-0.03	0	-0.47	-0.71
7	NM_006247	PPP5C	0	0.01	-0.18	-0.37	-0.41	-0.28
7	NM_006283	TACC1	0	0.19	0	-0.15	-0.32	-0.54
7	NM_006341	MAD2L2	0	-0.05	-0.23	-0.45	-0.59	-0.42
7	NM_006405	TM9SF1	0	0.01	-0.18	-0.05	-0.38	-0.57
7	NM_006429	CCT7	0	-0.01	-0.1	-0.35	-0.41	-0.34
7	NM_006443	C6orf108	0	0.07	-0.11	-0.47	-0.49	-0.73
7	NM_006596	POLQ	0	-0.19	-0.21	-0.34	-0.51	-0.52
7	NM_006706	TCERG1	0	0.04	-0.11	-0.39	-0.53	-0.4
7	NM_006759	UGP2	0	0.24	-0.33	-0.55	-0.5	-0.36
7	NM_006784	WDR3	0	0.02	-0.12	-0.39	-0.33	-0.5
7	NM_006819	STIP1	0	0.01	-0.19	-0.19	-0.39	-0.4
7	NM_006861	RAB35	0	-0.16	-0.18	-0.42	-0.31	-0.48
7	NM_006899	IDH3B	0	0.01	-0.22	-0.32	-0.29	-0.39
7	NM_006910	RBBP6	0	-0.1	-0.25	-0.22	-0.2	-0.68
7	NM_007002	ADRM1	0	-0.05	-0.31	-0.35	-0.33	-0.73
7	NM_007006	CPSF5	0	0.01	-0.09	-0.34	-0.69	-0.6
7	NM_007033	RER1	0	-0.13	-0.11	-0.12	-0.55	-0.63
7	NM_007042	RPP14	0	0.04	-0.25	-0.5	-0.31	-0.46
7	NM_007070	GLMN	0	-0.17	-0.29	-0.26	-0.28	-0.64
7	NM_007240	DUSP12	0	-0.13	-0.3	-0.35	-0.5	-0.43
7	NM_007254	PNKP	0	-0.05	-0.26	-0.23	-0.51	-0.36
7	NM_007375	TARDBP	0	0.13	-0.17	-0.23	-0.28	-0.56
7	NM_012089	ABCB10	0	0.16	-0.08	-0.3	-0.31	-0.55
7	NM_012117	CBX5	0	0.24	-0.05	-0.23	-0.48	-0.61
7	NM_012140	SLC25A1(	0	0.57	-0.18	-0.8	-0.46	-0.66
7	NM_012318	LETM1	0	-0.07	-0.2	-0.31	-0.47	-0.63
7	NM_012381	ORC3L	0	0.1	-0.41	-0.34	-0.48	-0.59
7	NM_012405	ICMT	0	0.04	-0.19	-0.2	-0.38	-0.61
7	NM_012456	TIMM10	0	0.15	0.05	-0.32	-0.4	-0.24
7	NM_013245	VPS4A	0	0.03	-0.18	-0.29	-0.48	-0.36
7	NM_013281	FLRT3	0	0.52	-0.1	-0.13	-0.31	-0.52
7	NM_013319	TERE1	0	-0.13	-0.17	-0.24	-0.51	-0.59
7	NM_013384	LASS2	0	0	0.09	-0.18	-0.47	-0.63
7	NM_013438	UBQLN1	0	-0.13	-0.26	-0.23	-0.38	-0.66
7	NM_013442	STOML2	0	0.09	-0.2	-0.31	-0.44	-0.67
7	NM_014002	IKBKE	0	-0.14	-0.25	-0.26	-0.61	-0.38
7	NM_014026	DCPS	0	-0.06	-0.26	-0.31	-0.42	-0.46
7	NM_014180	MRPL22	0	0.12	-0.44	-0.44	-0.59	-0.46
7	NM_014310	RASD2	0	-0.07	-0.47	-0.39	-0.48	-0.37
7	NM_014366	GNL3	0	-0.2	-0.24	-0.23	-0.46	-0.6
7	NM_014554	SENP1	0	0.01	-0.29	-0.24	-0.32	-0.61
7	NM_014612	C9orf10	0	-0.08	-0.08	-0.1	-0.25	-0.69
7	NM_014630	ZNF592	0	0.22	-0.25	-0.07	-0.51	-1.01

7	NM_014671	UBE3C	0	0.14	0.03	-0.2	-0.21	-0.51
7	NM_014708	KNTC1	0	0.56	-0.07	-0.26	-0.51	-0.72
7	NM_014962	BTBD3	0	0.45	-0.29	-0.24	-0.49	-0.61
7	NM_015362	DERP6	0	-0.24	-0.26	-0.31	-0.35	-0.66
7	NM_015456	COBRA1	0	-0.25	-0.36	-0.33	-0.38	-0.5
7	NM_015629	PRPF31	0	0.07	-0.1	-0.29	-0.52	-0.36
7	NM_015679	TRUB2	0	0.1	-0.18	-0.08	-0.3	-0.59
7	NM_015874	RBPSUH	0	-0.11	-0.09	-0.3	-0.45	-0.8
7	NM_015956	MRPL4	0	0.16	-0.02	-0.33	-0.37	-0.29
7	NM_015969	MRPS17	0	0.12	-0.17	-0.18	-0.45	-0.37
7	NM_015971	MRPS7	0	-0.11	-0.14	-0.13	-0.4	-0.38
7	NM_015989	CSAD	0	-0.17	-0.12	-0.35	-0.57	-0.47
7	NM_016048	ISOC1	0	0.06	-0.27	-0.43	-0.37	-0.6
7	NM_016086	DUSP24	0	0.1	-0.22	-0.32	-0.63	-0.67
7	NM_016222	DDX41	0	0.01	-0.03	-0.27	-0.49	-0.49
7	NM_016226	VPS29	0	0.28	-0.25	-0.35	-0.2	-0.64
7	NM_016263	FZR1	0	-0.01	-0.13	-0.06	-0.36	-0.41
7	NM_016271	RNF138	0	0.01	-0.15	-0.33	-0.41	-0.42
7	NM_016275	SELT	0	-0.02	-0.11	-0.25	-0.51	-0.64
7	NM_016281	TAOK3	0	-0.16	-0.33	-0.43	-0.48	-0.45
7	NM_016292	TRAP1	0	-0.03	-0.13	-0.3	-0.4	-0.56
7	NM_016299	HSPA14	0	-0.01	-0.14	-0.15	-0.19	-0.64
7	NM_016381	TREX1	0	0.02	-0.37	-0.39	-0.41	-0.61
7	NM_016422	RNF141	0	-0.04	-0.16	-0.22	-0.44	-0.67
7	NM_016486	LOC51249	0	-0.21	-0.16	-0.31	-0.33	-0.6
7	NM_016491	MRPL37	0	0.03	-0.22	-0.38	-0.51	-0.56
7	NM_016553	NUP62	0	0.1	-0.33	-0.15	-0.57	-0.45
7	NM_016594	FKBP11	0	-0.02	-0.12	-0.23	-0.39	-0.55
7	NM_016638	ARL6IP4	0	-0.03	-0.12	-0.32	-0.36	-0.39
7	NM_016653	ZAK	0	0.03	-0.1	-0.37	-0.4	-0.46
7	NM_016819	OGG1	0	0.04	-0.34	-0.35	-0.56	-0.39
7	NM_017409	HOXC10	0	-0.02	0.08	-0.09	-0.46	-0.51
7	NM_017410	HOXC13	0	0.29	0.21	0.04	-0.22	-0.88
7	NM_017421	COQ3	0	-0.06	-0.27	-0.32	-0.51	-0.45
7	NM_017590	RoXaN	0	0.1	-0.22	-0.4	-0.4	-0.43
7	NM_017668	NDE1	0	0.39	-0.3	-0.09	-0.63	-0.65
7	NM_017823	DUSP23	0	0.07	-0.07	-0.22	-0.23	-0.36
7	NM_017895	DDX27	0	-0.04	-0.08	-0.17	-0.32	-0.94
7	NM_017979	SMAP-1	0	-0.02	-0.15	-0.18	-0.29	-0.51
7	NM_018010	ESRRBL1	0	-0.04	0.01	-0.26	-0.56	-0.47
7	NM_018062	FANCL	0	0.01	-0.29	-0.21	-0.47	-0.69
7	NM_018124	NM_01812	0	0.07	-0.1	-0.27	-0.66	-0.76
7	NM_018157	hSyn	0	-0.06	-0.18	-0.09	-0.29	-0.48
7	NM_018163	FLJ10634	0	0.04	-0.26	-0.35	-0.6	-0.53
7	NM_018183	SBNO1	0	0.01	-0.18	-0.2	-0.57	-0.64
7	NM_018233	FLJ10826	0	-0.06	-0.25	-0.21	-0.43	-0.49
7	NM_018256	WDR12	0	0.35	0	-0.19	-0.32	-0.29
7	NM_018388	MBNL3	0	0.03	0	-0.3	-0.31	-0.78
7	NM_018592	NM_01859	0	-0.11	-0.15	-0.12	-0.39	-0.71
7	NM_018660	ZNF395	0	0.19	0.31	-0.37	-0.35	-0.86
7	NM_019014	POLR1B	0	0.02	-0.33	-0.13	-0.45	-0.6
7	NM_019105	TNXB	0	-0.03	0.07	0.21	-0.4	-0.62

7	NM_019842	KCNQ5	0	0.16	-0.3	-0.22	-0.57	-0.43
7	NM_020158	EXOSC5	0	0.04	-0.09	-0.35	-0.36	-0.69
7	NM_020362	HT014	0	-0.19	-0.25	-0.25	-0.42	-0.46
7	NM_020365	EIF2B3	0	0.25	-0.28	-0.33	-0.31	-0.41
7	U73377	SHC1	0	0.2	-0.05	-0.1	-0.35	-0.37
7	X05299	CENPB	0	0.03	-0.1	-0.26	-0.33	-0.62
7	X52005	MYL4	0	0.16	-0.06	0.29	-0.58	-1.12
8	AB002359	PFAS	0	0.03	-0.39	-0.52	-0.68	-0.75
8	AB006198	SART1	0	-0.09	-0.44	-0.34	-0.55	-0.77
8	AB023148	PHLPPL	0	-0.1	-0.22	-0.47	-0.39	-0.72
8	AB046829	KIAA1609	0	-0.16	-0.45	-0.56	-0.58	-0.75
8	AF000416	EXTL2	0	0.13	-0.81	-0.62	-0.63	-0.72
8	AF007152	ABHD3	0	-0.06	-0.58	-0.32	-0.55	-0.54
8	AF015592	CDC7	0	0.1	-0.58	-0.45	-0.77	-0.93
8	AF038183	D15Wsu7	0	-0.2	-0.33	-0.32	-0.58	-0.56
8	AF054996	IMP4	0	-0.24	-0.38	-0.32	-0.56	-0.67
8	AF055029	LOC15116	0	-0.17	-0.31	-0.1	-0.43	-1.17
8	AF059531	HRMT1L3	0	-0.22	-0.53	-0.33	-0.44	-0.71
8	AF070525	GRPEL1	0	-0.25	-0.19	-0.69	-0.65	-0.53
8	AF070559	LOC93081	0	-0.12	-0.48	-0.38	-0.81	-0.9
8	AF075119	CTMP	0	-0.42	-0.39	-0.24	-0.4	-0.93
8	AF086130	LOC44116	0	-0.32	-0.15	-0.28	-0.82	-0.87
8	AF116702	UBE3A	0	-0.31	-0.37	-0.42	-0.59	-0.62
8	AF130091	KCTD9	0	-0.34	-0.27	-0.42	-0.58	-0.69
8	AF143676	NRM	0	-0.09	-0.26	-0.51	-0.85	-1.06
8	AF147307	FLJ21687	0	-0.35	-0.37	-0.53	-0.67	-0.86
8	AF147311	NT5C	0	0.04	-0.14	-0.27	-0.57	-0.99
8	AF147374	ELAVL2	0	0.03	-0.23	-0.48	-0.61	-0.83
8	AF155657	GPSM3	0	-0.06	-0.28	-0.45	-0.82	-0.66
8	AF215923	RAP1GDS	0	0.03	-0.1	-0.44	-0.36	-1.02
8	AF218014	C8orf20	0	-0.2	-0.29	-0.24	-0.7	-0.93
8	AF233453	PRKCBP1	0	-0.21	-0.37	-0.39	-0.81	-0.8
8	AF265210	FANCE	0	-0.24	-0.61	-0.39	-0.5	-0.93
8	AF275798	CCT5	0	-0.06	-0.36	-0.49	-0.75	-0.65
8	AF282874	PVRL3	0	-0.29	-0.43	-0.19	-0.44	-0.87
8	AF283645	MFTC	0	-0.32	-0.43	-0.46	-0.48	-0.61
8	AF294326	CBFB	0	-0.08	-0.35	-0.57	-0.88	-0.51
8	AF301222	NY-REN-4	0	-0.18	-0.44	-0.41	-0.6	-0.7
8	AF304163	SH3BGRL	0	0.02	-0.05	-0.31	-0.8	-0.92
8	AF312678	FGFRL1	0	0.03	-0.53	-0.49	-0.77	-0.96
8	AJ006835	RNU17D	0	-0.5	-0.4	-0.44	-0.58	-0.72
8	AJ007015	NCL	0	-0.2	-0.15	-0.27	-0.55	-0.77
8	AJ227860	COTL1	0	-0.44	-0.54	-0.49	-0.58	-0.9
8	AJ290954	DMRTA1	0	0.14	-0.2	-0.28	-0.68	-0.87
8	AK000441	CXorf44	0	-0.09	-0.17	-0.62	-0.49	-0.71
8	AK000799	C14orf65	0	-0.16	-0.27	-0.32	-0.42	-0.92
8	AK001171	ELOF1	0	-0.32	-0.31	-0.3	-0.49	-0.55
8	AK001225	SHB	0	-0.17	-0.48	-0.49	-0.54	-0.73
8	AK001520	SPINK5L3	0	-0.17	-0.33	-0.51	-0.8	-0.63
8	AK001526	2'-PDE	0	-0.15	-0.47	-0.01	-0.5	-0.77
8	AK002107	RAB3B	0	-0.27	-0.45	-0.15	-0.68	-0.7
8	AK021945	MGC1320	0	-0.09	-0.23	-0.4	-0.79	-0.69

8	AK022241	FLJ10774	0	-0.14	-0.28	-0.27	-0.54	-0.86
8	AK022587	LAS1L	0	0.02	-0.23	-0.51	-0.46	-0.69
8	AK023018	AK023018	0	-0.21	-0.43	-0.4	-0.63	-0.86
8	AK023245	FLJ21144	0	-0.24	-0.58	-0.21	-0.65	-0.86
8	AK023335	FLJ13273	0	-0.28	-0.55	-0.21	-0.44	-1.22
8	AK023723	HS3ST3B1	0	-0.12	-0.29	-0.53	-0.78	-0.7
8	AK023843	PGF	0	-0.2	-0.43	-0.33	-0.54	-0.92
8	AK024137	FLJ14075	0	-0.04	-0.29	-0.28	-0.47	-0.85
8	AK024394	STK35	0	-0.21	-0.44	-0.38	-0.51	-0.95
8	AK024476	CHTF18	0	0.06	-0.38	-0.12	-0.87	-0.93
8	AK024512	FLJ20859	0	-0.16	-0.4	-0.15	-0.29	-1.24
8	AK024556	SPRY4	0	0.1	-0.48	-0.77	-0.67	-0.83
8	AK024689	HHIP	0	-0.16	-0.51	-0.67	-0.73	-0.71
8	AK024716	RRS1	0	-0.26	-0.33	-0.4	-0.48	-0.56
8	AK024747	CCDC5	0	-0.13	-0.37	-0.1	-0.95	-0.76
8	AK024750	NRIP3	0	-0.11	-0.5	-0.29	-0.66	-1.07
8	AK024917	DDAH1	0	-0.09	-0.34	-0.32	-0.73	-0.88
8	AK025470	RGNEF	0	0.09	-0.54	-0.34	-0.57	-0.93
8	AK025522	LOC44014	0	-0.22	-0.56	-0.45	-0.64	-0.7
8	AK025577	FLJ21924	0	-0.28	-0.37	-0.42	-0.68	-0.8
8	AK025639	FLJ21986	0	-0.16	-0.39	-0.29	-0.61	-0.91
8	AK025695	TMED8	0	-0.41	-0.61	-0.45	-0.69	-0.78
8	AK025712	ZNF574	0	-0.24	-0.39	-0.42	-0.64	-1.23
8	AK025905	SOX17	0	-0.04	-0.33	-0.47	-0.84	-0.67
8	AK025994	RHBDL6	0	-0.16	-0.34	-0.51	-0.36	-0.6
8	AK026046	SSB1	0	-0.15	-0.44	-0.35	-0.49	-0.75
8	AK026098	TSGA14	0	-0.11	-0.32	-0.32	-0.64	-0.63
8	AK026151	PRKCBP1	0	-0.26	-0.52	-0.34	-0.83	-0.88
8	AK026277	FLJ22624	0	-0.22	-0.42	-0.45	-0.64	-0.92
8	AK026593	C16orf33	0	0.02	-0.5	-0.58	-0.84	-0.88
8	AK026673	TTL	0	-0.28	-0.43	-0.34	-0.45	-0.68
8	AK026835	TFB2M	0	-0.32	-0.37	-0.38	-0.59	-0.45
8	AK027067	SUV39H2	0	0.45	-0.56	-0.42	-0.64	-0.88
8	AK027118	LOC90637	0	-0.32	-0.33	-0.29	-0.21	-1.03
8	AK027129	YRDC	0	-0.16	-0.73	-0.75	-0.61	-0.64
8	AL110170	LOC20091	0	-0.19	-0.26	-0.22	-0.42	-0.91
8	AL117607	LOC20327	0	-0.19	-0.36	-0.42	-0.52	-0.65
8	AL117629	WDR51A	0	0.07	-0.41	-0.4	-0.81	-0.91
8	AL137579	SNX26	0	-0.2	-0.35	-0.36	-0.5	-0.53
8	AL157480	SH3BP1	0	-0.03	-0.24	-0.67	-0.88	-0.8
8	AL160132	MGC3731	0	0.02	-0.38	-0.46	-0.74	-0.79
8	AL162049	USP10	0	-0.19	-0.28	-0.27	-0.51	-0.66
8	AL365411	LOC56931	0	-0.43	-0.3	-0.32	-0.49	-0.67
8	BC005219	NRAS	0	0.13	-0.41	-0.61	-0.56	-0.65
8	BC005946	TUBA6	0	-0.04	-0.42	-0.54	-0.63	-0.78
8	D17252	D17252	0	-0.12	-0.39	-0.39	-0.66	-1.03
8	D42046	DNA2L	0	0.16	-0.4	-0.55	-0.45	-0.7
8	D63487	KIAA0153	0	0.05	-0.28	-0.43	-0.64	-0.59
8	D79991	NUP188	0	-0.16	-0.47	-0.53	-0.7	-1.04
8	D82345	TMSL8	0	-0.04	-0.12	-0.23	-0.71	-0.78
8	L36587	L36587	0	-0.42	-0.51	-0.29	-0.58	-0.94
8	M23161	MCFD2	0	-0.01	-0.3	-0.5	-0.8	-0.75

8	NM_000057	BLM	0	-0.12	-0.4	-0.56	-1.24	-0.46
8	NM_000127	EXT1	0	-0.09	-0.31	-0.28	-0.65	-0.83
8	NM_000169	GLA	0	-0.12	-0.45	0.14	-0.68	-0.79
8	NM_000178	GSS	0	-0.03	-0.31	-0.64	-0.49	-0.82
8	NM_000185	SERPIND1	0	-0.39	-0.65	-0.46	-0.36	-0.84
8	NM_000268	NF2	0	0.04	-0.29	-0.37	-0.5	-0.77
8	NM_000274	OAT	0	-0.05	-0.34	-0.44	-0.57	-0.92
8	NM_000356	TCOF1	0	-0.09	-0.39	-0.43	-0.57	-0.44
8	NM_000400	ERCC2	0	-0.2	-0.38	-0.44	-0.56	-0.49
8	NM_000565	IL6R	0	0.03	-0.35	-0.12	-0.59	-0.84
8	NM_000666	ACY1	0	-0.29	-0.09	-0.56	-0.19	-0.87
8	NM_000745	CHRNA5	0	0.1	-0.63	-0.24	-0.4	-1.01
8	NM_000883	IMPDH1	0	-0.15	-0.52	-0.57	-0.39	-0.55
8	NM_000884	IMPDH2	0	0	0	-0.3	-0.41	-1.2
8	NM_000923	PDE4C	0	-0.17	-0.4	-0.47	-0.54	-0.63
8	NM_000958	PTGER4	0	-0.03	-0.28	-0.38	-0.63	-0.71
8	NM_001048	SST	0	0	-0.41	-0.56	-0.61	-0.6
8	NM_001114	ADCY7	0	0.09	-0.4	-0.68	-0.78	-0.83
8	NM_001269	CHC1	0	-0.32	-0.46	-0.3	-0.89	-0.89
8	NM_001323	CST6	0	-0.55	-0.29	0.11	-0.83	-1.21
8	NM_001333	CTSL2	0	-0.14	-0.25	-0.06	-0.59	-0.97
8	NM_001379	DNMT1	0	0.14	-0.36	-0.53	-1	-0.79
8	NM_001387	DPYSL3	0	-0.02	-0.38	-0.65	-0.95	-0.75
8	NM_001425	EMP3	0	-0.07	-0.14	-0.18	-0.51	-1.33
8	NM_001508	GPR39	0	-0.16	-0.27	-0.23	-0.84	-0.93
8	NM_001516	GTF2H3	0	-0.01	-0.21	-0.57	-0.63	-0.82
8	NM_001614	ACTG1	0	-0.38	-0.18	-0.37	-0.44	-0.65
8	NM_001689	ATP5G3	0	-0.01	-0.29	-0.39	-0.54	-0.69
8	NM_001707	BCL7B	0	-0.29	-0.46	-0.37	-0.54	-0.54
8	NM_001747	CAPG	0	-0.06	-0.27	-0.43	-0.77	-1.11
8	NM_001748	CAPN2	0	-0.17	-0.3	-0.5	-0.62	-0.77
8	NM_001814	CTSC	0	-0.01	-0.13	-0.26	-0.49	-1.01
8	NM_001821	CHML	0	-0.23	-0.46	-0.66	-0.68	-0.84
8	NM_001929	DGUOK	0	-0.29	-0.21	-0.42	-0.51	-0.74
8	NM_001932	MPP3	0	-0.23	-0.51	-0.32	-0.49	-0.65
8	NM_001950	E2F4	0	-0.3	-0.29	-0.36	-0.68	-0.5
8	NM_002109	HARS	0	-0.1	-0.38	-0.47	-0.57	-0.54
8	NM_002157	HSPE1	0	-0.02	-0.39	-0.44	-0.66	-0.59
8	NM_002205	ITGA5	0	-0.3	-0.41	-0.53	-0.72	-0.78
8	NM_002238	KCNH1	0	-0.02	-0.37	-0.41	-0.83	-0.9
8	NM_002256	KISS1	0	-0.32	-0.28	-0.39	-0.44	-0.96
8	NM_002410	MGAT5	0	-0.07	-0.28	-0.03	-0.34	-1.14
8	NM_002444	MSN	0	0.13	-0.34	-0.63	-0.7	-0.84
8	NM_002455	MTX1	0	-0.19	-0.39	-0.42	-0.59	-0.77
8	NM_002468	MYD88	0	-0.31	-0.37	-0.25	-0.45	-0.71
8	NM_002482	NASP	0	-0.23	-0.33	-0.65	-0.54	-0.92
8	NM_002532	NUP88	0	0.03	-0.32	-0.48	-0.43	-0.77
8	NM_002553	ORC5L	0	-0.11	-0.27	-0.24	-0.54	-0.7
8	NM_002668	PLP2	0	-0.21	-0.39	-0.26	-0.69	-1.02
8	NM_002687	PNN	0	-0.33	-0.41	-0.27	-0.26	-0.75
8	NM_002694	POLR2C	0	-0.26	-0.53	-0.44	-0.69	-0.69
8	NM_002737	PRKCA	0	0.13	-0.11	-0.32	-0.73	-0.88

8	NM_002755	MAP2K1	0	0.13	-0.16	-0.72	-0.66	-0.65
8	NM_002795	PSMB3	0	-0.07	-0.24	-0.39	-0.53	-1.01
8	NM_002829	PTPN3	0	-0.14	-0.31	-0.18	-0.59	-0.62
8	NM_002907	RECQL	0	0.1	-0.25	-0.51	-0.69	-0.77
8	NM_002949	MRPL12	0	0.14	-0.31	-0.52	-0.55	-0.88
8	NM_002953	RPS6KA1	0	-0.23	-0.53	-0.14	-0.65	-0.8
8	NM_003082	SNAPC1	0	0.04	-0.32	-0.32	-0.52	-1.2
8	NM_003090	SNRPA1	0	-0.34	-0.49	-0.49	-0.88	-0.8
8	NM_003095	SNRPF	0	-0.44	-0.2	-0.55	-0.4	-0.64
8	NM_003146	SSRP1	0	0.07	-0.26	-0.56	-0.76	-0.88
8	NM_003276	TMPO	0	0.13	-0.29	-0.66	-0.99	-0.55
8	NM_003311	PHLDA2	0	-0.16	-0.51	-0.61	-0.86	-0.76
8	NM_003329	TXN	0	-0.27	-0.32	-0.18	-0.73	-0.97
8	NM_003365	UQCRC1	0	-0.21	-0.31	-0.62	-0.51	-0.79
8	NM_003404	YWHAB	0	-0.17	-0.38	-0.24	-0.54	-0.58
8	NM_003463	PTP4A1	0	0.03	-0.44	-0.89	-0.54	-0.89
8	NM_003642	HAT1	0	-0.2	-0.65	-0.64	-0.52	-1.02
8	NM_003656	CAMK1	0	-0.06	-0.41	-0.52	-0.62	-0.46
8	NM_003687	PDLIM4	0	-0.29	-0.07	-0.49	-0.47	-0.83
8	NM_003815	ADAM15	0	-0.05	-0.2	-0.18	-0.64	-0.85
8	NM_003821	RIPK2	0	0.1	-0.43	-0.35	-0.73	-0.75
8	NM_003844	TNFRSF1(	0	0.05	-0.49	-0.35	-0.42	-0.79
8	NM_003875	GMPS	0	-0.12	-0.29	-0.68	-0.8	-0.79
8	NM_004053	BYSL	0	-0.17	-0.31	-0.42	-0.39	-0.62
8	NM_004247	U5-116KD	0	-0.14	-0.42	-0.58	-0.63	-0.65
8	NM_004427	PHC2	0	-0.1	-0.22	-0.52	-0.49	-0.91
8	NM_004674	ASH2L	0	-0.33	-0.45	-0.2	-0.52	-0.98
8	NM_004705	PRKRIR	0	-0.25	-0.27	-0.48	-0.51	-0.54
8	NM_004725	BUB3	0	-0.09	-0.44	-0.38	-0.67	-0.71
8	NM_004741	NOLC1	0	-0.35	-0.33	-0.44	-0.64	-0.77
8	NM_004804	WDR39	0	-0.09	-0.36	-0.46	-0.62	-0.67
8	NM_004875	POLR1C	0	-0.19	-0.39	-0.45	-0.63	-1.1
8	NM_004904	CREB5	0	-0.45	-0.5	-0.6	-0.64	-0.7
8	NM_004960	FUS	0	-0.18	-0.36	-0.63	-0.68	-0.95
8	NM_004965	HMGN1	0	-0.3	-0.37	-0.43	-0.7	-0.86
8	NM_004966	HNRPF	0	-0.15	-0.1	-0.34	-0.32	-1.12
8	NM_005033	EXOSC9	0	0.08	-0.37	-0.71	-0.94	-0.73
8	NM_005045	RELN	0	-0.02	-0.54	-0.36	-0.74	-1.01
8	NM_005049	PWP2H	0	-0.3	-0.61	-0.5	-0.48	-0.55
8	NM_005124	NUP153	0	-0.17	-0.29	-0.51	-0.54	-0.79
8	NM_005134	PPP4R1	0	-0.02	-0.46	-0.51	-0.43	-1.1
8	NM_005156	ROD1	0	-0.29	-0.47	-0.37	-0.59	-0.85
8	NM_005219	DIAPH1	0	-0.01	-0.45	-0.62	-0.78	-0.69
8	NM_005444	RQCD1	0	-0.27	-0.41	-0.32	-0.53	-0.82
8	NM_005452	C6orf11	0	-0.23	-0.27	-0.12	-0.38	-0.82
8	NM_005499	UBA2	0	-0.1	-0.51	-0.6	-0.53	-0.77
8	NM_005510	DOM3Z	0	-0.11	-0.34	-0.14	-0.57	-1.02
8	NM_005520	HNRPH1	0	-0.35	-0.37	-0.09	-0.57	-0.86
8	NM_005585	SMAD6	0	-0.03	-0.6	-0.42	-0.67	-0.99
8	NM_005717	ARPC5	0	-0.31	-0.36	-0.4	-0.48	-0.57
8	NM_005723	TSPAN5	0	-0.11	-0.17	-0.43	-0.59	-0.7
8	NM_005837	POP7	0	-0.22	-0.46	-0.38	-0.78	-0.78

8	NM_005968	HNRPM	0	-0.08	-0.3	-0.43	-0.47	-0.72
8	NM_006002	UCHL3	0	-0.19	-0.35	-0.51	-0.67	-0.91
8	NM_006117	PECI	0	-0.04	-0.45	-0.43	-0.46	-1.14
8	NM_006191	PA2G4	0	-0.3	-0.4	-0.55	-0.51	-0.99
8	NM_006203	PDE4D	0	-0.45	-0.33	-0.73	-0.7	-0.61
8	NM_006245	PPP2R5D	0	-0.14	-0.24	-0.25	-0.44	-0.77
8	NM_006322	TUBGCP3	0	0.14	-0.36	-0.3	-0.42	-0.85
8	NM_006367	CAP1	0	0.09	-0.42	-0.52	-0.57	-0.71
8	NM_006392	NOL5A	0	-0.14	-0.34	-0.32	-0.45	-1.26
8	NM_006395	APG7L	0	-0.15	-0.27	-0.67	-0.79	-0.71
8	NM_006452	PAICS	0	-0.07	-0.29	-0.48	-0.6	-1.12
8	NM_006459	SPFH1	0	-0.07	-0.22	-0.4	-0.74	-1.04
8	NM_006503	PSMC4	0	-0.14	-0.36	-0.45	-0.76	-0.62
8	NM_006516	SLC2A1	0	-0.08	-0.07	-0.51	-0.64	-0.75
8	NM_006570	RRAGA	0	-0.22	-0.28	-0.26	-0.5	-0.71
8	NM_006670	TPBG	0	0.02	-0.17	-0.54	-0.9	-0.83
8	NM_006747	SIPA1	0	0.1	-0.3	-0.3	-0.51	-0.98
8	NM_006806	BTG3	0	-0.03	-0.19	-0.46	-0.73	-0.8
8	NM_006808	SEC61B	0	0	-0.35	-0.38	-0.64	-1.12
8	NM_006839	IMMT	0	-0.05	-0.14	-0.3	-0.52	-0.97
8	NM_006845	KIF2C	0	-0.15	-0.21	-0.54	-0.92	-0.97
8	NM_006947	SRP72	0	-0.14	-0.31	-0.56	-0.51	-0.85
8	NM_007040	HNRPUL1	0	0.01	-0.17	-0.11	-0.31	-1.12
8	NM_007192	SUPT16H	0	-0.05	-0.23	-0.32	-0.5	-0.8
8	NM_007208	MRPL3	0	-0.09	-0.3	-0.39	-0.48	-0.79
8	NM_007217	PDCD10	0	-0.37	-0.48	-0.52	-0.61	-0.74
8	NM_007260	LYPLA2	0	0.04	-0.2	-0.38	-0.52	-0.97
8	NM_007279	U2AF2	0	-0.24	-0.3	-0.45	-0.55	-0.7
8	NM_012091	ADAT1	0	-0.25	-0.5	-0.36	-0.73	-0.97
8	NM_012099	ASE-1	0	-0.25	-0.75	-0.63	-0.61	-0.83
8	NM_012247	SEPHS1	0	-0.05	-0.33	-0.43	-0.82	-0.61
8	NM_012310	KIF4A	0	0.14	-0.25	-0.49	-0.97	-0.78
8	NM_013248	NXT1	0	0.11	-0.46	-0.52	-0.69	-0.64
8	NM_013393	FTSJ2	0	-0.19	-0.5	-0.38	-0.58	-0.53
8	NM_013447	EMR2	0	-0.16	-0.19	-0.39	-0.94	-0.53
8	NM_014052	YWHAB	0	-0.32	-0.47	-0.31	-0.54	-0.9
8	NM_014092	RBM15	0	-0.45	-0.32	-0.48	-0.53	-0.61
8	NM_014143	CD274	0	0.17	-0.35	-0.65	-0.66	-0.55
8	NM_014239	EIF2B2	0	-0.41	-0.45	-0.4	-0.46	-1.06
8	NM_014339	IL17R	0	-0.02	-0.22	-0.39	-0.67	-0.76
8	NM_014363	SACS	0	0.02	-0.41	-0.48	-0.65	-0.81
8	NM_014445	SERP1	0	-0.25	-0.33	-0.35	-0.47	-0.56
8	NM_014501	UBE2S	0	-0.06	-0.38	-0.53	-0.83	-0.88
8	NM_014521	SH3BP4	0	-0.21	-0.41	-0.4	-0.39	-0.84
8	NM_014705	DOCK4	0	-0.23	-0.72	-0.5	-0.69	-0.65
8	NM_014711	CP110	0	0.14	-0.53	-0.24	-0.13	-1.3
8	NM_014771	RNF40	0	-0.26	-0.37	-0.07	-0.38	-0.92
8	NM_014833	POM121	0	-0.23	-0.32	-0.34	-0.64	-0.76
8	NM_014889	PITRM1	0	-0.17	-0.33	-0.33	-0.63	-1.02
8	NM_014963	KIAA0963	0	-0.29	-0.34	-0.47	-0.59	-0.62
8	NM_015509	NECAP1	0	-0.06	-0.38	-0.58	-0.67	-0.94
8	NM_015640	PAI-RBP1	0	0.11	-0.27	-0.54	-0.42	-0.95

8	NM_015697	COQ2	0	0.07	-0.35	-0.49	-0.64	-0.75
8	NM_015884	MBTPS2	0	-0.33	-0.34	-0.17	-0.56	-0.69
8	NM_015938	NMD3	0	-0.35	-0.33	-0.34	-0.48	-0.61
8	NM_015960	CUTC	0	-0.37	-0.36	-0.34	-0.55	-0.58
8	NM_015972	POLR1D	0	-0.09	-0.42	-0.37	-0.56	-0.89
8	NM_016034	MRPS2	0	-0.2	-0.26	-0.35	-0.6	-0.58
8	NM_016072	GOLT1B	0	-0.02	-0.29	-0.18	-0.44	-1.02
8	NM_016095	Pfs2	0	-0.13	-0.4	-0.58	-0.78	-0.71
8	NM_016126	C1orf41	0	-0.07	-0.27	-0.36	-0.48	-0.71
8	NM_016146	TRAPPC4	0	-0.31	-0.44	-0.64	-0.67	-0.78
8	NM_016171	PTMA	0	0.06	-0.46	-0.22	-0.79	-1.04
8	NM_016195	MPHOSPH	0	-0.35	-0.52	-0.38	-0.66	-0.98
8	NM_016338	IPO11	0	-0.03	-0.23	-0.85	-0.57	-0.57
8	NM_017425	SPA17	0	0.01	-0.41	-0.26	-0.52	-0.76
8	NM_017444	CHRAC1	0	-0.08	-0.16	-0.39	-0.56	-0.71
8	NM_017518	NM_01751	0	-0.21	-0.48	-0.38	-0.48	-0.55
8	NM_017645	FAM29A	0	-0.27	-0.54	-0.43	-0.81	-0.92
8	NM_017647	FTSJ3	0	-0.17	-0.42	-0.49	-0.57	-0.67
8	NM_017721	FLJ20241	0	-0.31	-0.35	-0.4	-0.31	-0.82
8	NM_017735	FLJ20272	0	-0.01	-0.39	-0.45	-0.49	-0.6
8	NM_017746	TEX10	0	-0.13	-0.27	-0.49	-0.95	-0.57
8	NM_017755	NSUN2	0	-0.24	-0.55	-0.5	-0.61	-0.72
8	NM_017802	FLJ20397	0	-0.18	-0.19	-0.36	-0.43	-1.2
8	NM_017807	OSGEP	0	-0.38	-0.53	-0.51	-0.43	-0.64
8	NM_017819	RG9MTD1	0	-0.61	-0.62	-0.47	-0.69	-0.74
8	NM_017845	COMMD8	0	-0.19	-0.34	-0.32	-0.38	-0.73
8	NM_017853	TXNL4B	0	-0.41	-0.42	-0.36	-0.49	-0.56
8	NM_017906	PAK1IP1	0	-0.54	-0.51	-0.39	-0.59	-0.89
8	NM_017998	C9orf40	0	0.09	-0.33	-0.37	-0.56	-0.78
8	NM_018060	FLJ10326	0	-0.07	-0.11	-0.26	-0.36	-1.02
8	NM_018122	FLJ10514	0	-0.07	-0.41	-0.58	-0.58	-0.85
8	NM_018192	LEPREL1	0	-0.13	-0.49	-0.41	-0.6	-1.08
8	NM_018270	C20orf20	0	0.13	-0.23	-0.47	-0.76	-0.63
8	NM_018319	TDP1	0	-0.17	-0.41	-0.3	-0.81	-1.07
8	NM_018390	PLCXD1	0	-0.3	-0.56	-0.44	-0.64	-0.61
8	NM_018509	PRO1855	0	-0.02	-0.46	-0.56	-0.7	-0.83
8	NM_019109	ALG1	0	-0.12	-0.36	-0.15	-0.41	-0.78
8	NM_019117	KLHL4	0	-0.17	-0.27	-0.36	-0.69	-0.76
8	NM_020153	FLJ21827	0	-0.11	-0.23	-0.24	-0.52	-0.96
8	NM_020230	PPAN	0	0.11	-0.26	-0.41	-0.68	-0.92
8	NM_020315	PDXP	0	-0.19	-0.33	-0.46	-0.66	-0.65
8	NM_020401	NUP107	0	0.16	-0.32	-0.48	-0.86	-0.72
8	NM_030752	TCP1	0	-0.07	-0.36	-0.41	-0.65	-0.55
8	S81522	EEF1B2	0	-0.15	-0.27	-0.52	-0.6	-0.6
8	U12597	TRAF2	0	-0.16	-0.43	-0.12	-0.75	-0.74
8	U27655	RGS3	0	-0.62	-0.78	-0.47	-0.72	-0.66
8	U62823	U62823	0	-0.06	-0.28	-0.37	-0.75	-0.89
8	U81002	C15orf23	0	0.13	-0.56	-0.44	-0.61	-0.8
8	Z36811	Z36811	0	-0.15	-0.44	-0.33	-0.62	-0.97
9	AB010098	CORO2B	0	-0.46	-0.47	-0.49	-0.95	-1.42
9	AB014574	KIAA0674	0	-1.01	-0.38	-0.43	-0.97	-1.6
9	AB037715	FRMD4A	0	-0.04	-0.45	-0.47	-0.85	-1.09

9	AB040927	SH3MD2	0	-0.72	-0.45	-0.7	-0.84	-0.77
9	AB050716	LCN7	0	0.04	-0.8	-0.54	-0.91	-1.05
9	AF052109	AF052109	0	-0.29	-0.44	-0.36	-1.2	-1.21
9	AF086164	AF086164	0	-0.43	-0.54	-0.54	-1.02	-1.01
9	AF086526	AF086526	0	-0.38	-0.67	-0.7	-1.08	-1.21
9	AF118124	MCL1	0	-0.66	-0.81	-0.63	-0.65	-0.88
9	AF169796	RAD18	0	-0.42	-0.51	-0.65	-0.8	-1.1
9	AF301463	SMURF2	0	-0.25	-0.75	-0.62	-0.61	-0.92
9	AK001630	ETS1	0	-0.89	-0.89	-0.8	-0.92	-1.38
9	AK002195	ARHGAP1	0	-0.26	-0.65	-0.88	-1.21	-1.34
9	AK021604	C12orf2	0	-0.52	-0.8	-0.71	-0.74	-1.03
9	AK021705	LOC13988	0	-0.59	-0.44	-0.36	-0.88	-0.98
9	AK022738	AK022738	0	-0.29	-0.79	-0.59	-1.13	-1.17
9	AK022872	DCLRE1B	0	0.06	-0.53	-0.87	-1.04	-1.06
9	AK023043	E2F7	0	0.08	-0.72	-0.65	-0.99	-1.09
9	AK023106	SLC25A22	0	-0.13	-0.34	-0.66	-1.02	-1.01
9	AK023408	C20orf172	0	-0.15	-0.68	-0.49	-1.18	-1.42
9	AK023726	ACD	0	-0.28	-0.62	-0.62	-1.03	-0.91
9	AK023881	ARPC5L	0	-0.68	-0.6	-0.9	-0.69	-0.78
9	AK024292	SGOL1	0	-0.35	-0.66	-0.44	-1.26	-1.31
9	AK024326	MGC2603	0	-0.16	-0.45	-0.78	-1.31	-0.99
9	AK024361	FLJ14299	0	-0.28	-0.54	-0.41	-0.85	-0.98
9	AK024577	KBTBD2	0	-0.27	-0.32	-0.79	-1.08	-1.25
9	AK024598	AKAP12	0	-0.94	-0.62	-1.13	-1.15	-1.16
9	AK025489	FLJ40869	0	-0.7	-0.81	-0.45	-0.69	-1.1
9	AK025523	C2orf26	0	-0.56	-0.82	-1.07	-0.88	-1.55
9	AK025624	ANP32E	0	-0.84	-0.41	-0.58	-0.85	-1.53
9	AK025798	LOC20354	0	-0.46	-0.56	-0.46	-0.71	-1.28
9	AK025835	AK025835	0	-0.21	-0.82	-0.4	-0.25	-1.71
9	AK026068	ASAM	0	-0.04	-0.32	-0.51	-0.99	-1.15
9	AK026181	AK026181	0	-0.08	-0.35	-1.14	-1.36	-0.99
9	AK026447	FLJ22794	0	-0.94	-0.79	-0.86	-0.7	-1.66
9	AK026813	STEAP2	0	-0.08	-0.43	-0.56	-0.8	-1.05
9	AK027065	C20orf59	0	-0.4	-0.71	-0.45	-0.94	-1.21
9	AL080156	TIPARP	0	-0.58	-0.71	-1.21	-1.29	-1.11
9	AL133651	C19orf14	0	-0.14	-0.54	-0.38	-0.9	-1.08
9	AL137555	C9orf88	0	-0.38	-0.38	-0.78	-0.97	-1.27
9	AL162035	LOC81691	0	-0.17	-0.63	-0.56	-0.87	-0.85
9	BI769977	ANXA2	0	-0.26	-0.7	-0.63	-0.85	-0.71
9	D16988	CALM2	0	-0.22	-0.27	-0.65	-1.05	-0.91
9	D31765	POP1	0	-0.15	-0.64	-0.62	-1.02	-1.09
9	D31885	ARL6IP	0	-0.03	-0.55	-0.32	-1.08	-1.43
9	D80008	KIAA0186	0	0.09	-0.59	-0.67	-0.92	-1.16
9	J03048	HPX	0	-0.19	-0.25	-0.54	-1.09	-1.37
9	L39061	TAF1B	0	-0.43	-0.45	-0.94	-0.62	-0.99
9	M73239	HGF	0	-0.29	-0.46	-0.41	-0.91	-1.09
9	NM_000167	GK	0	-0.57	-0.37	-0.44	-0.98	-0.87
9	NM_000251	MSH2	0	-0.03	-0.49	-0.77	-1.06	-1.07
9	NM_000322	RDS	0	-0.02	-0.45	-0.52	-0.67	-1.23
9	NM_000346	SOX9	0	-0.11	-0.48	-0.93	-1.26	-1.18
9	NM_000759	CSF3	0	-0.16	-0.48	-0.98	-1.11	-0.86
9	NM_000903	NQO1	0	-0.33	-0.5	-0.14	-1.08	-1.7

9	NM_001066	TNFRSF1I	0	-0.49	-0.59	-0.73	-0.91	-1.25
9	NM_001211	BUB1B	0	-0.29	-0.66	-0.36	-0.99	-1.58
9	NM_001233	CAV2	0	-0.08	-0.41	-0.51	-0.91	-0.95
9	NM_001283	AP1S1	0	-0.39	-0.4	-0.68	-0.88	-0.89
9	NM_001709	BDNF	0	-0.77	-0.98	-0.84	-1.07	-1.05
9	NM_001758	CCND1	0	-0.09	-0.24	-0.89	-1.23	-1.39
9	NM_001790	CDC25C	0	-0.06	-0.46	-0.39	-1.23	-1.21
9	NM_001813	CENPE	0	-0.06	-0.58	-0.73	-1.1	-1.21
9	NM_001905	CTPS	0	-0.22	-0.64	-0.87	-0.98	-1.12
9	NM_001983	ERCC1	0	-0.09	-0.52	-0.89	-1.07	-1.25
9	NM_002089	CXCL2	0	-0.56	-0.89	-0.84	-1.06	-1.26
9	NM_002149	HPCAL1	0	-0.35	-0.48	-0.57	-0.98	-1.32
9	NM_002266	KPNA2	0	-0.03	-0.51	-0.49	-1.2	-1.36
9	NM_002620	PF4V1	0	-0.11	-0.5	-0.7	-1.15	-0.78
9	NM_002756	MAP2K3	0	-0.55	-0.84	-0.97	-1.36	-1.25
9	NM_002771	PRSS3	0	-0.35	-0.6	-0.69	-0.56	-1.41
9	NM_002819	PTBP1	0	-0.47	-0.66	-0.89	-1.05	-1.21
9	NM_002835	PTPN12	0	-0.26	-0.32	-0.49	-0.66	-1.23
9	NM_002875	RAD51	0	-0.13	-0.34	-0.72	-0.92	-1.18
9	NM_002883	RANGAP1	0	-0.32	-0.8	-0.56	-1.18	-1.24
9	NM_002916	RFC4	0	-0.13	-0.8	-0.68	-1.25	-1.11
9	NM_002999	SDC4	0	-0.29	-0.38	-0.85	-1.24	-1.05
9	NM_003028	SHB	0	-0.14	-0.33	-0.5	-0.81	-1.24
9	NM_003056	SLC19A1	0	-0.32	-0.55	-0.7	-1.15	-1.3
9	NM_003137	SRPK1	0	-0.05	-0.46	-0.54	-0.99	-1.4
9	NM_003370	VASP	0	-0.28	-0.5	-0.78	-0.69	-0.94
9	NM_003405	YWHAH	0	-0.31	-0.65	-0.71	-0.98	-1.23
9	NM_003505	FZD1	0	-0.37	-0.66	-0.89	-0.88	-1.13
9	NM_003541	HIST1H4K	0	-0.15	-0.29	-0.71	-1.23	-1.39
9	NM_003579	RAD54L	0	0.03	-0.59	-0.7	-1.03	-0.94
9	NM_003633	ENC1	0	-0.34	-0.77	-1.17	-1.14	-0.8
9	NM_003798	CTNNAL1	0	-0.53	-0.66	-0.39	-0.75	-0.98
9	NM_003878	GGH	0	-0.11	-0.31	-0.48	-1.15	-1.3
9	NM_004526	MCM2	0	-0.03	-0.49	-0.73	-1.26	-1.26
9	NM_004566	PFKFB3	0	-0.27	-0.38	-0.87	-0.83	-0.95
9	NM_004595	SMS	0	-0.01	-0.45	-0.72	-1.18	-1.42
9	NM_004603	STX1A	0	-0.23	-0.51	-0.81	-0.9	-0.77
9	NM_004635	MAPKAPK	0	-0.34	-0.64	-0.57	-0.87	-1.31
9	NM_004697	PRPF4	0	-0.16	-0.61	-0.56	-0.8	-1.47
9	NM_004702	CCNE2	0	-0.21	-0.51	-0.92	-0.91	-1.1
9	NM_005026	PIK3CD	0	-0.13	-0.41	-0.71	-0.88	-0.88
9	NM_005032	PLS3	0	-0.46	-0.68	-0.97	-0.7	-1.47
9	NM_005066	SFPQ	0	-0.28	-0.59	-0.88	-0.78	-0.97
9	NM_005102	FEZ2	0	-0.22	-0.4	-0.61	-0.63	-1.35
9	NM_005211	CSF1R	0	-0.17	-0.54	-0.58	-0.79	-0.92
9	NM_005226	EDG3	0	-0.33	-0.23	-0.64	-1.03	-1.39
9	NM_005230	ELK3	0	-0.58	-0.42	-0.84	-1.07	-1.41
9	NM_005261	GEM	0	-0.5	-0.81	-0.58	-0.89	-1.07
9	NM_005281	GPR3	0	-0.6	-0.62	-0.9	-0.67	-0.98
9	NM_005431	XRCC2	0	0.05	-0.56	-0.72	-1.31	-1.06
9	NM_005496	SMC4L1	0	-0.51	-0.72	-0.65	-1.23	-1.26
9	NM_005563	STMN1	0	-0.16	-0.84	-0.44	-0.79	-1.04

9	NM_006086	TUBB3	0	0.04	-0.37	-0.76	-1.04	-1.05
9	NM_006114	TOMM40	0	-0.23	-0.52	-0.61	-0.83	-1.04
9	NM_006496	GNAI3	0	-0.19	-0.56	-0.51	-0.74	-1.01
9	NM_006527	SLBP	0	-0.42	-0.66	-0.74	-1.06	-1.22
9	NM_006938	SNRPD1	0	-0.03	-0.4	-0.65	-0.81	-1.56
9	NM_007027	TOPBP1	0	-0.2	-0.6	-0.74	-0.85	-1.38
9	NM_007075	WDR45	0	-0.66	-0.74	-0.64	-0.68	-0.83
9	NM_007370	RFC5	0	-0.02	-0.62	-0.52	-0.99	-1.14
9	NM_012081	ELL2	0	-0.14	-0.5	-0.6	-0.95	-1.08
9	NM_012333	MYCBP	0	0.02	-0.43	-0.57	-0.88	-1.05
9	NM_012383	OSTF1	0	-0.2	-0.43	-0.64	-0.65	-1.17
9	NM_012429	SEC14L2	0	-0.15	-0.22	-0.87	-0.95	-0.77
9	NM_012482	ZNF281	0	-0.63	-0.91	-0.82	-1	-0.89
9	NM_013241	FHOD1	0	-0.2	-0.86	-0.47	-0.88	-1.47
9	NM_013285	GNL2	0	-0.19	-0.54	-0.58	-0.63	-1.25
9	NM_013381	TRHDE	0	-0.51	-0.72	-0.73	-0.87	-1.25
9	NM_014096	SLC43A3	0	-0.45	-0.56	-0.46	-1.12	-1.15
9	NM_014252	SLC25A15	0	-0.2	-0.6	-0.68	-0.83	-0.85
9	NM_014316	CARHSP1	0	-0.12	-0.39	-0.42	-1.08	-0.91
9	NM_014317	TPRT	0	-0.09	-0.46	-0.58	-0.69	-1.1
9	NM_014325	CORO1C	0	-0.43	-0.75	-0.6	-0.9	-0.96
9	NM_014463	LSM3	0	-0.46	-0.41	-0.52	-0.76	-1.1
9	NM_015895	GMNN	0	0.01	-0.62	-0.45	-0.8	-1.07
9	NM_015908	ARS2	0	-0.67	-0.76	-0.65	-0.93	-1.43
9	NM_015934	NOP5/NOL	0	-0.24	-0.32	-0.39	-0.64	-1.33
9	NM_015984	UCHL5	0	-0.51	-0.55	-0.56	-0.7	-0.88
9	NM_016025	DREV1	0	-0.05	-0.5	-0.76	-0.95	-1.25
9	NM_016113	TRPV2	0	-0.1	-0.53	-0.49	-0.98	-0.83
9	NM_016240	SCARA3	0	-0.14	-0.86	-0.8	-1.06	-1.25
9	NM_016310	POLR3K	0	-0.09	-0.59	-0.52	-0.94	-1.12
9	NM_016391	HSPC111	0	-0.23	-0.54	-0.63	-0.76	-1.12
9	NM_016404	HSPC152	0	-0.14	-0.46	-1.16	-0.97	-0.81
9	NM_016434	RTEL1	0	-0.2	-0.28	-0.99	-1.12	-1.13
9	NM_016445	PLEK2	0	-0.14	-0.72	-0.83	-1.23	-0.97
9	NM_016448	RAMP	0	0.21	-0.5	-0.85	-1.01	-1.2
9	NM_016545	IER5	0	-0.28	-0.69	-0.8	-1.28	-1.13
9	NM_016639	TNFRSF12	0	-0.25	-0.58	-0.9	-0.84	-0.59
9	NM_017723	FLJ20245	0	-0.04	-0.93	-0.7	-1.03	-0.91
9	NM_017816	LYAR	0	-0.39	-0.73	-0.68	-0.7	-1.04
9	NM_017882	CLN6	0	-0.34	-0.58	-0.67	-0.84	-0.91
9	NM_018057	SLC6A15	0	-0.16	-0.79	-0.09	-0.97	-1.39
9	NM_018098	ECT2	0	-0.25	-0.59	-0.62	-0.97	-1.06
9	NM_018186	FLJ10706	0	-0.03	-0.43	-0.65	-1.1	-1.15
9	NM_018324	THEDC1	0	-0.37	-0.28	-0.57	-0.85	-1.26
9	NM_018455	BM039	0	-0.08	-0.43	-0.74	-1.11	-1.18
9	NM_018518	MCM10	0	-0.01	-0.66	-0.92	-1.34	-0.87
9	NM_018584	CaMKIINa	0	-0.3	-0.55	-0.95	-1.07	-1.2
9	NM_018946	NANS	0	-0.28	-0.68	-0.69	-0.76	-1.16
9	NM_019005	FLJ20323	0	0.02	-0.39	-0.71	-0.92	-1.16
9	NM_019025	SMOX	0	-0.29	-0.24	-0.75	-0.63	-1.41
9	NM_019847	ANKH	0	-0.02	-0.07	-0.94	-1.05	-0.86
9	NM_020156	C1GALT1	0	-0.43	-0.54	-0.27	-0.66	-1.33

9	NM_020380	CASC5	0	-0.24	-0.31	-0.45	-1.08	-1.06
9	NM_020529	NFKBIA	0	-0.53	-0.82	-0.85	-1.3	-1.19
9	U52054	EMB	0	-0.38	-0.44	-0.82	-1.14	-1.35
9	U94354	LFNG	0	-0.31	-0.58	-1.14	-1.4	-0.96
9	X58377	IL11	0	-0.72	-0.83	-0.99	-0.79	-0.9
9	X67155	KIF23	0	-0.64	-0.7	-0.77	-1.54	-1.15
9	X79986	X79986	0	-0.32	-0.38	-0.84	-1.17	-1.18
9	X91221	SLC8A1	0	-0.44	-0.53	-0.6	-0.93	-1.07
9	Z36789	Z36789	0	-0.42	-0.27	-0.12	-0.52	-1.67
10	AB024704	TPX2	0	0.07	-0.69	-0.77	-1.42	-2.01
10	AB035124	CENPH	0	0.01	-0.41	-0.86	-1.56	-1.87
10	AB037784	AADACL1	0	-0.35	-0.91	-0.97	-1.23	-1.37
10	AF025441	OIP5	0	-0.14	-0.47	-0.46	-1.3	-1.5
10	AF086324	CARD10	0	-0.45	-0.45	-0.69	-1.31	-1.46
10	AF087966	CCBE1	0	-0.32	-0.57	-0.46	-1.3	-1.51
10	AF169351	PTPRQ	0	-0.15	-0.93	-1.34	-1.57	-1.83
10	AF192403	ELTD1	0	-0.14	-0.86	-0.95	-1.65	-1.77
10	AK001164	AK001164	0	-0.23	-0.64	-0.74	-0.99	-1.73
10	AK001379	ASPM	0	0.02	-0.47	-0.86	-1.71	-1.7
10	AK001469	GNPNAT1	0	-0.36	-0.6	-1.13	-1.34	-1.42
10	AK001581	FLJ10719	0	-0.19	-0.73	-0.84	-1.61	-1.7
10	AK021443	AK021443	0	-0.45	-0.66	-0.83	-1.63	-2.27
10	AK022611	PCNT1	0	-0.19	-0.49	-0.42	-1.52	-1.31
10	AK022613	FANCD2	0	0.02	-0.24	-0.46	-1.59	-1.85
10	AK023035	FLJ12973	0	-0.14	-0.57	-0.99	-1.52	-1.95
10	AK023998	FLJ25416	0	-0.32	-0.92	-1.09	-1.58	-1.7
10	AK026100	AK026100	0	0.26	-0.29	-1.1	-1.59	-1.65
10	AK027121	MLF1IP	0	-0.39	-0.72	-0.72	-1.26	-1.7
10	BE874471	VIM	0	-0.25	-0.93	-1.21	-1.72	-2.12
10	D12485	ENPP1	0	-0.05	-1.06	-1.03	-1.23	-1.3
10	D17184	H2A	0	-0.16	-0.38	-0.85	-1.59	-1.87
10	D28450	H2AFZ	0	-0.09	-0.51	-0.66	-1.36	-1.49
10	D38553	BRRN1	0	-0.26	-0.97	-1	-1.86	-1.98
10	D55716	MCM7	0	-0.06	-0.7	-0.91	-1.68	-1.8
10	D86978	NUP205	0	0.09	-0.69	-0.65	-1.29	-1.4
10	M59040	CD44	0	-0.1	-0.33	-0.51	-1.1	-2.04
10	M96577	E2F1	0	-0.56	-0.5	-0.71	-1.6	-1.85
10	NM_000946	PRIM1	0	0.09	-0.64	-0.59	-1.32	-1.57
10	NM_001033	RRM1	0	0.02	-0.43	-0.83	-1.44	-1.6
10	NM_001165	BIRC3	0	0.07	-0.61	-1.31	-1.76	-1.06
10	NM_001274	CHEK1	0	-0.17	-0.59	-0.8	-1.26	-1.4
10	NM_001699	AXL	0	-0.39	-0.51	-0.67	-1.28	-1.79
10	NM_001743	CALM2	0	-0.43	-0.6	-0.58	-1.25	-1.78
10	NM_001789	CDC25A	0	-0.11	-1.06	-1.09	-1.66	-2.05
10	NM_001798	CDK2	0	-0.38	-0.65	-0.87	-1.47	-1.33
10	NM_001946	DUSP6	0	0.17	-0.1	-1.67	-1.64	-1.57
10	NM_002131	HMGA1	0	-0.46	-0.57	-0.62	-1.48	-2.15
10	NM_002185	IL7R	0	-0.23	-0.98	-0.68	-1.43	-1.35
10	NM_002421	MMP1	0	-0.63	-1.04	-0.84	-1.44	-1.96
10	NM_002526	NT5E	0	0.14	-0.46	-0.82	-1.74	-1.59
10	NM_002592	PCNA	0	0.36	-0.35	-1.59	-1.68	-1.38
10	NM_002632	PGF	0	-0.36	-0.95	-1.12	-1.2	-1.85

10	NM_002867	RAB3B	0	-0.34	-1.02	-0.48	-1.68	-1.43
10	NM_002872	RAC2	0	0.03	-0.29	-0.9	-1.39	-2.06
10	NM_002915	RFC3	0	-0.07	-0.55	-1.08	-1.88	-1.69
10	NM_003046	SLC7A2	0	-0.34	-0.66	-1.48	-1.33	-1.34
10	NM_003115	UAP1	0	0.03	-0.91	-0.87	-1.3	-1.42
10	NM_003202	TCF7	0	-0.3	-1.14	-0.17	-1.35	-1.85
10	NM_003318	TTK	0	0.19	-0.69	-0.56	-1.45	-1.73
10	NM_003384	VRK1	0	-0.13	-0.59	-0.64	-1.17	-1.69
10	NM_003511	HIST1H2A	0	-0.24	-0.53	-0.9	-1.85	-1.76
10	NM_003520	HIST1H2B	0	-0.05	-0.59	-0.61	-1.35	-1.62
10	NM_003523	HIST1H2B	0	-0.33	-0.5	-0.91	-1.69	-2.21
10	NM_003686	EXO1	0	0.18	-0.6	-0.98	-1.27	-1.31
10	NM_003981	PRC1	0	0.91	-0.49	-0.43	-1.71	-2.19
10	NM_004336	BUB1	0	-0.16	-0.47	-0.67	-1.78	-2.09
10	NM_004811	LPXN	0	-0.41	-1.44	-0.52	-1.91	-2.02
10	NM_005100	AKAP12	0	-0.4	-0.73	-1.01	-1.31	-1.36
10	NM_005192	CDKN3	0	-0.45	-0.78	-1.13	-1.68	-1.94
10	NM_005320	HIST1H1D	0	0.09	-0.35	-0.84	-1.64	-1.68
10	NM_005325	HIST1H1A	0	0.05	-0.7	-0.98	-1.61	-1.88
10	NM_005566	LDHA	0	-0.67	-1.2	-0.37	-1.18	-1.74
10	NM_006101	KNTC2	0	-0.18	-0.7	-0.76	-1.39	-1.52
10	NM_006231	POLE	0	-0.29	-0.63	-0.48	-1.41	-1.59
10	NM_006397	RNASEH2	0	-0.16	-0.55	-0.76	-1.28	-1.61
10	NM_006739	MCM5	0	-0.05	-0.68	-0.89	-1.66	-1.82
10	NM_006829	C10orf116	0	-0.1	-0.22	-0.34	-1.15	-2.04
10	NM_006851	GLIPR1	0	-0.51	-0.67	-0.82	-1.53	-1.65
10	NM_007057	ZWINT	0	-0.37	-0.69	-0.8	-1.56	-1.8
10	NM_007211	C12orf2	0	-0.01	-0.48	-0.59	-1.12	-1.63
10	NM_007317	KIF22	0	0.02	-0.53	-0.68	-1.45	-1.99
10	NM_007350	PHLDA1	0	-0.42	-0.65	-1.11	-1.66	-1.64
10	NM_012242	DKK1	0	0.08	-0.88	-0.81	-1.67	-1.77
10	NM_012302	LPHN2	0	0.04	-0.23	-0.64	-1.18	-1.65
10	NM_012417	PITPNC1	0	-0.36	-0.86	-1.24	-1.51	-1.46
10	NM_014029	RAC2	0	0.17	-0.21	-1.58	-1.79	-1.98
10	NM_014109	ATAD2	0	0.08	-0.32	-0.94	-1.86	-1.99
10	NM_014321	ORC6L	0	-0.28	-0.76	-0.97	-1.3	-1.65
10	NM_014750	DLG7	0	-0.33	-0.61	-0.73	-1.39	-1.93
10	NM_014783	ARHGAP1	0	-0.58	-0.75	-0.69	-1.75	-1.89
10	NM_016109	ANGPTL4	0	-0.13	-0.18	-1.84	-1.61	-1.47
10	NM_016352	CPA4	0	0.06	-0.63	-0.09	-1.22	-1.85
10	NM_016539	SIRT6	0	-0.39	-0.53	-0.75	-1.36	-1.44
10	NM_017915	FLJ20641	0	-0.1	-0.97	-0.73	-1.31	-1.45
10	NM_017955	CDCA4	0	-0.47	-0.6	-0.81	-1.66	-1.62
10	NM_018101	CDCA8	0	-0.03	-0.65	-0.49	-1.39	-2.17
10	NM_018154	ASF1B	0	-0.09	-0.79	-1.07	-1.71	-2.11
10	NM_018685	ANLN	0	-0.4	-0.51	-0.47	-1.38	-1.62
10	NM_020183	ARNTL2	0	-0.25	-0.62	-0.89	-1.33	-2.01
10	NM_020238	INCENP	0	-0.13	-0.62	-0.59	-1.29	-1.53
10	S68954	MT1G	0	-0.08	-0.27	-0.57	-1.44	-1.51
10	U35622	ETV4	0	-0.25	-0.58	-0.99	-1.6	-1.59
10	U90908	ARHGAP2	0	0.21	-0.49	-1.34	-1.66	-1.59
10	X74794	MCM4	0	0.07	-0.38	-0.76	-1.43	-1.63

10	X75684	TM4SF1	0	-0.3	-0.8	-0.26	-1.36	-1.5
10	X97261	MT1L	0	-1.1	-0.21	-0.74	-1.4	-1.75
10	Z25433	PLK4	0	0.22	-0.28	-0.41	-1.52	-1.77
11	AB040957	KIAA1524	0	0.38	-0.67	-0.78	-1.51	-2.54
11	AF070552	CDT1	0	-0.02	-0.71	-0.98	-1.75	-2.63
11	AF235023	HCAP-G	0	-0.22	-0.72	-1.06	-1.96	-2.29
11	AJ001348	LY6K	0	-0.27	-1.1	-1.01	-2.72	-3.69
11	AJ223352	HIST1H2B	0	-0.31	-0.62	-0.94	-1.77	-2.29
11	AK001380	ASPM	0	0.16	-0.48	-0.44	-1.77	-2.44
11	AK002114	DEPDC1B	0	-0.05	-0.57	-0.86	-1.63	-2.36
11	AL136794	RACGAP1	0	-0.2	-0.66	-0.66	-1.79	-2.41
11	AY009951	HHIP	0	-0.48	-1.5	-1.57	-2.41	-2.96
11	D14678	KIFC1	0	-0.06	-0.73	-0.64	-2.14	-2.68
11	L19778	HIST1H2A	0	-0.02	-0.8	-1.03	-2.36	-2.98
11	M25753	CCNB1	0	-0.03	-0.78	-0.78	-1.92	-2.45
11	NM_000270	NP	0	0.02	-0.95	-2.06	-2.17	-2.45
11	NM_001034	RRM2	0	-0.13	-0.79	-1.04	-2.21	-2.82
11	NM_001067	TOP2A	0	-0.16	-0.5	-0.48	-1.92	-2.72
11	NM_001237	CCNA2	0	-0.3	-0.69	-0.96	-1.91	-2.46
11	NM_001255	CDC20	0	0	-0.81	-0.82	-2.29	-3.4
11	NM_002276	KRT19	0	0.02	-0.71	-0.99	-1.94	-2.43
11	NM_003258	TK1	0	0.39	-0.35	-0.83	-1.88	-2.4
11	NM_003504	CDC45L	0	-0.09	-0.42	-1.06	-1.94	-2.16
11	NM_003509	HIST1H2A	0	-0.15	-0.74	-1.21	-2.44	-3.5
11	NM_003513	HIST1H2A	0	-0.23	-0.56	-1.13	-1.94	-2.45
11	NM_003521	HIST1H2B	0	-0.3	-0.82	-1.62	-3.02	-3.96
11	NM_003522	HIST1H2B	0	-0.15	-0.65	-1.36	-2.19	-3.29
11	NM_003525	HIST1H2B	0	-0.3	-0.64	-0.89	-1.89	-3.03
11	NM_003529	HIST1H3A	0	0.08	-0.45	-1.21	-2.07	-2.48
11	NM_003531	HIST1H3C	0	-0.02	-0.48	-1.18	-2.52	-3.44
11	NM_003533	HIST1H3I	0	-0.58	-0.84	-0.74	-1.73	-2.53
11	NM_003534	HIST1H3G	0	0.06	-0.51	-1.24	-2.46	-3.44
11	NM_003535	HIST1H3J	0	-0.08	-0.75	-1.06	-2.35	-3.46
11	NM_003537	HIST1H3B	0	-0.07	-0.51	-1.08	-2.37	-3.26
11	NM_003538	HIST1H4A	0	-0.13	-0.62	-1.17	-1.92	-2.45
11	NM_003544	HIST1H4B	0	0.05	-0.32	-0.84	-1.43	-2.57
11	NM_004217	AURKB	0	0.28	-0.48	-0.79	-2.03	-3.44
11	NM_004523	KIF11	0	-0.39	-0.9	-0.99	-1.82	-2.24
11	NM_004701	CCNB2	0	-0.05	-0.57	-0.64	-1.92	-3
11	NM_005030	PLK1	0	-0.27	-0.79	-0.89	-1.93	-2.49
11	NM_005322	HIST1H1B	0	-0.24	-0.58	-1.13	-2.66	-3.81
11	NM_005328	HAS2	0	0.02	-0.92	-1.2	-2	-2.1
11	NM_005429	VEGFC	0	-0.4	-1.26	-1.55	-2.1	-2.73
11	NM_005573	LMNB1	0	0	-0.43	-0.56	-2.12	-2.57
11	NM_005593	MYF5	0	0.9	0.06	-0.58	-1.77	-2.56
11	NM_005978	S100A2	0	-0.2	-0.65	-0.94	-1.79	-2.46
11	NM_006342	TACC3	0	-0.84	-0.81	-0.77	-1.99	-2.95
11	NM_006461	SPAG5	0	-0.13	-0.83	-0.67	-2.74	-2.36
11	NM_006528	TFPI2	0	0.05	-0.8	-0.64	-2.15	-2.32
11	NM_007019	UBE2C	0	-0.26	-0.77	-0.82	-2.51	-3.04
11	NM_014791	MELK	0	-0.04	-0.79	-1.08	-1.85	-2.47
11	NM_016359	NUSAP1	0	-0.26	-0.54	-0.6	-1.81	-2.31

11	NM_018131	C10orf3	0	-0.18	-0.82	-0.78	-2.08	-3.06
11	NM_018410	DKFZp762	0	-0.32	-0.93	-0.97	-2.31	-2.86
11	NM_145904	HMGA1	0	-0.35	-0.57	-0.83	-1.38	-2.5
11	U17077	BENE	0	-0.05	-1.32	-1.42	-2.07	-2.26
11	U26662	NPTX2	0	0.03	-0.32	-0.76	-2.02	-2.72
11	U27768	RGS4	0	-0.31	-0.92	-1.32	-2.26	-2.17
11	U74612	FOXM1	0	-0.03	-0.57	-0.62	-1.69	-2.49
12	AJ227912	DUSP1	0	-1.01	-1.17	-1.49	-1.58	-1.61
12	AL117565	AXUD1	0	-2.06	-1.87	-1.85	-1.45	-1.91
12	D16875	RHOB	0	-1.17	-1.1	-1.35	-1.36	-1.71
12	M14584	IL6	0	-1.17	-1.02	-1.08	-1.21	-1.25
12	NM_000710	BDKRB1	0	-0.55	-1.08	-1.55	-1.87	-2.24
12	NM_001570	IRAK2	0	-0.99	-1.01	-0.86	-1.08	-1.39
12	NM_001717	BNC1	0	-0.76	-1.3	-1.65	-1.79	-1.94
12	NM_001886	CRYBA4	0	-1.02	-1.09	-1.47	-1.34	-1.23
12	NM_001964	EGR1	0	-0.5	-0.89	-1.28	-1.06	-1.41
12	NM_002050	GATA2	0	-0.68	-1.3	-1.17	-1.2	-1.2
12	NM_002203	ITGA2	0	-0.39	-1.1	-1.28	-1.37	-1.3
12	NM_003897	IER3	0	-1.85	-1.7	-1.72	-1.75	-1.66
12	NM_004040	RHOB	0	-1.11	-0.92	-1.2	-1.14	-1.32
12	NM_004203	PKMYT1	0	-0.5	-1.07	-1.2	-1.85	-1.46
12	NM_004219	PTTG1	0	-1.67	-0.85	-0.67	-1.65	-1.95
12	NM_004405	DLX2	0	-1.35	-1.82	-1.92	-2.13	-1.97
12	NM_004417	DUSP1	0	-0.78	-1.1	-1.38	-1.43	-1.06
12	NM_004419	DUSP5	0	-1.1	-1.64	-1.82	-2.08	-1.77
12	NM_004431	EPHA2	0	-0.71	-1.07	-1.5	-2.14	-2.08
12	NM_004591	CCL20	0	-1.96	-1.56	-1.76	-2.01	-2.01
12	NM_005415	SLC20A1	0	-0.32	-0.84	-1.79	-1.74	-1.54
12	NM_005450	NOG	0	-0.84	-0.89	-1.14	-1.6	-1.6
12	NM_005475	LNK	0	-0.52	-0.97	-1.25	-1.69	-1.8
12	NM_005904	SMAD7	0	-1.4	-1.69	-1.69	-1.42	-1.71
12	NM_006290	TNFAIP3	0	-1.17	-1.21	-1	-1.11	-1.28
12	NM_006733	FSHPRH1	0	-0.82	-1.21	-1.26	-1.26	-1.77
12	NM_006809	TOMM34	0	-1.15	-0.76	-1.04	-1.2	-1.73
12	NM_012145	DTYMK	0	-0.76	-1.22	-0.9	-1.33	-1.87
12	NM_013246	CLCF1	0	-0.93	-1.56	-1.64	-1.65	-2.02
12	NM_013259	TAGLN3	0	-0.56	-1.19	-1.3	-1.25	-1.43
12	NM_013376	SERTAD1	0	-0.74	-0.81	-1.31	-1.28	-1.11
12	NM_015193	ARC	0	-1.03	-1.49	-1.43	-1.54	-1.46
12	NM_017975	FLJ10036	0	-1.11	-0.95	-1.11	-1.41	-2.04
13	D28449	ID3	0	-0.61	-1.68	-1.98	-3.09	-2.9
13	M17017	IL8	0	-3.02	-3.25	-3.63	-3.32	-3.57
13	NM_001523	HAS1	0	-0.56	-1.91	-2.38	-2.51	-2.6
13	NM_001657	AREG	0	-1.04	-1.54	-2.89	-3.43	-3.73
13	NM_002309	LIF	0	-2.02	-2.72	-2.76	-2.75	-2.78
13	NM_003155	STC1	0	-0.69	-1.03	-2.54	-2.82	-3.51
13	NM_004418	DUSP2	0	-1.85	-2.94	-3.16	-3.16	-2.83
13	NM_005438	FOSL1	0	-0.94	-1.64	-1.69	-2.45	-3.07

Supplementry Table 2 GO attributes by cluster

Cluster	P	P-adj	GO Attribute
0	2.50E-14	<0.001	0006936: muscle contraction
0	1.10E-10	<0.001	0007517: muscle development
0	5.50E-09	<0.001	0008307: structural constituent of muscle
0	5.50E-09	<0.001	0043292: contractile fiber
0	1.60E-07	<0.001	0006937: regulation of muscle contraction
0	2.30E-07	<0.001	0006941: striated muscle contraction
0	3.50E-07	<0.001	0005790: smooth endoplasmic reticulum/smooth ER
0	1.40E-06	<0.001	0051239: regulation of organismal physiological process
0	1.60E-06	<0.001	0005523: tropomyosin binding
0	3.60E-06	<0.001	0050874: organismal physiological process
0	4.40E-06	<0.001	0008092: cytoskeletal protein binding
0	8.00E-06	0.003	0009887: organogenesis
0	9.70E-06	0.003	0009653: morphogenesis
0	1.30E-05	0.004	0048513: organ development/development of an organ
0	1.40E-05	0.004	0030017: sarcomere
0	1.40E-05	0.004	0005509: calcium ion binding
0	1.70E-05	0.004	0030016: myofibril/striated muscle fiber/striated muscle fibre
0	2.10E-05	0.008	0005861: troponin complex
0	5.90E-05	0.033	0005865: striated muscle thin filament
0	5.90E-05	0.033	0006942: regulation of striated muscle contraction
0	6.10E-05	0.033	0015629: actin cytoskeleton
0	9.80E-05	0.049	0007275: development
1	2.40E-16	<0.001	0006936: muscle contraction
1	2.30E-14	<0.001	0007517: muscle development
1	1.20E-13	<0.001	0009887: organogenesis
1	3.40E-13	<0.001	0048513: organ development/development of an organ
1	5.90E-13	<0.001	0006941: striated muscle contraction
1	1.10E-11	<0.001	0009653: morphogenesis
1	2.80E-09	<0.001	0007275: development
1	4.60E-09	<0.001	0030017: sarcomere
1	6.40E-09	<0.001	0030016: myofibril/striated muscle fiber/striated muscle fibre
1	2.40E-08	<0.001	0043292: contractile fiber
1	3.80E-07	<0.001	0005515: protein binding/protein amino acid binding
1	5.20E-07	<0.001	0006937: regulation of muscle contraction
1	1.70E-06	0.001	0008307: structural constituent of muscle
1	5.70E-06	0.005	0005863: striated muscle thick filament
1	6.10E-06	0.005	0051239: regulation of organismal physiological process
1	1.10E-05	0.008	0050874: organismal physiological process
1	2.80E-05	0.021	0005578: extracellular matrix (sensu Metazoa)
1	3.80E-05	0.027	0031012: extracellular matrix
2	9.10E-06	0.009	0009653: morphogenesis
2	3.50E-05	0.023	0006695: cholesterol biosynthesis
3			
4	2.90E-08	<0.001	0007275: development
4	5.70E-08	<0.001	0009653: morphogenesis
4	1.50E-07	<0.001	0009887: organogenesis
4	4.20E-07	<0.001	0048513: organ development/development of an organ
4	2.40E-06	0.003	0005578: extracellular matrix (sensu Metazoa)
4	4.10E-06	0.003	0031012: extracellular matrix

4	4.10E-06	0.003	0006936:	muscle contraction
4	3.00E-05	0.013	0005583:	fibrillar collagen
4	6.50E-05	0.05	0000323:	lytic vacuole
4	6.50E-05	0.05	0005764:	lysosome
5	2.20E-05	0.007	0016126:	sterol biosynthesis
5	2.30E-05	0.031	0008970:	phospholipase A1 activity
5	4.20E-05	0.045	0008610:	lipid biosynthesis
5	4.30E-05	0.045	0006694:	steroid biosynthesis/steroidogenesis
6		0.05	0006325:	establishment and/or maintenance of chromatin architecture
7	7.50E-11	<0.001	0043231:	intracellular membrane-bound organelle
7	7.50E-11	<0.001	0043227:	membrane-bound organelle
7	1.50E-10	<0.001	0005737:	cytoplasm
7	4.60E-09	<0.001	0005622:	intracellular/protoplasm
7	1.80E-08	<0.001	0043226:	organelle
7	1.80E-08	<0.001	0043229:	intracellular organelle
7	4.00E-07	<0.001	0005654:	nucleoplasm
7	6.20E-07	<0.001	0015980:	energy deriv. by oxidation of org. compounds/chemoorganotrophy
7	7.00E-06	0.002	0044262:	cellular carbohydrate metabolism
7	1.00E-05	0.003	0006006:	glucose metabolism
7	1.10E-05	0.004	0044237:	cellular metabolism
7	1.20E-05	0.005	0006092:	main pathways of carbohydrate metabolism
7	1.40E-05	0.005	0000910:	cytokinesis/cell division
7	1.40E-05	0.005	0051301:	cell division
7	1.70E-05	0.005	0044238:	primary metabolism
7	3.00E-05	0.012	0019318:	hexose metabolism
7	3.70E-05	0.019	0005996:	monosaccharide metabolism
7	6.20E-05	0.03	0005739:	mitochondrion
7	7.10E-05	0.03	0043283:	biopolymer metabolism
7	0.0001	0.05	0006007:	glucose catabolism
8	1.20E-07	<0.001	0005730:	nucleolus
8	2.20E-06	0.002	0009127:	purine nucleoside monophosphate biosynthesis
8	2.20E-06	0.002	0009168:	purine ribonucleoside monophosphate biosynthesis
8	2.20E-06	0.002	0009167:	purine ribonucleoside monophosphate metabolism
8	2.20E-06	0.002	0009126:	purine nucleoside monophosphate metabolism
8	4.70E-06	0.006	0006396:	RNA processing
8	6.40E-06	0.006	0016072:	rRNA metabolism
8	6.60E-06	0.006	0009161:	ribonucleoside monophosphate metabolism
8	6.60E-06	0.006	0009156:	ribonucleoside monophosphate biosynthesis
8	1.10E-05	0.011	0009124:	nucleoside monophosphate biosynthesis
8	1.10E-05	0.011	0009123:	nucleoside monophosphate metabolism
8	1.30E-05	0.011	0016070:	RNA metabolism
8	2.30E-05	0.016	0007046:	ribosome biogenesis
8	3.40E-05	0.024	0046037:	GMP metabolism
8	3.40E-05	0.024	0006177:	GMP biosynthesis
8	5.40E-05	0.039	0006364:	rRNA processing
9	2.40E-07	0.001	0000279:	M phase/M-phase
9	6.60E-06	0.003	0006950:	response to stress
9	1.50E-05	0.011	0003684:	damaged DNA binding
9	1.60E-05	0.011	0007049:	cell cycle/cell-division cycle
9	2.10E-05	0.015	0006281:	DNA repair
9	2.90E-05	0.019	0000278:	mitotic cell cycle
9	4.10E-05	0.046	0006974:	response to DNA damage stimulus

10	3.50E-17	<0.001	0007049: cell cycle/cell-division cycle
10	1.60E-16	<0.001	0005694: chromosome
10	9.10E-15	<0.001	0000278: mitotic cell cycle
10	3.20E-14	<0.001	0006259: DNA metabolism
10	5.30E-13	<0.001	0000279: M phase/M-phase
10	3.50E-12	<0.001	0006260: DNA replication/DNA biosynthesis/DNA synthesis
10	3.90E-12	<0.001	0006261: DNA-dependent DNA replication
10	5.90E-12	<0.001	0007067: mitosis
10	7.10E-12	<0.001	0000087: M phase of mitotic cell cycle/M-phase of mitotic cell cycle
10	9.10E-11	<0.001	0000074: regulation of cell cycle/cell cycle control
10	1.90E-09	<0.001	0000910: cytokinesis/cell division
10	1.90E-09	<0.001	0051301: cell division
10	1.00E-08	<0.001	0005660: delta-DNA polymerase cofactor complex
10	1.80E-08	<0.001	0008283: cell proliferation
10	2.40E-08	<0.001	0005659: delta DNA polymerase complex
10	3.60E-08	<0.001	0000775: chromosome, pericentric region/centromere
10	8.70E-08	<0.001	0042575: DNA polymerase complex
10	1.80E-07	<0.001	0000086: G2/M transition of mitotic cell cycle
10	2.10E-07	<0.001	0030894: replisome
10	2.40E-07	<0.001	0051329: interphase of mitotic cell cycle
10	2.40E-07	<0.001	0051325: interphase/karyostasis/resting phase
10	2.60E-07	<0.001	0005657: replication fork/replication focus
10	3.50E-07	<0.001	0051338: regulation of transferase activity/transferase regulator
10	3.50E-07	<0.001	0045859: regulation of protein kinase activity
10	3.90E-07	<0.001	0043283: biopolymer metabolism
10	1.20E-06	<0.001	0000785: chromatin
10	1.40E-06	0.001	0050790: regulation of enzyme activity
10	1.60E-06	0.001	0000075: cell cycle checkpoint
10	1.60E-06	0.002	0000776: kinetochore
10	1.80E-06	0.002	0000079: regul. of cyclin dep. protein kinase activity/regul. of CDK activ
10	3.20E-06	0.003	0043228: non-membrane-bound organelle
10	3.20E-06	0.003	0043232: intracellular non-membrane-bound organelle
10	4.80E-06	0.004	0006271: DNA strand elongation/DNA replication elongation
10	7.60E-06	0.006	0008094: DNA-dep ATPase activity/DNA dep ATPase activity
10	7.70E-06	0.006	0005634: nucleus
10	9.60E-06	0.008	0006270: DNA replication initiation
10	1.10E-05	0.008	0000082: G1/S transition of mitotic cell cycle
10	1.40E-05	0.009	0006139: nucleobase, nucleoside, nucleotide and nucleic acid metabolism
10	2.00E-05	0.013	0031497:
10	2.60E-05	0.015	0051052: regulation of DNA metabolism
10	2.90E-05	0.028	0007093: mitotic checkpoint
10	3.10E-05	0.028	0005819: spindle
10	3.80E-05	0.036	0005663: DNA replication factor C complex
10	4.60E-05	0.037	0000786: nucleosome
10	5.00E-05	0.039	0007088: regulation of mitosis
10	6.00E-05	0.042	0006275: regulation of DNA replication
10	7.20E-05	0.046	0048519: negative regulation of biological process
11	1.20E-20	<0.001	0007049: cell cycle/cell-division cycle
11	3.60E-20	<0.001	0000279: M phase/M-phase
11	1.90E-19	<0.001	0000278: mitotic cell cycle
11	3.20E-19	<0.001	0007067: mitosis
11	4.20E-19	<0.001	0000087: M phase of mitotic cell cycle/M-phase of mitotic cell cycle

11	1.60E-16	<0.001	0000910: cytokinesis/cell division
11	1.60E-16	<0.001	0051301: cell division
11	1.00E-15	<0.001	0000074: regulation of cell cycle/cell cycle control
11	1.30E-14	<0.001	0006259: DNA metabolism
11	3.40E-11	<0.001	0006261: DNA-dependent DNA replication
11	6.10E-11	<0.001	0005694: chromosome
11	1.10E-10	<0.001	0006260: DNA replication/DNA biosynthesis/DNA synthesis
11	4.60E-10	<0.001	0000075: cell cycle checkpoint
11	2.60E-09	<0.001	0000086: G2/M transition of mitotic cell cycle
11	6.80E-09	<0.001	0005660: delta-DNA polymerase cofactor complex
11	1.60E-08	<0.001	0005659: delta DNA polymerase complex
11	2.80E-08	<0.001	0008283: cell proliferation
11	5.60E-08	<0.001	0042575: DNA polymerase complex
11	6.50E-08	<0.001	0043283: biopolymer metabolism
11	1.20E-07	<0.001	0051329: interphase of mitotic cell cycle
11	1.20E-07	<0.001	0051325: interphase/karyostasis/resting phase
11	2.20E-07	0.001	0007093: mitotic checkpoint
11	5.70E-07	0.001	0005634: nucleus
11	1.00E-06	0.003	0007088: regulation of mitosis
11	1.00E-06	0.003	0000079: regul. of cyclin dep. protein kinase activ./regul. of CDK activity
11	6.30E-06	0.01	0006270: DNA replication initiation
11	6.30E-06	0.01	0030894: replisome
11	6.50E-06	0.01	0000082: G1/S transition of mitotic cell cycle
11	7.40E-06	0.01	0005657: replication fork/replication focus
11	7.90E-06	0.01	0050794: regulation of cellular process
11	9.60E-06	0.013	0006139: nucleobase, nucleoside, nucleotide and nucleic acid metabolism
11	1.10E-05	0.013	0043228: non-membrane-bound organelle
11	1.10E-05	0.013	0043232: intracellular non-membrane-bound organelle
11	1.70E-05	0.015	0051052: regulation of DNA metabolism
11	1.80E-05	0.015	0005819: spindle
11	1.90E-05	0.015	0050789: regulation of biological process/regulation
11	1.90E-05	0.015	0051244: regulation of cellular physiological process
11	2.10E-05	0.016	0007052: mitotic spindle organization and biogenesis
11	2.10E-05	0.016	0007051: spindle organization and biogenesis
11	2.30E-05	0.028	0008284: positive regulation of cell proliferation
11	2.50E-05	0.028	0000786: nucleosome
11	2.80E-05	0.028	0005663: DNA replication factor C complex
11	3.00E-05	0.03	0051338: regulation of transferase activity/transferase regulator
11	3.00E-05	0.03	0045859: regulation of protein kinase activity
11	3.40E-05	0.03	0000785: chromatin
11	4.20E-05	0.036	0050791: regulation of physiological process
11	4.40E-05	0.038	0006275: regulation of DNA replication
11	4.80E-05	0.038	0042127: regulation of cell proliferation
11	6.10E-05	0.04	0006334: nucleosome assembly
12	6.70E-16	<0.001	0007049: cell cycle/cell-division cycle
12	1.50E-14	<0.001	0000278: mitotic cell cycle
12	6.60E-14	<0.001	0000279: M phase/M-phase
12	9.40E-13	<0.001	0000074: regulation of cell cycle/cell cycle control
12	9.50E-13	<0.001	0007067: mitosis
12	1.20E-12	<0.001	0000087: M phase of mitotic cell cycle/M-phase of mitotic cell cycle
12	2.80E-12	<0.001	0006259: DNA metabolism
12	2.60E-11	<0.001	0000910: cytokinesis/cell division

12	2.60E-11	<0.001	0051301: cell division
12	4.80E-11	<0.001	0000086: G2/M transition of mitotic cell cycle
12	3.10E-10	<0.001	0008283: cell proliferation
12	3.90E-10	<0.001	0000075: cell cycle checkpoint
12	4.00E-09	<0.001	0051329: interphase of mitotic cell cycle
12	4.00E-09	<0.001	0051325: interphase/karyostasis/resting phase
12	1.70E-08	<0.001	0006261: DNA-dependent DNA replication
12	2.30E-08	<0.001	0000079: regul. of cyclin dep. protein kinase activ./regul. of CDK activity
12	7.90E-08	<0.001	0043283: biopolymer metabolism
12	8.70E-08	<0.001	0008284: positive regulation of cell proliferation
12	1.10E-07	<0.001	0006260: DNA replication/DNA biosynthesis/DNA synthesis
12	1.90E-07	<0.001	0050794: regulation of cellular process
12	2.00E-07	<0.001	0007093: mitotic checkpoint
12	2.20E-07	<0.001	0000082: G1/S transition of mitotic cell cycle
12	3.00E-07	<0.001	0005694: chromosome
12	5.30E-07	<0.001	0050789: regulation of biological process/regulation
12	5.80E-07	<0.001	0042127: regulation of cell proliferation
12	9.30E-07	<0.001	0007088: regulation of mitosis
12	1.50E-06	<0.001	0051244: regulation of cellular physiological process
12	3.50E-06	0.001	0050791: regulation of physiological process
12	4.80E-06	0.001	0006139: nucleobase, nucleoside, nucleotide and nucleic acid metabolism
12	5.40E-06	0.001	0006950: response to stress
12	5.70E-06	0.002	0006270: DNA replication initiation
12	1.20E-05	0.006	0051242: positive regulation of cellular physiological process
12	1.40E-05	0.008	0048522: positive regulation of cellular process
12	1.50E-05	0.009	0051052: regulation of DNA metabolism
12	1.70E-05	0.009	0043119: positive regulation of physiological process
12	2.60E-05	0.018	0051338: regulation of transferase activity/transferase regulator
12	2.60E-05	0.018	0045859: regulation of protein kinase activity
12	2.70E-05	0.018	0005634: nucleus
12	4.10E-05	0.027	0006275: regulation of DNA replication
12	4.50E-05	0.027	0006793: phosphorus metabolism
12	4.50E-05	0.027	0006796: phosphate metabolism
12	5.90E-05	0.03	0008083: growth factor activity
13	1.00E-05	0.005	0008283: cell proliferation
13	1.60E-05	0.008	0007267: cell-cell signaling/cell-cell signalling
13	2.80E-05	0.012	0005576: extracellular region/extracellular
13	4.00E-05	0.017	0005102: receptor binding/receptor ligand
13	4.50E-05	0.018	0005125: cytokine activity
13	4.50E-05	0.018	0042221: response to chemical substance
13	6.00E-05	0.02	0042127: regulation of cell proliferation
13	8.10E-05	0.02	0005615: extracellular space/intercellular space
13	0.00021	0.041	0009628: response to abiotic stimulus
13	0.00022	0.041	0016477: cell migration

Supplementary Table 4: Predicted and Tested CRM Regions

region	chromosome	strand	start coordinate	stop coordinate
Positive control CRMs				
ACTA1 (prom)	1	+	225875728	225877726
CAV3	3	+	8749393	8751391
COX6A2	16	+	31346483	31348481
TNNT2	1	+	198077778	198079776
DMD	X	+	32981672	32983670
PhylCRM predictions				
ACTA1 (PhylCRM)	1	+	225852506	225854504
CSRP3	11	+	19179244	19181242
HSPB3	5	+	53787965	53789963
PDLIM3/SORBS2	4	+	186863082	186865080
CACNG1	17	+	62477578	62479576
MEF2C	5	+	88164527	88166525
Negative control regions				
MGLL	3	+	129031135	129033133
CLC	19	+	44947497	44949495
GAP43	3	+	116777470	116779468
CPM	12	+	67659795	67661793
BDKRB2	14	+	95762300	95764298
HBZ	16	+	148530	150528
EDG5	19	+	10199535	10201533
KRT1B	12	+	51369942	51371940
IGFBP4	17	+	35868970	35870968

Supplementary Methods

Supplementary Information is available on the Nature Methods website and on our lab website, http://the_brain.bwh.harvard.edu/.

A. Construction of length-matched background sets against which foreground gene sets are evaluated in Lever

The following procedure is similar to the procedure we described previously in a *Drosophila* context[1]. We first ordered the search regions in each gene set by length. We defined the "foreground regions" to be those regions upstream and downstream of the genes that belong to a given foreground Gene Set, and we defined the "non-foreground regions" to be the collection of all other regions (i.e., regions not upstream or downstream of genes that belong to a given foreground Gene Set). For each foreground region, we took the 2 non-foreground regions occurring directly above and below it in the length-based ranking as background regions. In the event that two or more foreground regions did not have background regions ranked between them, we continued to extend above and below them in the ranking so that the center of this local collection of background regions was the same as the center of their associated foreground regions. Hence, for each foreground region, we were able to initially associate 2 length-matched background regions. We measured the AUC statistic for the lengths of the foreground and the background gene regions accumulated thus far and repeated the procedure of adding more non-foreground regions to the background set of gene regions until this AUC was close to 0.5, and until the background set was at least 10 times as large (and up to 40 times as large) as the foreground set, so that the distribution of the lengths of the foreground set of gene regions is similar to that of the background set of gene regions. The "PhylCRM_preprocess" program that generates the length-matched background sets of gene regions has a user-defined tolerance for what "close" means; in this study, we employed a tolerance of ± 0.02, i.e., for all foreground and background gene sets

considered in this paper, we required an AUC between 0.48 and 0.52 when ranking the foreground and background genes according to their lengths (AUC = 0.5 implies no difference between the distribution of lengths of foreground genes and that of the background genes).

B. Description of PhylCRM scoring scheme

The increasing number of sequenced genomes provides the opportunity for improved identification of regulatory regions by scanning for noncoding loci under negative selective pressure. To accomplish this, the evolutionary conservation must be scored in a way that the evolutionary history of the organisms is appropriately quantified; conservation of a locus between species sharing a recent ancestor should be weighted less than conservation between species that diverged long ago.

1. Scoring scheme and algorithm, one motif

In this section, we develop the scoring scheme for the case of only of one motif; in Section 2 we extend the scoring scheme to incorporate multiple motifs.

We begin with some notation. Given a base sequence g of length L from the genome being searched for TF binding site motif matches, let $a^{(i)}$, $i \in \{1,..,n\}$ denote the sequences aligned to g from each of the n organisms under consideration. We use $(g_j \ldots g_{j+k-1})$ to denote the subsequence of g beginning at position j and of length k, and we use $\left(a_j^{(i)} \ldots a_{j+k-1}^{(i)}\right)$ to denote the corresponding subsequence in the i'th alignment to g. Similarly, let H denote the (n + 1) × $|L|$-dimensional matrix storing both g and the $a^{(i)}$; thus, $H_{0,\bullet} = g$, $H_{i,\bullet} = a^{(i)}$, and $H_{\bullet,j}$ denotes the alignment column at position j (note that the $\bullet$ is used here to denote the collection of all values for that index position; see **Supplementary Fig. 1a** online). Finally, let T be the tree indicating the phylogeny of g and the $a^{(i)}$, let $\{v_\delta\}$ denote the ancestral vertices in T, and let $\{\tau_\varepsilon\}$ denote the branch lengths (see **Supplementary Fig. 1b** online).

For a given TF binding site motif of length m, let $M(\alpha,j)$ be the $4\times m$ matrix indicating the probability of observing the letter $\alpha \in \{A,C,G,T\}$ at position $j = 1,..,m$ of the motif (i.e., M is the frequency-derived probability matrix[2]), and let $Q(\alpha)$ denote the genomic frequency of letter α. For each position $j \in \{1,\ldots,L\}$ of g, we evaluate the degree to which $(g_j,\ldots g_{j+m-1})$ matches M with the quantity[2]:

$$\textbf{Eqn. 1)} \qquad \lambda(j) = \sum_{k=j}^{j+m-1} \log_2\left(\frac{M(g_k,k)}{Q(g_k)}\right)$$

This quantity is the commonly used position weight matrix score[2]. If $\lambda(j)$ is greater than a user-specified cutoff c, which is usually set to 1 or 2 standard deviations below the motif mean for the standard likelihood ratio score of the PWM model M and the genomic frequencies given by Q, we evaluate the degree to which this motif match is conserved throughout the phylogeny using an evolutionary model first suggested by Halpern and Bruno[3] and developed by Moses, Eisen and colleagues[4,5] (henceforth referred to as the MEHB model). In their approach, the degree of evolutionary conservation for the match to the TF binding site motif is scored by taking the log-likelihood ratio of observing the given collection of sequences throughout the phylogeny under the MEHB model as compared to a neutral model of evolutionary change:

$$\textbf{Eqn. 2)} \qquad \varphi(j) = \sum_{k=j}^{j+m-1} \log_2\left(\frac{P_{MEHB}\left(H_{\bullet,k}\middle|T,M,Q\right)}{P_{neutral}\left(H_{\bullet,k}\middle|T,Q\right)}\right) - c$$

Here, $P_{MEHB}\left(H_{\bullet,k}\middle|T,M,Q\right)$ represents the probability of observing $H_{\bullet,k}$ under the evolutionary model where nucleotide substitutions occur along T with a frequency specified by the MEHB proportionality (i.e., with fewer changes expected at the most

conserved positions of the motif; see **Supplementary Fig. 1c** online), and $P_{neutral}\left(H_{\bullet,k}\middle|T,Q\right)$ represents the probability of observing $H_{\bullet,k}$ under a neutral evolutionary model (either Jukes-Cantor[6] or Hasegawa-Kishino-Yano[7]). We have schematized how these probabilities are computed for a small phylogenetic tree in **Supplementary Fig. 1c** online.

Let ξ be an array of length L (i.e., the same length as g) and initialized so that, for all j, $\xi(j) = 0$. When a match to the motif M is made (i.e., $\lambda(j) > c$) in g beginning at position j, then, for $k = j,.., j+m-1$, ξ is updated according to:

Eqn. 3) $$\xi(k) = \max(\varphi(j)/m, \xi(k))$$

Here, the max is taken so that, in the event of overlapping motif matches, both matches contribute to the score, but there is no double-counting of scores. This rationale is schematized in **Supplementary Fig. 1d** online, where $\xi(j)$ is schematized for a sequence g and motif M. Note that we shall refer to quantity $\xi(j)$ as the "positional score for M" at j.

We wish to find sub-windows of the base sequence g that have a statistically significant over-representation of high-scoring matches to M. We do this by deriving the probability distribution function of the sub-windows of a fixed size within an *a priori* specified size range that best fits our data. We then use this probability distribution function in order to evaluate the enrichment of better scoring sub-windows of this size as compared to a given query sub-window under consideration. We also use the derived probability distribution

functions in order to combine the scores from several motifs of interest in the Fuzzy Boolean logic framework (see Section **3.** below).

Specifically, for each window size we derive the shape and the parameters of the null distribution. This is done by fitting a mixture model of three probability distribution functions – Delta, Uniform and Gamma – on a collection of sequences g_b of total length L_b that are believed not to be enriched for matches to motif M (we henceforth refer to this as the "background" sequence). Briefly, the Delta function is used to model the jump in score that occurs when a window of genomic sequence contains the initial portion of a motif at its left-most or right-most edge; the Uniform distribution is used to model the increase in score that occurs as the window contains an increasingly greater portion of the motif at either of its edges; finally, the Gamma distribution is then used for the bulk of the distribution to model an increasing number of binding sites and their evolutionary conservation.

Let w_j be a window of sequence in g of length $|w|$ and beginning at position j; we wish to evaluate whether this window is enriched for instances of M. Consider the following quantity:

Eqn. 4) $$\Xi(w_j) = \sum_{j'=j}^{j+|w|-1} \xi(j')$$

For a motif M and fixed *a priori* window size |w|, we wish to model the distribution of scores $\Xi(w_j) = \sum_{j'=j}^{j+|w|-1} \xi(j')$ under the null hypothesis of no motif enrichment. We shall refer to $\Xi(w_j)$ as the "window score" of w_j and, for a given window w_j, we shall determine

whether $\Xi(w_j)$ is statistically significantly large by estimating the p-value with respect to the modeled distribution at $\Xi(w_j)$.

In order to see how well the window scores $\Xi(w_j)$ are modeled by this mixture of three distributions, we considered the four motifs utilized in this paper: MRF, MEF2, SRF and Tead (see **Supplementary Fig. 2** online). For this analysis we utilized the foreground and background 75-kb regions shown in **Supplementary Fig. 4** online, where the foreground sequences contain a collection of 27 CRMs known to drive expression in muscle and background regions are a collection of 1,080 75-kb regions surrounding genes that were not up- or down-regulated during our time-course analysis of myogenesis. In **Supplementary Fig. 2** online, we have plotted the empirical distribution of $\Xi(w_{100})$ (blue curve) for each of these four motifs, as well as the fitted mixture model (red curve). As can be seen, the match between the fitted and empirical curves is very precise (we note that the fit for Tead is somewhat worse, as it is an infrequently occurring motif, and there are thus very few windows of genomic sequence comprising the right tail of the empirical distribution).

We then define the "output score" for the window to be the negative-log of its corresponding p-value:

Eqn. 5) $$\text{output score} = -\log_{10} P(\Xi(w)).$$

In **Supplementary Fig. 2** online, we have plotted the empirical output score (blue curve) for each of the four motifs mentioned above, as well as the output score from the fitted mixture model (red curve).

Finally, there are two related technical issues that must be addressed in building the array of positional scores ξ. First, due to the difficulties in aligning distant genomes, as well as the presence of sequencing gaps resulting from a genome being incompletely sequenced, there may not be any alignment to g at position j in genome $a^{(i)}$. Thus, it is not clear how to evaluate **Eqn. 2** in the presence of such missing data. Second, there is the possibility that a binding site may be truly present in g but lost (due to evolution) in $a^{(i)}$, particularly if $a^{(i)}$ and g are greatly diverged. In such a situation, it is possible that the quantity φ of **Eqn. 2** will be negative, which is undesirable since it is reasonable to assume that observing the presence of a motif match in a window w_j should increase (not decrease) the window score $\Xi(w_j)$, even if this match is not well-conserved. We handle these issues in a similar fashion by restricting to an appropriate sub-tree of the original tree. In the first scenario, the branches corresponding to genomes with missing alignments are removed; in the second scenario, any binding sites not scoring above the user-specified cutoff for determining a motif match are removed (**Supplementary Fig. 1e** online). We note, however, that for the second scenario it is also possible to run the program so that the entire phylogeny for which alignments are available is considered, even if there is not a motif match in some genomes (such a mode might be used, for example, in attempting to identify exclusively those TF binding sites conserved throughout the phylogeny, as was done in the original work by Moses *et al.*[5]).

2. Flexible scoring scheme and algorithm, multiple motifs

In this section, we assume the case of multiple motifs M_n, $n=1,..,N$. Let $\xi_n(j)$ hold the positional scores of motif M_n. We desire a means of measuring whether a given window w_j is enriched for motif matches. We allow flexibility in the scoring scheme by allowing the user to address the situation of potentially overlapping motifs (refer to the "-DEOVERLAP" option in the algorithms). A naïve approach would be to first define the array:

Eqn. 6) $$\hat{\xi}(j) = \max_n \{\xi_n(j)\}.$$

The score for a window w_j could then be obtained by calculating the significance of:

Eqn. 7) $$\hat{\Xi}(w_j) = \sum_{j'=j}^{j+|w|-1} \hat{\xi}(j').$$

This method has the advantage of appropriately handling overlapping motifs. Unfortunately, it has the disadvantage that the behavior of the score is dominated by the degree of enrichment for the most frequently occurring motifs. For example, assuming similar degrees of degeneracy, a motif of width 6 occurs more than twice as frequently as a motif of width 12, but the contribution of each match of the 6-mer motif to $\hat{\Xi}$ is half that of the motif of width 12.

Therefore, we describe an alternative means of scoring multiple motifs when the "-DEOVERLAP" option is specified (which is the option we employed in our Warner *et al.* manuscript). First, define:

Eqn. 8) $$\widetilde{\xi}_n(j) = \begin{cases} \xi_n(j) \; if \; \xi_n(j) = \max_{n'}\{\xi_{n'}(j)\} \\ 0 \; otherwise \end{cases}$$

Similar to the case of one motif, this step removes the possibility that the score for different motifs could be double-counted at position *j*, but also ensures that each position receives the score of the motif that best matches it. We shall refer to the $\widetilde{\xi}_n$ as the "de-overlapped" positional score; this de-overlapping step is schematized in **Supplementary Fig. 3a** online. The de-overlapping step is also performed for the background sequences g_b.

From now on, let $\widetilde{\Xi}_n(w_j)$ be the window score of w_j (with or without the "-DEOVERLAP" option specified), and let $\gamma_n(\widetilde{\Xi}_n;|w|)$ be the corresponding mixture distribution of scores $\widetilde{\Xi}_n$ (see **Eqn. 7**) for a motif M_n for a given window length $|w|$ under the null hypothesis of no enrichment.

3. Combinations of several motifs in Fuzzy logic framework

We wish to utilize the mixture distributions $\gamma_n(\widetilde{\Xi}_n;|w|)$ for a motif M_n in order to determine the statistical significance of observing a given degree of clustering and evolutionary conservation for the set of motifs. In the case of one motif, this computation was straightforward, as the statistical significance was directly obtainable from the tail of the appropriate mixture of Delta, Uniform and Gamma distributions. For many motifs we have developed a rich vocabulary of scoring schemes, in order to model the combinatorial interactions between the TFs under consideration.

For simplicity, take the case of two motifs M_n and M_m. It is possible to calculate statistical significance using a "restrictively-defined tail" (**Supplementary Fig. 3b** online):

Eqn. 9) $$P\left(\tilde{\Xi}_n, \tilde{\Xi}_m\right) = P_n\left(\tilde{\Xi}_n\right) P_m\left(\tilde{\Xi}_m\right) = \left(\int_{\tilde{\Xi}_n}^{\infty} \gamma_n(\Xi;|w|)d\Xi\right)\left(\int_{\tilde{\Xi}_m}^{\infty} \gamma_m(\Xi;|w|)d\Xi\right)$$

(note: $P\left(\tilde{\Xi}_n, \tilde{\Xi}_m\right)$ does not refer to the joint distribution of the random variables $\tilde{\Xi}_n$ and $\tilde{\Xi}_m$).

We take the "output score" to be $-\log\left(P_n\left(\tilde{\Xi}_n\right) P_m\left(\tilde{\Xi}_m\right)\right) = -\log\left(P_n\left(\tilde{\Xi}_n\right)\right) - \log\left(P_m\left(\tilde{\Xi}_m\right)\right)$, and so the output score is additive in the number of motifs. Hence, a given window can achieve significance if it is greatly enriched for matches to *either* motif one or motif two (OR combination).

Conversely, it is also possible to calculate statistical significance of a combination of distributions using a "generously defined tail" (**Supplementary Fig. 3c** online):

Eqn. 10) $$\begin{aligned} P\left(\tilde{\Xi}_n, \tilde{\Xi}_m\right) &= 1 - \left(\int_0^{\tilde{\Xi}_n} \gamma_n(\Xi;|w|)d\Xi\right)\left(\int_0^{\tilde{\Xi}_m} \gamma_m(\Xi;|w|)d\Xi\right) \\ &= P_n\left(\tilde{\Xi}_n\right) + P_m\left(\tilde{\Xi}_m\right) - P_n\left(\tilde{\Xi}_n\right) P_m\left(\tilde{\Xi}_m\right) \end{aligned}$$

Here, if $\tilde{\Xi}_n = 0$ (the window score is zero), then $P_n\left(\tilde{\Xi}_n\right) = 1$ and so $P\left(\tilde{\Xi}_n, \tilde{\Xi}_m\right) = 1$ and so the window score $-\log\left(P\left(\tilde{\Xi}_n, \tilde{\Xi}_m\right)\right) = 0$ (and similarly for the case where $\tilde{\Xi}_m = 0$). Thus, using this tail, a window must be enriched for *both* motifs (AND combination) under consideration in order to be statistically significant.

Finally, it is possible to define the combination of the distributions in more complicated ways. For example, the following combination would assign a high score to windows of sequence that are enriched for the first motif but specifically not enriched for the second (NOT combination; **Supplementary Fig. 3d** online):

Eqn. 11)

$$P\left(\tilde{\Xi}_n, \tilde{\Xi}_m\right) = 1 - \left(\int_0^{\tilde{\Xi}_n} \gamma_n(\Xi;|w|)d\Xi\right)\left(\int_{\tilde{\Xi}_m}^{\infty} \gamma_m(\Xi;|w|)d\Xi\right)$$
$$= 1 - P_m\left(\tilde{\Xi}_m\right) + P_n\left(\tilde{\Xi}_n\right)P_m\left(\tilde{\Xi}_m\right)$$

The cases we have described, Eqns. 9-11, can be thought of as Fuzzy logic rules for the discrete Boolean logical functions (M_n OR M_m), (M_n AND M_m), and (M_n AND NOT M_m). In general, we define the "output score" for a Fuzzy logic combination of multiple motifs to be the negative-log of the corresponding P (see Eqns 9-11):

Eqn. 12) $$\text{output score} = -\log_{10}\left(P\left(\tilde{\Xi}_n, \tilde{\Xi}_m\right)\right).$$

We have implemented PhylCRM so that a variety of different tails are possible, in order to allow the evaluation of a more nuanced view of *cis* regulatory logic. A summary of all Fuzzy logic combinations considered is listed below:

a. OR combinations of arbitrarily many motifs

b. AND combinations of arbitrarily many motifs

c. The following four classes of compound combinations involving up to 4 motifs:

1) (M_1 AND NOT M_2) (two motifs)

2) ((M_1 AND M_2) OR M_3) (three motifs)

3) ((M_1 OR M_2) AND M_3) (three motifs)

4) ((*M1* AND *M2*) AND NOT *M3*) (three motifs)

5) ((*M1* AND *M2* AND *M3*) AND NOT *M4*) (four motifs)

Thus, if one would like to find CRMs enriched for any subset of the motifs under consideration, the OR mode is more appropriate; conversely, if one wishes to specifically identify CRMs enriched for matches to all the motifs under consideration, the AND mode is more appropriate.

C. Evaluation of ability of PhylCRM to identify CRMs

We obtained a phylogenetic tree of 11 vertebrate genomes from the ENCODE multiple sequence alignment working group[8] (**Supplementary Figure 4a** online) and a set of 27 CRMs previously compiled by Wasserman *et al.*[9] that are known to drive expression in muscle and to be regulated by at least one of the four well known myogenic TFs: a) MEF2, b) Serum Response Factor (SRF), c) Tead, and d) the myogenic regulatory factors (MRFs) MyoD, Myogenin, Myf5 and Myf6 (note that the motifs for the MRFs are currently indistinguishable and thus are encompassed by a single, general MRF motif)[9]. Here, we examined windows ranging between 50 and 500 bp (increment size of 50 bp), and utilized the phylogenetic tree derived by the ENCODE multiple sequence alignment working group[8]. The tree is input to PhylCRM in Newick format:

(((((((human:0.006690,chimp:0.007571):0.024272,
macaque:0.059256):0.107134,(mouse:0.077017,rat:0.081728):0.252613):0.023026,(dog:
0.147731,cow:0.159182):0.03945):0.262899,opossum:0.371073):0.189124,chicken:0.454
691):0.279364,(fugu:0.732855,zebrafish:0.782561):0.156067)

The versions of the genomes that we used are:

- human (hg 17)
- chimp (Nov 2003, panTro1)
- macaque (Jan 2006, rheMac2)
- mouse (May 2004, mm7)
- rat (Jun 2003, rn3)
- dog (May 2005, canFam2)
- cow (Mar 2005, bosTau2)

- opossum (Jun 2005, monDom2)
- chicken (Feb 2004, galGal2)
- zebrafish (May 2005, danRer3)
- Fugu (Aug 2002, fr1)

We compiled a "foreground" human gene set consisting of the 75-kb sequence regions surrounding each of these 27 known CRMs, and also a length-matched random "background" set of genomic regions not believed to contain muscle CRMs. We first masked out any coding regions and repetitive elements, and then searched the foreground and background gene sets with PhylCRM in order to identify windows of sequence significantly enriched for clusters of high-scoring, evolutionarily conserved matches to these four myogenic motifs. We assigned to each foreground and background region the score of its highest scoring PhylCRM window ranging between 10 bp and 500 bp, and then determined whether the foreground gene set scored higher than the background gene set by evaluating the AUC.

Without the use of phylogenetic conservation, we observed statistically significant enrichment for these motifs within this positive control foreground gene set (AUC = 0.64 ± 0.05; $P < 0.01$ calculated by the Wilcoxon-Mann-Whitney[10] (WMW) statistic; **Supplementary Figure 4b** online). When utilizing all 11 available vertebrate genomes, the degree of foreground enrichment increased significantly (AUC = 0.81 ± 0.05; $P < 10^{-7}$ by WMW; **Supplementary Figure 4c** online), demonstrating that the use of evolutionary conservation can increase discriminatory power.

Next, we evaluated whether the use of a subset of species in PhylCRM might yield higher foreground enrichment than the use of all available vertebrate genomes for this positive control set of myogenic CRMs. To evaluate such subsets, we systematically added those branches extending from each preceding common ancestor of human (**Supplementary Figure 4d** online). We observed the greatest degree of enrichment when using all available vertebrate genomes except those of chicken, pufferfish and zebrafish (AUC = 0.82 ± 0.05; $P < 10^{-8}$ by WMW), indicating that a judicious choice of sub-tree could yield improved performance. Finally, as a negative control we scanned the foreground and background regions with a permuted form of the four considered motifs and observed no enrichment (AUC = 0.41 ± 0.06; $P > 0.05$ by WMW; **Supplementary Figure 4e** online).

From this analysis, we concluded that PhylCRM can detect enrichment of motifs within 75-kb regions of genomic sequence within an appropriate gene set, and that the utilization of many aligned genomes increases the power of PhylCRM.

D. Comparison of PhylCRM to other CRM prediction methods

There are many available computational tools for CRM identification, and a full comparison of PhylCRM against each of them is beyond the scope of this present study. Therefore, we have selected two computational tools against which to compare PhylCRM, as they have similar goals of taking as input a collection of TF binding site motifs and outputting target CRMs.

We compared the performance of PhylCRM to two other algorithms: Comet (which utilizes a hidden Markov model (HMM) based approach and does not utilize information on the evolutionary conservation of the TF binding site motifs) and Stubb (which also utilizes an HMM-based approach and incorporates information on evolutionary conservation across up to two species of interest – one base genome plus one alignment genome). We selected two data sets for comparison: 1) the collection of 27 known muscle CRMs previously compiled by Wasserman *et al.*[9] (the results of PhylCRM analysis for this collection of CRMs is shown in **Supplementary Fig. 4** online), and 2) the collection of "sarcomeric genes" from **Fig. 4** and **Supplementary Fig. 6** of the manuscript. Thus, these were the two sequence sets that were most carefully examined in our manuscript.

First, we took as a "foreground" set of sequences the 27 75-kb regions containing each of the known muscle CRMs (i.e., we considered the 75-kb regions within which the CRMs were located) as well as a length-matched background set of sequences (data #1). Next, we took as a "foreground" set of sequences the set of the 75-kb regions around

transcription start of the 46 known sarcomeric genes, as well as a length-matched set of background sequences (data #2). Because of computational limitations of the Stubb algorithm in handling large amounts of sequence, we had to reduce the size of the background data sets from what we used to generate the results shown in the main body of our manuscript (in this comparison, we used the same background to evaluate the results from all three programs – PhylCRM, Comet, and Stubb – in order to ensure that they were compared in a fair and systematic way). Consequently, the performance of PhylCRM shown below is slightly different from the results shown in **Supplementary Figure 4** online.

We ran the three programs by varying the input parameters in order to obtain the best performance from each program. We compared Comet, PhylCRM and Stubb by utilizing the same measure of performance as that utilized in the main text, namely, the AUC statistic that indicates the degree to which foreground sequences are ranked higher than background sequences (see the table below for a summary of the results). First, we observed that when no phylogeny was utilized the performance of PhylCRM on data #1 was AUC = 0.70 ± 0.06 (error represents 1 standard deviation determined by applying bootstrap) ($P < 10^{-3}$); this is within the margin of error of the performance observed for Comet (AUC = 0.70 ± 0.05, $P < 10^{-4}$) and for Stubb (AUC = 0.68 ± 0.05, $P < 10^{-3}$) on data #1. On the sarcomeric gene set (data #2), without utilizing phylogeny, PhylCRM (AUC = 0.64 ± 0.05, $P < 10^{-2}$) was within the margin of error of Comet (AUC = 0.60 ± 0.05, $P > 0.01$), but better than Stubb (AUC = 0.49 ± 0.05, $P > 0.1$).

We then examined how PhylCRM compares with Stubb in the case when information on the evolutionary conservation of the binding sites is utilized. We note that Stubb currently can consider conservation between only two species, while PhylCRM can utilize arbitrarily many genomes. On data #1, using the phylogenetic tree: Human/Chimp/Macaque/Mouse/Rat/Dog/Cow/Opossum, the performance of PhylCRM (AUC = 0.81 ± 0.06, $P < 10^{-6}$) was within the margin of error of Stubb when using human and mouse (AUC = 0.80 ± 0.05, $P < 10^{-6}$). We note that many of the CRMs in data set #1 were originally discovered in mouse and other non-human species[11], and this bias in the creation of this positive control data set may have resulted in their being better conserved in mouse. Using the same phylogenetic tree (Human/Chimp/Macaque/Mouse/ Rat/Dog/Cow/Opossum) but now considering the Sarcomeric gene set (data #2), PhylCRM (AUC = 0.74 ± 0.05, $P < 10^{-6}$) performed significantly better than Stubb (AUC = 0.59 ± 0.04, $P > 0.01$) when Stubb was run utilizing human and mouse.

Table S1: Summary of algorithm comparison

Algorithm:	Wasserman data: (without utilizing phylogeny)	Wasserman data: (with phylogeny)	Sarcomeric data: (without utilizing phylogeny)	Sarcomeric data: (with phylogeny
Stubb	AUC = 0.68 ± 0.05	AUC = 0.80 ± 0.05	AUC = 0.49 ± 0.05	AUC = 0.59 ± 0.04
PhylCRM	AUC = 0.70 ± 0.06	AUC = 0.81 ± 0.06	AUC = 0.64 ± 0.05	AUC = 0.74 ± 0.05
Comet	AUC=0.70 ± 0.05	N/A	AUC = 0.60 ± 0.05	N/A

From these comparisons we conclude that that PhylCRM performs comparably to the other algorithms on the collection of 27 known CRMs, and better on the Sarcomeric gene

set. Additionally, PhylCRM has the added feature of being able to score CRMs using a rich vocabulary of Fuzzy Boolean logic rules in order to discover nuanced *cis* regulatory codes (in the preceding comparisons, we utilized the OR combination for simplicity, although the performance could possibly be improved with a different combination of TF binding site motifs but would have complicated a direct comparison with the other algorithms). We show that in all of the datasets considered, using phylogeny information helps to improve the performance (this is also shown in **Supplementary Figure 4** online). Also, we expect that the performance of PhylCRM will continue to improve on these data sets (and other data sets) as more mammalian genomes are sequenced.

E. Lever

The statistical framework of Lever is based upon principles used by other groups for gene set enrichment analysis[12,13] and utilizes permutation-based corrections for multiple hypothesis testing[14]. However, in contrast to gene set enrichment analysis[12,13], in the Lever framework genes are ranked by a sequence-based, rather than an expression-based, scoring function, and each combination of motifs gives rise to a distinct scoring function. For each gene set and scoring function, the ranking power of the function is statistically assessed by calculating the enrichment for highly scoring genes within the gene set. Thus, Lever simultaneously calculates and assesses the enrichment for many gene sets across many motif combinations (i.e., GM-pairs).

1. Statistical assessment for enrichment

Let $g_1, g_2, \ldots g_G$ be a collection of G genes whose upstream/downstream/intronic regions are being searched for CRMs, and let $GS_1, GS_2, \ldots, GS_N$ be a collection of subsets of these genes. Within each subset GS_j, the genes g_i which are elements of it will be labeled as either being "foreground" or "background". To denote this labeling, we use the matrix Y where:

Eqn. 1)

$$Y_{i,j} = \begin{cases} 1 & \text{if } g_i \text{ is a foreground gene in set } GS_j \\ 0 & \text{if } g_i \text{ is a background gene in set } GS_j \\ \bullet & \text{if } g_i \notin GS_j \end{cases}$$

The final value (•) of the above equation serves as a set membership indicator, which is used for efficient processing in order to assemble all of the required sets of genes. Specifically, information on set membership is required in a later permutation-based approach for evaluation of statistical significance, during which the assignment of genes

to the various gene sets changes. Let $F_{S_j} \subset GS_j$ and $B_{S_j} \subset GS_j$ be the sets of all foreground and background genes, respectively, within GS_j, and let $\left|F_{GS_j}\right|$ and $\left|B_{GS_j}\right|$ be the number of foreground and background genes, respectively, within GS_j. Finally, let MC_k , $k = 1,..,M$ denote a given collection of combinations of motifs, and let the matrix $X=(X_{i,k})$, $i=1,..,G$, $k = 1,..,M$, where $X_{i,k}$ denote the PhylCRM score (see **Supplementary Figures 1-4** online) of the maximum scoring window within the flanking sequence of g_i when scanning it with a motif combination MC_k.

Our goal is to determine which combinations of motifs MC_k are significantly enriched within the various gene sets GS_j. We consider the ranked PhylCRM scores for each combination of motifs and utilize the AUC statistic of the ranked scores in order to evaluate this enrichment. The AUC statistic is broadly applied for bipartite ranking problems and for comparisons of performance of binary classifiers[15]:

Eqn. 2) $$AUC\left(GS_j, MC_k\right) = \left(\frac{1}{\left|F_{GS_j}\right|\left|B_{GS_j}\right|}\right)\left(\sum_{i:\,Y_{i,j}=1}\ \sum_{i':Y_{i',j}=0} I_{[X_{i,k}>X_{i',k}]} + \frac{1}{2} I_{[X_{i,k}=X_{i',k}]}\right)$$

where I is the indicator function taking the value of "1" if the statement in brackets is true and "0" otherwise. The AUC of a ranking function takes values in the range [0,1], and is the probability that a randomly chosen positive instance (a member of the foreground set) will rank higher than a randomly chosen negative instance (a member of the background). It will take the value "1" if all of the genes in the foreground rank higher than genes in the background, the value "0" if all of the genes in the foreground rank lower than genes

in the background, and a value close to 0.5 if the ordering of foreground genes is not biased toward higher or lower ranks.

2. Adjustment for multiple hypothesis testing

An explicit goal of Lever is to evaluate many pairings of gene sets and motifs or motif combinations simultaneously, in order to identify motif combinations exhibiting statistically significant enrichment in specific gene sets (we refer to a matching of a gene set and a motif combination (GS_j, MC_k) as a GM-pair). The evaluation of so many GM-pairs, however, necessitates a mechanism to correct for multiple hypothesis testing. Observe that AUC scores of distinct pairings (GS_j, MC_k) and ($GS_{j'}$, $MC_{k'}$) are not independent under the null hypothesis of no enrichment, since GS_j and $GS_{j'}$ may contain common genes and MC_k and $MC_{k'}$ may contain common motifs. Consequently, a simple Bonferroni correction for multiple hypothesis testing is overly conservative and would cause many biologically relevant pairings (GS_j, MC_k) to be missed. Therefore, we applied a permutation-based approach for evaluation of statistical significance that takes into account the non-independence of the hypotheses.

For a given gene g_i let $\vec{Y}_i = \left(Y_{i,1}, \quad Y_{i,2}, \quad \ldots \quad Y_{i,S-1}, \quad Y_{i,N}\right)$ be the row vector of Y indicating membership of g_i in each of the sets GS_j, $j = 1,..,N$ and let $\vec{X}_i = \left(X_{i,1}, \quad X_{i,2}, \quad \ldots \quad X_{i,M-1}, \quad X_{i,M}\right)$ be the row vector of X indicating the PhylCRM score of g_i for each combination of motifs MC_k $k = 1,..,M$. Let π be a fixed permutation of $\{1,..,G\}$ (where G is the total number of genes).

Next, let:

Eqn. 3) $$AUC\left(GS_j, MC_k, \pi\right) = \left(\frac{1}{\left|F_{GS_j}\right|\left|B_{GS_j}\right|}\right)\left(\sum_{i: Y_{i,j}=1}\ \sum_{i': Y_{i',j}=0} I_{[X_{\pi(i),k} > X_{\pi(i'),k}]} + \frac{1}{2} I_{[X_{\pi(i),k} = X_{\pi(i'),k}]}\right)$$

This is the AUC computed for the GM-pair (GS_j, MC_k) when the class labels are permuted. Observe that, as desired, the definition of this permutation preserves all correlations in values of AUC statistics between pairings (GS_j, MC_k) and ($GS_{j'}$, $MC_{k'}$) resulting from genes being elements of both GS_j and GS_k and motifs being elements of both MC_k and $MC_{k'}$.

We use the permutation approach in order to evaluate the significance of the values AUC(GS_j, MC_k) when controlling for false discovery rate (FDR) and family-wise error rate for multiple comparisons. Let $\{\pi_l\}_{l=1}^{P}$ be a collection of P randomly chosen permutations over the gene labels. Because different gene sets GS_j , $j = 1,..,N$ contain different numbers of genes, and because different motif combinations can result in more or fewer ties in PhylCRM scores between distinct genes (for example, AND combinations involving many motifs may result in many genes having a PhylCRM score of "0"), the variance of AUC(GS_j, MC_k) is not constant across pairings (GS_j, MC_k). Let:

Eqns. 4 and 5)

$$\mu_{j,k} = \frac{1}{P}\sum_{l=1}^{P} AUC\left(GS_j, MC_k, \pi_l\right)$$

$$\sigma_{j,k} = \left(\frac{1}{P-1}\sum_{l=1}^{P}\left(AUC\left(GS_j, MC_k, \pi_l\right) - \mu_{j,k}\right)^2\right)^{1/2}$$

We normalize the AUC(GS_j, MC_k) value by applying the z-transformation:

Eqn. 6) $$AUC\left(GS_j, MC_k\right)' = \frac{AUC\left(GS_j, MC_k\right) - \mu_{j,k}}{\sigma_{j,k}}$$

Following the method of Subramanian *et al.*[13], for family-wise error rate estimation of significance for each value AUC(GS_j, MC_k)′, we take the maximum of the normalized AUC statistics across all gene set and motif combination pairings within a given permutation:

Eqn. 7) $$U_{\pi_l} = \max_{j,k}\left\{AUC\left(GS_j, MC_k, \pi_l\right)\right\}$$

The family-wise error rate estimate of statistical significance of a specific value AUC(GS_j, MC_k)′ is then given by:

Eqn. 8) $$P\left[AUC\left(GS_j, MC_k\right)'\right]_{FWER} = percentage\ of\ (l)\ s.t.\ U_{\pi_l} \geq AUC\left(GS_j, MC_k\right)$$

Similarly, the FDR estimate of statistical significance is obtained by utilizing the entire distribution of AUC(GS_j, MC_k, π_l)′ values and by calculating the FDR *Q*-values, denoted as *Q* in the main text and in the figures:

Eqn. 9) $$Q\left[AUC\left(GS_j, MC_k\right)'\right] = \frac{percentage\ of\ \left(j', k', l\right)\ s.t.\ AUC\left(GC_{j'}, MS_{k'}, \pi_l\right) \geq AUC\left(GS_j, MC_k\right)}{percentage\ of\ \left(j', k'\right)\ s.t.\ AUC\left(GC_{j'}, MS_{k'}\right) \geq AUC\left(GS_j, MC_k\right)}$$

In this paper, we report AUCs along with an error term that corresponds to one standard deviation of the bootstrap confidence interval[14].

3. Correction for AT/GC-rich motifs

We have observed that many genes of interest have G/C-rich flanking sequences; consequently, many gene sets will show artificially high enrichment for G/C-rich motifs. For the Lever screens shown in **Figure 4** and **Supplementary Figures 5-6**, we controlled

for this by first generating many permuted forms of each motif (50 for analyses involving the Xie *et al.*[16] motifs, and 100 for analyses involving the four motifs MRF/MEF2/SRF/Tead). For each gene of interest, we scored its 75-kb flanking noncoding sequence with permuted forms of the motifs. For each gene and each motif or combination of motifs, we *z*-transformed the PhylCRM scores (similarly to **Eqns. 4** and **5**) after calculating the mean and variance from the permuted forms of the motifs. This approach showed reduction of the artifacts described above.

PhylCRM and Lever software parameter settings

For all runs and all motifs considered in this study, as the threshold cutoff used by Lever and PhylCRM for calling a motif match, we used 2 standard deviations (SDs) below the motif average[17] and the "-THRESHOLD" setting in both of these programs. For the PhylCRM results shown in **Supplementary Figure 4**, we used the "-DEOVERLAP" option for the OR combination of the MRF/MEF2/SRF/Tead motifs. We observed very similar trends without the "-DEOVERLAP" option, *i.e.* without removing the overlaps between different motifs. In the rest of this study, we applied PhylCRM and Lever without the "-DEOVERLAP" option. For PhylCRM and Lever runs involving the MRF/MEF2/SRF/Tead motifs, we used windows ranging between 10 and 500 bp, and for runs involving the Xie *et al.*[16] motifs we used a window range of 25 to 500 bp since some of those motifs can be wider than 10 bp.

Gene sets examined in this study

For the Lever scans shown in **Supplementary Figure 5**, we examined each of the *k*-means expression clusters as an input library of foreground gene sets (we excluded cluster **C13** because it contained only 12 genes). For those shown in **Supplementary Figures 6** and **Figure 4,** we added to this collection by additionally considering gene sets based upon shared GO annotation terms (we considered the Biological Process, Molecular Function and Cellular Component terms). Specifically, significantly over-represented GO categories among the up- and down-regulated genes were determined using FuncAssociate[29]. Only the significantly (FDR ≤ 0.05) up- or down-regulated genes belonging to each of those GO categories were considered in constructing the corresponding reduced GO category gene sets. Nonredundant gene lists were created by matching Refseq sequences to common gene names using DAVID[30] and removing redundancies. Finally, we considered only those gene sets that contained at least 15 members. Also, if two gene sets were found to contain identical genes, one of the gene sets was dropped.

We noticed that numerous sarcomere-related GO categories, such as actin cytoskeleton, contractile fiber, structural constituent of muscle, muscle contraction, and muscle development, were enriched among the up-regulated genes. Sarcomeric genes might be especially likely to be co-regulated, as they are all components of a single protein complex utilized in muscle. However, the GO category "sarcomere" contained only 12 genes observed to be up-regulated in our study. Therefore, knowing that GO annotation of mammalian genes can be quite incomplete, we manually compiled from the literature a list of 46 sarcomeric genes that were up-regulated during the differentiation of myoblasts

into myotubes. This list of 46 genes included two genes (*ACTA1* and *CSRP3*) for which probes were not included on the microarrays utilized studying gene expression profiling, but for which RT-PCR experiments confirmed their up-regulation (**Supplementary Figure 8**).

F. Further discussion of interpretation of CRM enrichment results from Lever

We note that Lever identifies CRM enrichment within a given gene set. Of the six tested CRMs, the four that showed significant binding by MEF2, MyoD, and myogenin were the ones that are located next to genes involved in sarcomeric function, whereas the two that did not show significant binding by these factors are not. The MEF2 AND MRF motif combination within the up-regulated sarcomeric gene set was one of our top 10 GM-pairs in terms of AUC and *Q*-value from our Lever screen of 101 myogenic gene sets and the four known myogenic motifs MRF, MEF2, SRF and Tead (data provided in **Supplementary Table 3c**). Ranking by AUC values, the top 10 GM-pairs from that screen were:

Gene set	Boolean Motif combination	FDR Q-value (*Q*)	AUC
CONTRACTILE FIBER_up	OR(MRF,MEF2)	0	0.864706
CONTRACTILE FIBER_up	AND(MRF,MEF2)	0	0.856747
CONTRACTILE FIBER_up	COMPOUND(MRF AND (MEF2MEF2 OR SRF))	0.000028	0.846021
CONTRACTILE FIBER_up	OR(MRF,MEF2,SRF)	0.000028	0.842907
CONTRACTILE FIBER_up	COMPOUND(MRF AND (MEF2MEF2 OR Tead))	0.000037	0.8391
CONTRACTILE FIBER_up	COMPOUND(MEF2 OR (MRF AND SRF))	0.000033	0.828893
MUSCLE DEVELOPMENT_up	COMPOUND(MEF2 OR (MRF AND SRF))	0	0.828668
CONTRACTILE FIBER_up	COMPOUND(MEF2 AND (MRF OR SRF))	0.000077	0.828374
sarcomere_up	AND(MRF,MEF2)	0	0.821739
CONTRACTILE FIBER_up	COMPOUND(MEF2 AND (MRF OR Tead))	0.000035	0.819377

For experimental validation, we chose to examine simple Boolean motif combinations instead of compound Boolean combinations, because simple Boolean motif combinations would be easier to test in subsequent construction and analysis of synthetic CRMs. We also expected an AND motif combination to confer greater specificity of gene expression regulation than an OR motif combination. The MRF AND MEF2 motif combination for

the sarcomere_up gene set (FDR 0, AUC 0.822) scored slightly less well than the MRF AND MEF2 motif combination for the CONTRACTILE FIBER_up gene set (FDR *Q*-value = 0, AUC = 0.857). One of our positive control CRMs was for the gene *ACTA1*, which belongs to the sarcomere_up gene set and not to the CONTRACTILE FIBER_up gene set, and we were interested to see if there might be more than 1 functional CRM per gene at a given time point in a given cell type. It would be interesting to see if the predicted CRMs containing the MRF AND MEF2 motif combination for the CONTRACTILE FIBER_up gene set work with just as high a success rate.

To try to estimate what the anticipated CRM success rate might be for a given gene set, consider the following example. The figure below shows the degree to which all 46 sarcomeric genes are enriched for the MRF AND MEF2 TF binding site motif combination, as compared to a background set of 1840 (= 46*40) length-matched background genes that were not observed to be up- or down-regulated in this cell-type:

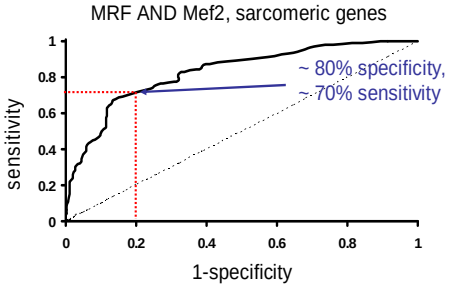

Sensitivity and specificity of MRF AND MEF2 for sarcomeric genes.

In looking at this figure, we see that at a given PhylCRM score threshold where 20% of background genes have a positive hit (i.e., a maximum-scoring window that we predict as

being a CRM) somewhere within their 75 kb regions around transcription start (80% specificity), 70% of sarcomeric genes (foreground) have such a positive hit within their 75 kb regions (i.e., 70% sensitivity). We note that sensitivity values for any given specificity can immediately be read off of the ROC curve, although for simplicity we use the 80% specificity / 70% sensitivity point for the following discussion. At this threshold, we can compile the following table of summary statistics indicating the fraction of true positives (TP), true negatives (TN), false positives (FP) and false negatives (FN), and also the positive predictive value (PPV) and misclassification error:

Estimation of summary statistics at a given score cutoff			
	Predicted Positive	Predicted Negative	
Foreground = 46	TP = 32	FN = 14	Sensitivity = TP/(TP + FN) = 70%
Background = 1840	FP = 368	TN = 1472	Specificity = TN/(FP + TN) = 80%
	PPV = TP/(TP + FP) = 8%		Misclassification error = (FP + FN)/(TP + FP + TN + FN) = 20%

Using the cutoff mentioned above, 20% of the background genes have a positive PhylCRM hit (i.e., predicted CRM) somewhere within 75 kb of transcription start, and 30% of the foreground genes do not have a predicted CRM, giving a misclassification error of 20% and positive predictive value (PPV) of 8%. We see three possible explanations for these results. First, some background genes containing a PhylCRM hit might be located close to a gene that is expressed in muscle and regulated by MRF AND MEF2; such PhylCRM hits would correspond to *bona fide* myogenic CRMs that were incorrectly placed into the background. Second, many of these PhylCRM hits might

represent CRMs that are targeted by TFs binding to the MRF AND MEF2 motifs but that do not drive expression in muscle. For example, MEF2 is known to regulate gene expression in the brain, and there are several bHLH TFs that are crucial for neuronal cell fate specification and are likely to have a binding site motif similar to the MRF motif bound by the myogenic bHLH TFs (MyoD, myogenin); thus, many of these hits could be true CRMs that drive expression in the brain rather than the muscle. Finally, it is possible that many of the PhylCRM hits are simply false predictions and are not actually CRMs. We have given this issue extensive thought, and we do not presently see a reliable means of estimating what fraction of MRF AND MEF2 hits adjacent to background genes fall into each of these three potential classes. We expect that prioritizing for experimental testing those significant PhylCRM hits that contain MRF AND MEF2 motifs and that are directly adjacent to sarcomeric genes, will lead to a greatly increased success rate in experimental validation of predicted CRMs functional in myogenic differentiation. In general, we believe that the results of Lever can be used to prioritize predicted CRMs for experimental testing, by picking for testing those candidate CRMs which lie next to genes that belong to significant scoring GM-pairs.

G. Position Weight Matrices utilized in this study:

We obtained from the supplementary data of Wasserman *et al.*[9] DNA binding site sequences corresponding to these 4 motifs from the supplementary data of that study, although we added additional myogenic MEF2 sites obtained from a SELEX experiment[18].

MRF:

$$\begin{bmatrix} A \\ C \\ G \\ T \end{bmatrix} \begin{bmatrix} 24 & 17 & 0 & 39 & 0 & 3 & 0 & 0 \\ 2 & 4 & 39 & 0 & 5 & 13 & 0 & 1 \\ 12 & 13 & 0 & 0 & 34 & 14 & 0 & 38 \\ 1 & 5 & 0 & 0 & 0 & 9 & 39 & 0 \end{bmatrix}$$

MEF2:

$$\begin{bmatrix} A \\ C \\ G \\ T \end{bmatrix} \begin{bmatrix} 6 & 3 & 107 & 73 & 113 & 117 & 114 & 1 & 125 & 17 \\ 97 & 9 & 0 & 0 & 0 & 0 & 0 & 1 & 0 & 2 \\ 4 & 1 & 0 & 0 & 2 & 0 & 1 & 0 & 0 & 103 \\ 18 & 112 & 18 & 52 & 10 & 8 & 10 & 123 & 0 & 3 \end{bmatrix}$$

SRF:

$$\begin{bmatrix} A \\ C \\ G \\ T \end{bmatrix} \begin{bmatrix} 0 & 0 & 13 & 14 & 10 & 4 & 14 & 8 & 6 & 0 \\ 20 & 20 & 0 & 0 & 0 & 0 & 0 & 1 & 0 & 0 \\ 0 & 0 & 0 & 0 & 4 & 0 & 2 & 0 & 14 & 18 \\ 0 & 0 & 7 & 6 & 6 & 16 & 4 & 11 & 0 & 2 \end{bmatrix}$$

Tead:

$$\begin{bmatrix} A \\ C \\ G \\ T \end{bmatrix} \begin{bmatrix} 4 & 9 & 0 & 12 & 0 & 0 & 0 & 0 & 4 & 0 & 1 \\ 6 & 0 & 12 & 0 & 0 & 0 & 12 & 11 & 1 & 6 & 4 \\ 1 & 3 & 0 & 0 & 0 & 0 & 0 & 0 & 0 & 6 & 6 \\ 1 & 0 & 0 & 0 & 12 & 12 & 0 & 1 & 7 & 0 & 1 \end{bmatrix}$$

H. Detailed experimental protocols, including primer sequences

Cell culture

Adult human skeletal myoblasts (Cambrex) were grown in SkGM2 medium (Cambrex) for optimal growth and differentiation potential. Myogenic differentiation was stimulated by switching the culture medium to DMEM with 2% horse serum (Sigma) when the cells reached about 70% confluence. All time points referred to in this study are with respect to the time of switching to differentiation medium. Mouse C2C12 cells (ATCC), mouse 3T3 cells (ATCC), and human lens epithelial cells (gift from Amy Donner) were cultured in DMEM (Invitrogen) with 10% fetal bovine serum (Sigma), respectively. HEK293T cells were a gift from Karen Cichowski.

RNA purification

Total RNA was isolated from primary human skeletal muscle cells using TRIzol reagent (Invitrogen) according to the manufacturer's protocols. For microarray experiments, total RNA was further purified with RNeasy columns (Qiagen).

Gene expression profiling microarray experiments

Microarrays were synthesized and hybridized by the Harvard Partners Center for Genetics and Genomics. Briefly, each glass slide was spotted with the Human OligoLibrary^{TM} Release 1.0 that was designed by Compugen, Inc. and manufactured by Sigma-Genosys, Inc. This oligonucleotide library consists of 18,864 60-mers representing 18,664 unique genes. We extracted mRNA at 6 time points (–48 hrs, –24 hrs, 0 hrs, 12 hrs, 24 hrs, and 48 hrs relative to serum withdrawal). These time points were selected since prior studies in a related cell type (mouse C2C12 cells) demonstrated their

effectiveness for capturing key transcriptional events during myogenic differentiation[19,20]. For each time point, four hybridizations, consisting of duplicate hybridizations with Cy3 and Cy5 dye-reversal, were performed essentially as described previously[21].

Preprocessing and clustering of gene expression microarray data

Scanned TIF images were quantified with GenePix software (Axon Instruments). For each feature, the median pixel intensity of the local background was subtracted from the spot's median pixel intensity. We then applied variance stabilizing normalization[22] to normalize all single channels to each other. False discovery rates (FDRs) were calculated using Significance Analysis of Microarrays[23] (one class time-series and slope parameters) on the four replicate arrays. The arcsinh values of the four replicate arrays for each time point were then combined by taking the arithmetic mean and expressed as the fold-change relative to the first time point (–24 hrs). Changes in arcsinh values correspond to the following approximate ratios (arcsinh = linear): 0 = 1/1; 1 = 2.7/1; 2 = 7.5/1; 3 = 20/1, 4 = 55/1; 5 = 155/1, 6 = 405/1. Genes that were differentially expressed at a 5% FDR were clustered using *k*-means clustering by de Hoon's Cluster 3.0 software[24] (http://bonsai.ims.u-tokyo.ac.jp/~mdehoon/software/cluster/software.htm#ctv). Our choice of 14 clusters was determined empirically.

Western blotting

Cell nuclei extracts and cytoplasmic extracts were obtained from human skeletal myoblasts at –48, –24, 0, +24, and +48 hours with respect to stimulation of differentiation, according to standard protocols. Equal protein amounts were subjected to

standard SDS-PAGE. Western Blots were performed using SuperSignal West Femto Maximum Sensitivity Substrate (Pierce) according to the manufacturer's instructions. Blocking solution consisted of 5% nonfat dry milk in TBS-T (Tris Buffered Saline with 0.1% Tween 20) and washing solution was TBS-T.

The following antibodies used in Western blots were purchased from Santa Cruz: Myf5 (sc-302), MyoD (sc-760), Myogenin (sc-576), Myf6 (sc-784), SRF (sc-335), MEF2C (sc-13266), MEF2 (sc-10794), MEF2A (sc-313), and lamin B1 (sc-20682). Tead1 (or Tef-1) antibody was purchased from BD Biosciences Pharmingen (610923). All antibodies were probed at a 1:1,000 dilution in blocking solution, except for the lamin B1 and MEF2C antibodies which were probed at a 1:2,000 dilution. Anti-rabbit and anti-mouse HRP-conjugated secondary antibodies (as supplied by Pierce) were diluted 1:3,000 in blocking solution. Anti-goat secondary antibodies (Sigma) were diluted 1:300,000.

The Tead or Tef family of transcription factors are comprised of at least four mammalian members, Tead1 (TEF-1), Tead2 (TEF-4), Tead3 (TEF-5), and Tead4 (TEF-3)[25]. Tead4 and Tead2 are the only two members detectable in regenerating mouse skeletal muscle[25,26]. Tead1 is broadly expressed in many different embryonic tissues[27], but Tead1 knockout mice have severe cardiac defects suggesting a major role in cardiac development[28]. Tead3 is detectable in skeletal and cardiac muscle but is preferentially expressed in the developing placenta[29,30]. Since the immunogen used to develop the BD Pharmingen is 53% identical and 66% similar to Tead4 protein, it is possible that the antibody is cross-reactive with Tead4 or other Tead family members using a sensitive

Western blot detection system. At the time of submission of this paper, it was believed that Tef1 was the relevant Tead family member for myogenic differentiation[11], and BD Biosciences Pharmingen had no data for or against the cross-reactivity of their Tead1 antibody.

ChIP

Chromatin immunoprecipitations were carried out using a modified version of the Farnham protocol (http://mcardle.oncology.wisc.edu/Farnham/protocols/chips.html). 5 x 10^8 cells fixed at days 0, 1, and 2 of differentiation.

Cells were fixed with 1% formaldehyde at room temperature for 10 minutes with occasional agitation of the plates. 2.5 M glycine was added to the cell media for 5 minutes to stop the crosslinking reaction. The cells were then washed twice with ice-cold PBS and incubated in PBS with 20% trypsin-EDTA (Cambrex) for 10 min at 37ºC. 0.5 ml of FCS was added to inhibit trypsinization. The cells were then scraped and collected into 50-ml conical tubes and kept on ice. Cells were washed once with ice-cold PBS with PMSF (Sigma, 100 μM) and protease inhibitors (20 μl per ml, Sigma P8340), flash frozen in ethanol/dry ice, and kept @-70ºC until chromatin immunoprecipitation.

Frozen cells were thawed on ice, resuspended in ice-cold cell lysis buffer (5 mM PIPES pH 8.0, 85 mM KCl, 0.5% NP40, 1:50 protease inhibitor mix [Sigma catalog # P8340]), and incubated on ice for 10 minutes. Nuclei release was aided by dounce homogenization. Nuclei were pelleted by centrifugation and resuspended in room

temperature nuclei lysis buffer (50 mM Tris-Cl pH 8.1, 10 mM EDTA, 1% SDS, 1:50 protease inhibitor mix), followed by incubation on ice for 10 minutes. The nuclei were then sonicated to achieve chromatin fragments with an average length of 1,000 bp. The sonication conditions used were 9 sonications of 15-second pulses separated by 1-minute incubation on ice. Samples were centrifuged at high speed to remove cellular debris. The supernatant containing the sonicated chromatin was transferred to a 50-ml conical tube and diluted 1:10 with ice-cold dilution buffer (0.01% SDS, 1.1% Triton X-100, 1.2 mM EDTA, 16.7 mM Tris-Cl pH 8.1, 167 mM NaCl, 1:50 protease inhibitor mix). Chromatin was precleared by adding 50 μl of Protein A beads/Salmon Sperm DNA (Upstate Protein A/Salmon Sperm DNA, cat# 16-157) per ml and incubating on a rotating platform at 4ºC. 3 μg of antibody was used for each immunoprecipitation. The following antibodies were purchased from Santa Cruz: MyoD (sc-760), Myogenin (sc-576), SRF (sc-335), and MEF2 (sc-10794). 60 μl of Protein A/salmon sperm DNA beads were added to each sample and incubated on a rotating platform at 4°C for 1-2 hours. Samples were then microcentrifuged for 1 min and placed into fresh microcentrifuge tubes.

Immunoprecipitates were washed twice with ice-cold wash buffer 1 (20 mM Tris, pH 8.1, 150 mM NaCl, 2 mM EDTA, 0.1 % SDS, 1% Triton X-100), once with wash buffer 2 (20 mM Tris, pH 8.1, 500 mM NaCl, 2 mM EDTA, 0.1 % SDS, 1% Triton X-100), once with wash buffer 3 (10 mM Tris, pH 8.1, 250 mM LiCl, 2 mM EDTA, 1% NP-40, 1% deoxycholate), and once with ice-cold 4 M LiCl/TE. After the last wash and spin, all remaining buffer was carefully removed with a sterile 1-ml pipette. Antibody/protein/DNA complexes were eluted by adding 100 μl of IP elution buffer 1

(1% SDS, 1 mM EDTA, 10 mM Tris, pH 8.1) and incubated @65°C for 15 min. Samples were microcentrifuged for 3 minutes. Supernatants were then transferred to fresh microcentrifuge tubes. Samples were then eluted again with 150 µl of elution buffer 2 and incubated at 65°C for 15 min. Samples were then combined and incubated overnight at 65°C to reverse formaldehyde crosslinks.

To each tube, 250 µl TE and 5 µl of proteinase K (20 mg/ml) were added. The tubes were then incubated at 37ºC for 1 hour. To each tube, 55 µl of 4M LiCl was added. The samples were then extracted twice with 500 µl phenol/chloroform/isoamyl alcohol and once with 500 µl of chloroform. Then, 1 µl (10 mg) of glycogen to each sample and the samples were ethanol precipitated. After drying the pellets, the samples were resuspended in 150 µl of 10 mM Tris 8.5. Each IP was performed in triplicate for each individual chromatin sample.

In our ChIP assays, as positive controls we examined five previously described muscle CRMs, and as negative controls we examined two noncoding regions with no significant matches and eight noncoding regions with only a single significant match, to any of these five motifs. The positive control regions were as follows:

CAV3 (0.2 kb upstream of transcriptional start):

- myotube specific promoter; previously confirmed myogenin (MYF) binding site in mouse C2C12 cells[31]

COX6A2 (0.3 kb upstream of transcriptional start):

- myotube specific promoter; previously confirmed MRF (E-box) and MEF2 binding sites in mouse Sol8 and C2C12 cells[32]

ACTA1 (0.3 kb upstream of transcriptional start):

- promoter region
- 3 previously confirmed SRF sites in primary chicken muscle culture[33]
- previously confirmed Tead1 site in rat cardiomyocytes[34]

TNNT2 (0.1 kb upstream of transcriptional start):

- conserved Tead1 (M-CAT) site in chicken promoter was previously shown to be important for chicken skeletal muscle[35]
- MEF2 site was previously shown to be important for rat cardiac muscle expression[36]
- CArG boxes (SRF sites) were previously confirmed by footprinting in rat cardiomyocytes[36]

DMD (6.4 kb into 1st introns):

- myotube-specific enhancer
- three MRF sites and one MEF2 site required for activation in myotubes[37]

Primer sequences:

Gene Name	Forward Primer	Reverse Primer
ChIP primers		
ACTA1	ACCCTCGCCCCACCCCATCC	GGCCGCTTGTCCCTCTGCTC
BDKRB2	GCCCGGGCTCTTGCTCCAG	CTCCTCAGGGCCTCAGTTTCTTCAT
CAV3	GCCCTCTGCACCCTCTCCTG	CCGGCTGGGGCTGAAAATAC
CLC	TCCAGGGGGCAAATGAGGGTAAT	CATAAGAGACTGGGCGCGGTGGTTC
COX6A2	GCCTGTAATCCCAGCACTGT	AGCTGTTGTCCTGTGCCTCT
CPM	TGTGCCACGTGTCCTTTCATCATCAGTA	GCACCCAAATCCCCATCTCAGTCC
CSRP3	GTGGGGGCCTGGAGAAATGAT	AGCCACAGAACCAACCCACCTC
DMD	CTGCGACAAAATGGGCACTCAATA	CTGCGACAAAATGGGCACTCAATA
GAP43	CTGAGGCGGGGAGAGGAGAG	TGGGAAGTGGTTATTATGGGATTG
HBZ	GGCCTTGTCTGTCTTTTCCTCCATA	GGCAGCTCAGCACCCATCCT
HSPB3	GGACTAGTGCCTTCAACAGC	TAAAACAACGTGGGGGAGTA
EDG5	CTAGCCCATGTCCCCTCCCTGTGTAA	TCCCCCTGGCTGCTTGGTAGAGAAT
KRT2A	GCCCCTCACCGCCCTCTCCT	ATTATGCGCCTTGTCGATGCTCTC
MEF2C	AGGGCAGTCATGGAGAGGTC	TTATGGCAAGGGAGAACTGG
MGLL	CAAGGGGGATGGCACTAAACC	CTCCTACAGCCTGCGATGAAAAG
MTP	TTGGGTACTATCGGTGGAGA	GTGGGCAGAAAGGAGTTGAG
PTHR1	GGGGGTCCAAAGCGGGTCCTGTT	TCCTGGCCCCCTCCTCCCTTCAAA
TNNT2	TCTTTACCCCCAGCATCAGT	GGGACAAGGCTACAGGAACA
TOP2A	AAGTCTGCCCCACGGTCCTGA	CTCTGGGCCCTGCTTGCTCTTC
RT-PCR primers		
DMD	GCGCCTCCTAGACCTCCTC	ACCCGCAGTGCCTTGTTG
ACTA1	GCCCGAGCCGAGAGTAGCAGTTGT	CTCGCGGTTGGCCTTGGGATTG
COX6A2	CCAAAGGAGGCCACGGAGGAGCAG	GGTGGCCCGAGTGGAGATAGGAGTTGA
CAV3	TTGACCTGGTGAACCGAGAC	CGTGGACAACAGACGGTAGC
TNNT2	CTGAGCGGGAAAAGAAGAAGAAGATT	GTGGGGGCAGGCAGGAGTG
MYOD	AGCACTACAGCGGCGACT	GCGACTCAGAAGGCACGTC
MYOG	TAAGGTGTGTAAGAGGAAGTCG	CCACAGACACATCTTCCACTGT
MEF2C	CTCCCAGTCGGCTCAGTCATTG	CGAAGGGGTGGTGGTACGGTCTCTA
MEF2D	AAGCGGAAGTTTGGCCTGATGAAGAA	GCCGCTGGGATTGCTGAACTGC
SRF	ACTGCCTTCAGTAGGAACAA	TTCAAGCACACACACTCACT

TEAD4	TGTGGCAGGCGCAAAATCATCC	GTCCGGGTCCTGCTGCTGCTC
HSPB3	GGGGCTCGCCACTGACTGAA	AGACTGCGCTGCCCTGGTTTT
CSRP3	CTCTTCCCACAGATGGCACA	GAGAAGGTTATGGGAGGTGGC
CACNG1	ATGTCCCAGACCAAAATGCTG	CAGGTAGTGTTGTGGTGCTC
PDLIM3	ACTCCCTCCGGGATTGACTG	AGCTTAGCCGCAACTTTCAAG
ARGBP2	AACACAGGGCGTGATTCTCAG	TGGTCGAACGCTTCTAAAACC
RPS18	GATGGGCGGCGGAAAATAG	GCGTGGATTCTGCATAATGGT
Cloning primers		
DMD_BAM	CACCGGATCCCACGGCCATACAACCTCTACCTC	GGATCCTTCATCTCCACTGTCCCCATTCTA
PDLIM3_BAM	CACCGGATCCCTACCCGCCAGTGCTGTGTTGAG	GGATCCGGGAAGGCCTGGGGGAGAAG
MGLL_BAML	ACGCGGATCCCAAGGGGGATGGCACTAAACC	ACGCGGATCCCTCCTACAGCCTGCGATGAAAAG
CSRP3_BAM	ACGCGGATCCGTGGGGGCCTGGAGAAATGAT	ACGCGGATCCAGCCACAGAACCAACCCACCTC
Primers for cloning into pLKO.1 vector (RNAi)		
MYOG_shRNA_1	CCGGGCCCACAATCTGCACTCCCTTCTCGAGAAGGGAGTGCAGATTGTGGGCTTTTTG	AATTCAAAAAGCCCACAATCTGCACTCCCTTCTCGAGAAGGGAGTGCAGATTGTGGGC
MYOG_shRNA_2	CCGGGCACATCTGTTCTAGTCTCTTCTCGAGAAGAGACTAGAACAGATGTGCTTTTTG	AATTCAAAAAGCACATCTGTTCTAGTCTCTTCTCGAGAAGAGACTAGAACAGATGTGC
MYOG_shRNA_3	CCGGCCCAGACGAAACCATGCCCAACTCGAGTTGGGCATGGTTTCGTCTGGGTTTTTG	AATTCAAAAACCCAGACGAAACCATGCCCAACTCGAGTTGGGCATGGTTTCGTCTGGG
MEF2D_shRNA_1	CCGGCCCTGGTGACATCATCCCTTACTCGAGTAAGGGATGATGTCACCAGGGTTTTTG	AATTCAAAAACCCTGGTGACATCATCCCTTACTCGAGTAAGGGATGATGTCACCAGGG
MEF2D_shRNA_2	CCGGCAATGGCAACAGCCTAAACAACTCGAGTTGTTTAGGCTGTTGCCATTGTTTTTG	AATTCAAAAACAATGGCAACAGCCTAAACAACTCGAGTTGTTTAGGCTGTTGCCATTG
MEF2D_shRNA_3	CCGGCACATCAGCATCAAGTCAGAACTCGAGTTCTGACTTGATGCTGATGTGTTTTTG	AATTCAAAAACACATCAGCATCAAGTCAGAACTCGAGTTCTGACTTGATGCTGATGTG

SRF_3882F	CCGGCCCTTGGTGTATCCCTAATTACTCGAGTAATTAGGGATACACCAAGGGTTTTTG	AATTCAAAAACCCTTGGTGTATCCCTAATTACTCGAGTAATTAGGGATACACCAAGGG
SRF_2110F	CCGGGCTCAATTTGCTATGAGTATTCTCGAGAATACTCATAGCAAATTGAGCTTTTTG	AATTCAAAAAGCTCAATTTGCTATGAGTATTCTCGAGAATACTCATAGCAAATTGAGC
SRF_2934F	CCGGGAGAGGAGATTGATGTCCTTTCTCGAGAAAGGACATCAATCTCCTCTCTTTTTG	AATTCAAAAAGAGAGGAGATTGATGTCCTTTCTCGAGAAAGGACATCAATCTCCTCTC
HNF4alpha	CCGGCCGACAATGTGTGGTAGACAACTCGAGTTGTCTACCACACATTGTCGGTTTTTG	AATTCAAAAACCGACAATGTGTGGTAGACAACTCGAGTTGTCTACCACACATTGTCGG

Quantitative RT-PCR

Total RNA was reverse-transcribed using SuperScript III (Invitrogen) according to the manufacturer's protocols. Quantitative PCRs were performed using iQ^{TM} SYBR$^{®}$ Green Supermix (BioRad) and 0.2 μM primers with an iCycler iQ Real-Time PCR Detection System (BioRad).

Quantitative ChIP-PCR

ChIPs were performed in biological triplicate using a modified version of the Farnham protocol[38]. The following antibodies were used in ChIPs: MyoD (sc-760), myogenin (sc-576), SRF (sc-335), and MEF2 (sc-10794), all from Santa Cruz Biotechnology, Inc. We included SRF since we observed that several of our predicted CRMs contained SRF motif matches. Tead was not included since a suitable antibody was not available. As positive

controls, we examined five previously described muscle CRMs. Negative control genomic regions were chosen based on their not having any significant PhylCRM hits when considering the MRF, MEF2, SRF, or Tead motifs, and their being adjacent to genes called "present" in the expression microarray data but not up- or down-regulated at a FDR less than 0.1. Quantitative ChIP-PCRs were performed essentially as described above, except using 6 μl of immunoprecipitated DNA.

Luciferase reporter assays

Putative and control CRMs were cloned either upstream (BglII) or downstream (BamHI) of the luciferase reporter gene into pGL3-Promoter vector (Promega) in their native genomic orientation (i.e., upstream versus downstream of transcription, Watson versus Crick strand). As a positive control, we used one of the five previously known muscle CRMs used in our ChIPs. A negative control human noncoding genomic region not enriched for matches to these four motifs was indistinguishable from the corresponding enhancer-less empty vector negative control. C2C12 cells were cultured in 6-well plates (9.4 cm^2 per well) 24 hours prior to transfection at 3 x 10^4 cells per well for myoblasts or 1.5 x 10^5 cells per well for myotubes. The cells were then co-transfected in triplicate with 1 μg of experimental vector (pGL3-P with or without inserted region) and 50 ng of the normalization vector (pRL-TK) using FuGENE 6 transfection reagent (Roche) according to the manufacturer's protocols. Cell extracts were obtained from an aliquot of the proliferating myoblasts 24 hours after transfection. The remaining cell cultures were then switched to differentiation medium, and cell extracts were obtained after 96 hours in differentiation medium. Luciferase reporter assays were performed using the Dual-

Luciferase® Reporter Assay System (Promega) according to the manufacturer's protocols. Firefly luminescence intensities were normalized by the luminescence intensities of the internal *Renilla* control. We used C2C12 cells in these assays instead of primary adult human skeletal myoblasts because the primary cells failed to differentiate robustly after transfection.

shRNA knockdowns

Short hairpin RNA (shRNA) constructs directed against mouse RNA transcripts were generated essentially as described previously[39]. Lentiviral reagents were kindly provided by Karen Cichowski. For lentiviral production, HEK293T cells were transfected with the Δ8.2 lentiviral construct (encoding *gag, pol, rev)*, VSVG, and either empty pLKO.1 vector or the pLKO.1 vector containing a sequence for a shRNA specific for each of the muscle genes *MYOD*, *MYOG*, *MEF2D*, *SRF*, and the liver gene *HNF4α.* Three distinct shRNA constructs were created for each gene in order to control for off-targets effects. Lentivirus was titered by serial dilution followed by colony formation assays in medium containing puromycin. C2C12 cells (7×10^4) were plated on 100-mm plates 24 hours prior to infection. After infection at 5 multiplicities of infection of lentivirus, C2C12 cells were grown in growth media for 24 hours and selected in puromycin for 72 hours. Luciferase reporter assays were then performed as described above, except cells were plated onto 12-well plates and transfected with proportionately less of the reagents. Our MEF2C knockdowns resulted in extensive cell death, and thus could not be utilized here.

Creation of synthetic CRMs

To test the sufficiency of the inferred MRF AND MEF2 *cis* regulatory code for myogenic differentiation, we created a synthetic CRM containing consensus MRF and MEF2 binding sites arranged as in our newly discovered *ACTA1* CRM, but in the context of the *MGLL* negative control flanking sequence. The MGLL negative control region was selected as a template into which to place TF binding sites in order to experimentally test the MRF AND MEF2 *cis* regulatory code for myogenic differentiation. To create synthetic CRMs, we created variants of a shorter 167-bp *MGLL* negative control region by ligating segments of the original *MGLL* region or by ligating modified segments of the *MGLL* region such that the new construct would have two consensus MRF sites and one consensus MEF2 site. The reconstituted *MGLL* region served as a negative control. As positive controls, we used an SV40 enhancer, one of the five previously known muscle CRMs used in our ChIPs (DMD), and a novel CRM that we verified previously CRM (ACTA1, see **Fig. 5** of the manuscript). The TF binding sites were placed in the modified *MGLL* region such that they mimicked the position and orientation of our newly discovered *ACTA1* CRM. The sense (F) and antisense (R) strand of each segment were synthesized as single-stranded DNA oligonucleotides and were then annealed to form double-stranded DNA. The following oligonucleotides were used in the annealing reactions:

MGLL_SEG1_F	CCATGATGCATTCACCTCCCACCAGGCCCCACCTTCAACATTGGGGATTA CAGTTCAAAATGAGG
MGLL_SEG1_R	ATTTTGAACTGTAATCCCCAATGTTGAAGGTGGGGCCTGGTGGGAGGTGA ATGCATCATGGAGCT
MGLL_SEG2_F	TTTGGTGGGGACACAGATCCAAACCATATCAACTTGTAGGGGCAGAAAGA CGTCACCTTTAC
MGLL_SEG2_R	AGGTGACGTCTTTCTGCCCCTACAAGTTGATATGGTTTGGATCTGTGTCC

	CCACCAAACCTC
MGLL_SEG3_F	TTGAATTGCAACCCTTACCTTTTCATCGCAGGCTGTAGGAGA
MGLL_SEG3_R	GATCTCTCCTACAGCCTGCGATGAAAAGGTAAGGGTTGCAATTCAAGTAA
MGLL_SEG1_CAGCTG_F	CCATGATGCATTCACCTCCCACCAGGCCCCACCTTCAACATTGGGGCAGC
	TGGTTCAAAATGAGG
MGLL_SEG1_CAGCTG_R	ATTTTGAACCAGCTGCCCCAATGTTGAAGGTGGGGCCTGGTGGGAGGTGA
	ATGCATCATGGAGCT
MGLL_SEG2_ACTA1_PMEF2_F	TTTGGTGGGGACACAGATCCAAACCATATCAACTTGTAGGGGCAGAACTA
	AAAATAGTTTAC
MGLL_SEG2_ACTA1_PMEF2_R	ACTATTTTTAGTTCTGCCCCTACAAGTTGATATGGTTTGGATCTGTGTCC
	CCACCAAACCTC
MGLL_SEG3_CAGCTG_F	TTGAATTGCAACCCTTACCTTTTCATCGCAGGCTGCAGCTGA
MGLL_SEG3_CAGCTG_R	GATCTCAGCTGCAGCCTGCGATGAAAAGGTAAGGGTTGCAATTCAAGTAA

Segment 1 was designed to have a *SacI*-compatible end and segment 3 a *NheI*-compatible end such that an entire Seg1-Seg2-Seg3 sequence could be ligated into a pGL3-P vector that was previously digested with *NheI* and *SacI* and treated with alkaline phosphatase. The short MGLL sequence was reconstituted by ligating the following double-stranded segments: MGLL_SEG1, MGLL_SEG2, and MGLL_SEG3. The MGLL region with two MRF sites and one MEF2 site was created by ligating MGLL_SEG1_CAGCTG, MGLL_SEG2_ACTA_PMEF2, and MGLL_SEG3_CAGCTG.

References

1. Philippakis, A.A. et al. Expression-guided *in silico* evaluation of candidate *cis* regulatory codes for *Drosophila* muscle founder cells. *PLoS Computational Biology* 2(2006).
2. Stormo, G. DNA binding sites: representation and discovery. *Bioinformatics* 16, 16-23 (2000).
3. Halpern, A.L. & Bruno, W.J. Evolutionary distances for protein-coding sequences: modeling site-specific residue frequencies. *Mol. Biol. Evol.* 15, 910-7 (1998).
4. Moses, A.M., Chiang, D.Y., Kellis, M., Lander, E.S. & Eisen, M.B. Position specific variation in the rate of evolution in transcription factor binding sites. *BMC Evol Biol* 3, 19 (2003).
5. Moses, A.M., Chiang, D.Y., Pollard, D.A., Iyer, V.N. & Eisen, M.B. MONKEY: identifying conserved transcription-factor binding sites in multiple alignments using a binding site-specific evolutionary model. *Genome Biol.* 5, R98 (2004).
6. Holmquist, R., Cantor, C. & Jukes, T. Improved procedures for comparing homologous sequences in molecules of proteins and nucleic acids. *J Mol Biol* 64, 145-61 (1972).
7. Hasegawa, M., Kishino, H. & Yano, T. Dating of the human-ape splitting by a molecular clock of mitochondrial DNA. *J Mol Evol* 22, 160-74 (1985).
8. Margulies, E.H. et al. Analyses of deep mammalian sequence alignments and constraint predictions for 1% of the human genome. *Genome Res.* 17, 760-74 (2007).
9. Wasserman, W., Palumbo, M., Thompson, W., Fickett, J. & Lawrence, C. Human-mouse genome comparisons to locate regulatory sites. *Nat. Genet.* 26, 225-8 (2000).
10. Toutenburg, H. *Statistical Analysis of Designed Experiments*, (Springer-Verlag, New York, 2002).
11. Wasserman, W. & Fickett, J. Identification of regulatory regions which confer muscle-specific gene expression. *J. Mol. Biol.* 278, 167-181 (1998).
12. Mootha, V.K. et al. PGC-1alpha-responsive genes involved in oxidative phosphorylation are coordinately downregulated in human diabetes. *Nat. Genet.* 34, 267-73 (2003).
13. Subramanian, A. et al. Gene set enrichment analysis: a knowledge-based approach for interpreting genome-wide expression profiles. *Proc Natl Acad Sci U S A* 102, 15545-50 (2005).
14. Good, P.I. *Permutation, Parametric and Bootstrap Tests of Hypotheses*, (Springer, 2005).
15. Agarwal, P. & Graepel, T. Generalization Bounds for the Area under the ROC Curve. *Journal of Machine Learning Research* 6, 393-425 (2005).
16. Xie, X. et al. Systematic discovery of regulatory motifs in human promoters and 3' UTRs by comparison of several mammals. *Nature* 434, 338-45 (2005).
17. Hughes, J.D., Estep, P.W., Tavazoie, S. & Church, G.M. Computational identification of cis-regulatory elements associated with groups of functionally related genes in Saccharomyces cerevisiae. *J Mol Biol* 296, 1205-14 (2000).

18. Andres, V., Cervera, M. & Mahdavi, V. Determination of the consensus binding site for MEF2 expressed in muscle and brain reveals tissue-specific sequence constraints. *J. Biol. Chem.* 270, 23246-9 (1995).
19. Shen, X. et al. Genome-wide examination of myoblast cell cycle withdrawal during differentiation. *Dev Dyn* 226, 128-38 (2003).
20. Tomczak, K.K. et al. Expression profiling and identification of novel genes involved in myogenic differentiation. *FASEB J.* 18, 403-5 (2004).
21. Schena, M., Shalon, D., Davis, R.W. & Brown, P.O. Quantitative monitoring of gene expression patterns with a complementary DNA microarray. *Science* 270, 467-70 (1995).
22. Huber, W., von Heydebreck, A., Sultmann, H., Poustka, A. & Vingron, M. Variance stabilization applied to microarray data calibration and to the quantification of differential expression. *Bioinformatics* 18 Suppl 1, S96-104 (2002).
23. Tusher, V.G., Tibshirani, R. & Chu, G. Significance analysis of microarrays applied to the ionizing radiation response. *Proc Natl Acad Sci U S A* 98, 5116-21 (2001).
24. de Hoon, M.J., Imoto, S., Nolan, J. & Miyano, S. Open source clustering software. *Bioinformatics* 20, 1453-4 (2004).
25. Zhao, P. et al. Fgfr4 is required for effective muscle regeneration in vivo. Delineation of a MyoD-Tead2-Fgfr4 transcriptional pathway. *J Biol Chem* 281, 429-38 (2006).
26. Yockey, C.E., Smith, G., Izumo, S. & Shimizu, N. cDNA cloning and characterization of murine transcriptional enhancer factor-1-related protein 1, a transcription factor that binds to the M-CAT motif. *J Biol Chem* 271, 3727-36 (1996).
27. Jacquemin, P., Hwang, J.J., Martial, J.A., Dolle, P. & Davidson, I. A novel family of developmentally regulated mammalian transcription factors containing the TEA/ATTS DNA binding domain. *J Biol Chem* 271, 21775-85 (1996).
28. Chen, Z., Friedrich, G.A. & Soriano, P. Transcriptional enhancer factor 1 disruption by a retroviral gene trap leads to heart defects and embryonic lethality in mice. *Genes Dev* 8, 2293-301 (1994).
29. Jacquemin, P., Martial, J.A. & Davidson, I. Human TEF-5 is preferentially expressed in placenta and binds to multiple functional elements of the human chorionic somatomammotropin-B gene enhancer. *J Biol Chem* 272, 12928-37 (1997).
30. Jacquemin, P. et al. Differential expression of the TEF family of transcription factors in the murine placenta and during differentiation of primary human trophoblasts in vitro. *Dev Dyn* 212, 423-36 (1998).
31. Biederer, C.H. et al. The basic helix-loop-helix transcription factors myogenin and Id2 mediate specific induction of caveolin-3 gene expression during embryonic development. *J. Biol. Chem.* 275, 26245-51 (2000).
32. Wan, B. & Moreadith, R.W. Structural characterization and regulatory element analysis of the heart isoform of cytochrome c oxidase VIa. *J. Biol. Chem.* 270, 26433-40 (1995).

33. Chow, K.L. & Schwartz, R.J. A combination of closely associated positive and negative cis-acting promoter elements regulates transcription of the skeletal alpha-actin gene. *Mol. Cell. Biol.* 10, 528-38 (1990).
34. MacLellan, W.R., Lee, T.C., Schwartz, R.J. & Schneider, M.D. Transforming growth factor-beta response elements of the skeletal alpha-actin gene. Combinatorial action of serum response factor, YY1, and the SV40 enhancer-binding protein, TEF-1. *J Biol Chem* 269, 16754-60 (1994).
35. Mar, J.H. & Ordahl, C.P. M-CAT binding factor, a novel trans-acting factor governing muscle-specific transcription. *Mol. Cell. Biol.* 10, 4271-83 (1990).
36. Wang, G., Yeh, H.I. & Lin, J.J. Characterization of cis-regulating elements and trans-activating factors of the rat cardiac troponin T gene. *J. Biol. Chem.* 269, 30595-603 (1994).
37. Marshall, P., Chartrand, N. & Worton, R.G. The mouse dystrophin enhancer is regulated by MyoD, E-box-binding factors, and by the serum response factor. *J Biol Chem* 276, 20719-26 (2001).
38. Boyd, K.E. & Farnham, P.J. Coexamination of site-specific transcription factor binding and promoter activity in living cells. *Mol Cell Biol* 19, 8393-9 (1999).
39. Stewart, S.A. et al. Lentivirus-delivered stable gene silencing by RNAi in primary cells. *RNA* 9, 493-501 (2003).

Supplementary Results

A) Lever screen of 4 known myogenic regulatory motifs across 101 myogenic gene sets

As an initial positive control analysis, we applied Lever to systematically analyze the 101 myogenic gene expression clusters and GO categories when considering the four known myogenic motifs MRF, MEF2, SRF and Tead. We found that 41 out of the 101 gene sets showed significant enrichment ($Q \leq 0.05$) for at least one Boolean combination of these four motifs (**Supplementary Figure 6** online; **Supplementary Table 3b** online). Nearly all gene sets that showed statistically significant enrichment ($Q \leq 0.05$) for combinations of these four motifs were composed of up-regulated genes, consistent with the known functions of the corresponding TFs as transcriptional activators.

B) Experimental validation of CRMs predicted by PhylCRM

We first verified by Q-RT-PCR that these seven genes were up-regulated during differentiation (**Supplementary Figure 8** online). Western blot analyses confirmed that these myogenic TFs were differentially expressed at the protein level during differentiation (**Supplementary Figure 9** online). Next, chromatin immunoprecipitation (ChIP) assays followed by region-specific quantitative PCR (see **Methods**) showed that four of the six candidate CRMs were significantly enriched for binding by MEF2 ($P \leq 0.05$), MyoD ($P \leq 0.05$) and myogenin ($P \leq 0.005$) (**Figure 5b**). Positive control CRMs were also significantly enriched for binding by these TFs, while negative control regions were not (**Figure 5b**). Two of these four bound regions were also significantly occupied by SRF ($P \leq 0.05$) during differentiation. Interestingly, of the six tested CRMs, the four that showed significant binding by MEF2, MyoD, and myogenin were the ones that are located next to genes involved in sarcomeric function, whereas the two that did not show significant binding by these factors are not. Although this does not tell us what sequence features distinguish the active from the inactive CRMs, it does suggest that the choice of the likely target gene sets is important in predicting CRMs that are active in a given

condition (here, myogenic differentiation).

We performed luciferase assays for the four novel, candidate CRMs that were enriched for *in vivo* TF binding. All four of these candidate CRMs resulted in statistically significant ($P \leq 0.05$) activation of luciferase expression during myogenic differentiation (**Figure 5c**). In contrast, these same CRMs did not result in increased luciferase activity in either fibroblasts or lens epithelial cells (**Figure 5c**). To further validate that these four candidate CRMs drive expression specifically in response to myogenic differentiation, we disrupted myogenic differentiation by shRNA knockdown of MEF2D (one of two MEF2 isoforms up-regulated in myotubes), myogenin (the most up-regulated MRF member), or SRF (**Supplementary Figure 10** online). Knockdown of myogenin significantly reduced ($P \leq 0.05$) transcriptional activity of all four predicted human CRMs positive for luciferase reporter activity in C2C12 myotubes (**Supplementary Figure 11a** online), while knockdown of SRF or MEF2D reduced the transcriptional activity of different subsets of these CRMs (**Supplementary Figure 11b,c** online). We note as a caveat that this reduced luciferase activity could potentially have been due to indirect effects involving some other TF under the control of the myogenic regulators knocked down by the shRNAs. In each case the level of luciferase activity was proportional to the amount of TF knockdown for a given shRNA clone (**Supplementary Figures 10 and 11** online).

Finally, we tested the sufficiency of the MRF AND MEF2 motif combination for CRM activity by generating a synthetic CRM containing consensus MRF and MEF2 binding sites arranged as in our newly discovered *ACTA1* CRM, but in the context of the *MGLL* negative control flanking sequence (see **Methods**). This synthetic CRM failed to drive expression in a luciferase reporter construct, suggesting that there are further sequence requirements aside from the MRF and MEF2 motifs (**Supplementary Figure 12** online). We anticipate that further computational analyses with more candidate regulatory motifs, combined with further experimental testing, will help to identify additional sequence features that may be important for CRM activity.